Part I

Recent Climate Change (Past 200 Years)

Recent Change—Atmosphere

2

Martin Stendel, Else van den Besselaar, Abdel Hannachi, Elizabeth C. Kent, Christiana Lefebvre, Frederik Schenk, Gerard van der Schrier and Tim Woollings

Abstract

This chapter examines past and present studies of variability and changes in atmospheric variables within the North Sea region over the instrumental period; roughly the past 200 years. The variables addressed are large-scale circulation, pressure and wind, surface air temperature, precipitation and radiative properties (clouds, solar radiation, and sunshine duration). Temperature has increased everywhere in the North Sea region, especially in spring and in the north. Precipitation has increased in the north and decreased in the south. There has been a north-eastward shift in storm tracks, which agrees with climate model projections. Due to large internal variability, it is not clear which aspects of the observed changes are due to anthropogenic activities and which are internally forced, and long-term trends are difficult to deduce. The number of deep cyclones seems to have increased (but not the total number of cyclones). The persistence of circulation types seems to have increased over the past century, with 'more extreme' extreme events. Changes in extreme weather events, however, are difficult to assess due to changes in instrumentation, station relocations, and problems with digitisation. Without thorough quality control digitised datasets may be useless or even counterproductive. Reanalyses are useful as long as biases introduced by inhomogeneities are properly addressed. It is unclear to what extent circulation over the North Sea region is controlled by distant factors, especially changes in Arctic sea ice.

Electronic supplementary material Supplementary material is available in the online version of this chapter at 10.1007/978-3-319-39745-0_2.

M. Stendel (✉)
Department for Arctic and Climate, Danish Meteorological Institute (DMI), Copenhagen, Denmark
e-mail: mas@dmi.dk

E. van den Besselaar · G. van der Schrier
Royal Netherlands Meteorological Institute (KNMI), De Bilt, The Netherlands
e-mail: besselaar@knmi.nl

G. van der Schrier
e-mail: schrier@knmi.nl

A. Hannachi
Department of Meteorology, Stockholm University, Stockholm, Sweden
e-mail: a.hannachi@misu.su.se

E.C. Kent
National Oceanography Centre, Southampton, UK
e-mail: eck@noc.ac.uk

C. Lefebvre
German Meteorological Service (DWD), Hamburg, Germany
e-mail: Christiana.Lefebvre@dwd.de

F. Schenk
Bolin Centre for Climate Research, University of Stockholm, Stockholm, Sweden
e-mail: frederik.schenk@geo.su.se

T. Woollings
Atmospheric Physics, Clarendon Laboratory, University of Oxford, Oxford, UK
e-mail: Tim.Woollings@physics.ox.ac.uk

M. Quante and F. Colijn (eds.), *North Sea Region Climate Change Assessment*, Regional Climate Studies, DOI 10.1007/978-3-319-39745-0_2

2.1 Introduction

Situated in northern central Europe, the North Sea exhibits large climate variability with inflow of a wide range of air masses from arctic to subtropical. For this reason, it is difficult to differentiate between natural and externally forced variability, despite large amounts of historical data. This chapter examines past and present studies of variability and changes in atmospheric variables over the instrumental period; roughly the last 200 years. Research areas lacking consensus in the scientific community are highlighted to stimulate further research.

The main driver of atmospheric variability in the North Sea region is the North Atlantic Oscillation (NAO). Despite its apparent long-term irregularity, the NAO exhibits extended periods of positive or negative index values. No consensus exists with respect to the size of the fraction of interannual NAO variance that cannot be explained by random forcing and is therefore probably influenced by external forcing. Slowly varying natural factors with an effect on European climate, such as the Atlantic Multidecadal Oscillation (AMO), may superimpose long-term trends on atmospheric variability and so be difficult to distinguish from the anthropogenic climate change signal.

The source of atmospheric and surface data influences the results obtained, even in the comparatively data-rich North Sea region. Based on reanalysis data, several studies find positive trends in storm activity over the North Sea region and a northeast shift in storm tracks over the past few decades. However, studies based on direct or indirect historical records of long-term variations in pressure, wind or wind-related proxies, mostly do not identify robust long-term trends. This counter-intuitive result is explained by uncertainties in the long-term historical wind and atmospheric pressure observations, and additional uncertainties arising from the lack of quality control when digitising old data as well as potential biases in the reanalyses due to the fact that the underlying amount of available data is not constant in time. Nevertheless, the northeast shift in storm tracks appears to be a new phenomenon. In contrast, the increase in wind speed and storminess in the latter half of the 20th century does not seem to be unprecedented within the context of historical observations. There are indications of an increase in the number of deep cyclones (but not in the total number of cyclones). There are also indications that the persistence of circulation types has increased over the past century.

Temperatures have increased both over land and over the North Sea. There is a distinct signal in the number of frost days and the number of summer days. While there is a clear winter and spring warming signal over the Baltic Sea region, this is not as clear for the North Sea region. As expected, the variability in marine temperatures on seasonal timescales is less than for the land temperatures.

Precipitation over land and, but to a lesser extent, over sea is positively correlated with the NAO, and on longer time scales with the AMO. There are indications of an increase in precipitation in the north of the region and a decrease in the south, in agreement with the north-eastward shift in the storm tracks. There are also indications that extreme precipitation events have become more extreme and that return periods have decreased.

From the few datasets available on radiative properties, it may be concluded that there are non-negligible trends together with potential uncertainties and land-sea inhomogeneities which make it difficult to assess these quantities in detail.

Climate change in the North Sea region cannot be investigated in isolation. In particular, what the relation is between changes in the Arctic cryosphere and trends in storminess, number of cyclones, persistence of circulation anomalies and extreme events further south, is an open research question. As analyses of the latter often rely on small datasets covering relatively short time scales, it is difficult to draw statistically significant conclusions. It is therefore essential to make available the large amount of data from past decades that have not yet been digitised. However, it is essential to thoroughly quality-check the data.

2.2 Large-Scale Circulation

2.2.1 Circulation Over the North Sea Region in a Climatological Perspective

From a climatological perspective, the North Sea region is characterised by strong ocean-atmosphere interactions, especially during winter, compared to other regions at similar latitudes (Furevik and Nilsen 2005). These interactions involve transfer of momentum, moisture and various trace gases, mainly carbon dioxide (Takahashi et al. 2002). In addition to the recent warming trend (Delworth and Knutson 2000; Johannessen et al. 2004), the North Sea and nearby regions witnessed climate change during the early 20th century, which was large in comparison to similar latitudes elsewhere (von Storch and Reichardt 1997; Gönnert 2003).

Atmospheric circulation in the European/North Atlantic region plays an important role in the regional climate of the North Sea and surrounding land areas (Hurrell 1995; Slonosky et al. 2000, 2001). It is mainly described by the NAO (e.g. Hurrell et al. 2003) which is an expression of the zonality of the atmospheric flow. The North Sea region is controlled by two large-scale quasi-stationary atmospheric patterns, the Icelandic Low (IL) and the Azores High (AH) plus a thermally driven

system over Eurasia with high pressure in winter and low pressure in summer. The dominant flow is therefore westerly, although any other wind direction is also frequently observed, and one of the main factors controlling air-sea interactions in the North Sea region is wind stress. Large-scale processes also constitute one of the main driving mechanisms responsible for the connection between local processes and global change. It is therefore important to pay attention to the recent changes in large-scale flow directly affecting the North Sea region.

The remainder of Sect. 2.2 reviews the status of the large-scale atmospheric variability affecting the North Sea region by focusing on the major teleconnection patterns and their effect on the jet stream. The NAO can be seen as the European expression of a larger-scale phenomenon, the Arctic Oscillation (AO). The relationship between the NAO and AO is briefly discussed in the following section, while a general description of the NAO and its properties is given in Annex 1. The NAO varies on a wide range of time scales from days to decades, reflecting interactions with surface conditions including sea-surface temperature (SST) and sea ice. These changes translate into changes in pressure and winds (Sect. 2.3), temperature (Sect. 2.4) and precipitation (Sect. 2.5) and also affect other variables, like sunshine (Sect. 2.6).

2.2.2 NAO and AO

The strength of the westerlies and the eddy-driven jet stream over the North Atlantic and western Europe are controlled by various factors including the pressure difference between the IL and AH as the main centres of action of the NAO (Wanner et al. 2001; Hurrell et al. 2003; Budikova 2009). The NAO and its changes can be understood as signals in the surface pressure field of jet stream variation (Hurrell and Deser 2009) and, as such, are often referred to as the regional expression of the AO, which describes sea-level pressure variations between the Arctic and northern hemisphere lower latitudes (Budikova 2012) or, in other words, variability in the strength of the polar vortex. The AO, also termed the Northern Annular Mode (NAM), was first identified by Lorenz (1951) and named by Thompson and Wallace (1998). Its positive phase is characterised by low surface pressure in the Arctic and a generally zonal (west to east) jet stream, thus keeping cold air in the Arctic. When the AO index is negative, there is high pressure in the Arctic and a stronger meridional (north to south or vice versa) component of the jet stream so that cold air can extend to lower latitudes. With respect to the North Sea region, the state of the AO controls the westerly flow and the storm track.

The AO is strongly correlated with the NAO, and the latter can be viewed as the signature of the former over the North Atlantic region. Therefore, the discussion below and in Annex 1 focuses on the NAO. Note, however, that there is extensive literature on the relationship between the NAO and AO, including studies on the robustness and consistency of one versus the other (Ambaum et al. 2001). Even though the AO and NAO are strongly correlated, their relationship is not linear (Kravtsov et al. 2006; de Viron et al. 2013). A fully three-dimensional picture discussing the connection between the AO and stratospheric circulation anomalies is provided by, for example, Ripesi et al. (2012).

2.2.3 Temporal and Spatial Changes in the NAO

Given the importance of the NAO in the North Atlantic and European climate, substantial efforts have been made to understand its variability in order to gain insight into its potential predictability. The NAO index varies on a wide range of time scales ranging from days to decades. As Fig. A1.1 in Annex 1 shows, the long-term behaviour of the NAO is irregular, and there is large interannual and interdecadal variability, reflecting the interaction with the surface, including SST and sea ice. Focusing on the 20th century, a period with predominantly positive NAO index values prevailed in the 1920s, followed by mainly negative values in the 1960s. Since then, a positive trend has been observed, which means more zonal circulation with mild and wet winters and increased storminess in central and northern Europe, including the North Sea region (e.g. Hurrell et al. 2003). This was especially the case in the early 1990s, raising claims that this behaviour was ‘due to anthropogenic climate change’. After the mid-1990s, however, there was a tendency towards more negative NAO index values, in other words a more meridional circulation and according to Jones et al. (1997), Slonosky et al. (2000, 2001) and Moberg et al. (2006), the strongly positive NAO phase in the early 1990s should be seen as an element of multi-decadal variation comparable to that at the start of the 20th century rather than as a trend towards more positive NAO values. It should also be noted that the winter of 2010/2011 had one of the most negative NAO indices in the record (Jung et al. 2011; Pinto and Raible 2012).

Intraseasonal variability in the NAO can be reasonably well described by a Markov process or first-order autoregressive (AR1) model (Feldstein 2000), although the observed skewness of the NAO index (Woollings et al. 2010; Hannachi et al. 2012) or the particularly enhanced persistence of the negative phase (Barnes and Hartmann 2010) are not captured very well. Nonlinear Rossby wave breaking mechanisms have been proposed to explain the intraseasonal variability in the NAO (e.g. Benedict et al. 2004; Franzke et al. 2004; Woollings et al. 2008).

Interannual variability in the winter mean NAO index is also found to be linked to the intraseasonal transitions between the positive and negative phases of the NAO pattern (Luo et al. 2012).

Several studies have attempted to quantify the fraction of interannual NAO variance that can be explained by 'climate noise', namely by random sampling of the intraseasonal variations (Feldstein 2000; Keeley et al. 2009; Franzke and Woollings 2011). As the NAO exhibits no preferred periods on the interannual and longer timescale (Hurrell and Deser 2009), the results of these studies differ widely, meaning as yet no consensus on the fraction of interannual NAO variability that cannot be explained by such noise and which is thus likely to be forced externally (Stephenson et al. 2000; Feldstein 2002; Rennert and Wallace 2009). Several external forcing mechanisms have been proposed, including bottom boundary conditions of local SST (Rodwell et al. 1999; Marshall et al. 2001) and sea ice (Strong and Magnusdottir 2011), volcanoes (Fischer et al. 2007), solar activity (Shindell et al. 2001; Spangehl et al. 2010; Ineson et al. 2011), and even stratospheric influence (Blessing et al. 2005; Scaife et al. 2005), including the quasi-biennial oscillation (Marshall and Scaife 2009) and stratospheric water vapour trends (Joshi et al. 2006). Remote SST forcing of the NAO originating from as far as the Indian Ocean was proposed by Hoerling et al. (2001) and Kucharski et al. (2006), while Cassou (2008) proposed an influence of the Madden-Julian Oscillation, but no consensus has been reached.

The positive trend in the NAO from the 1960s to the 1990s has been a particular focus of interest, and it has been a concern that many climate models have been unable to simulate the observed trends (Gillett 2005). Even though some models simulate quite large natural variability (Selten et al. 2004; Semenov et al. 2008), they still fall short of the strongest observed 30-year trend (Scaife et al. 2009). While Gillett et al. (2003) suggested that anthropogenic forcing could have contributed to the positive NAO trend there is no agreement on this, and concerns over the ability of models to represent NAO variability mean that attribution attempts should be treated with caution. The downturn in the NAO since the mid-1990s has brought its relation to climate change under further doubt (Cohen and Barlow 2005).

The NAO pattern is not entirely stationary, neither geographically nor with respect to season (Fig. 2.1). Although the amplitude is greatest and the explained variance highest in winter, the NAO is present all year round with varying strength and position. In particular, there is a westward shift of the southern centre of action in spring and an eastward displacement of both centres in autumn. Portis et al. (2001) developed a seasonally and geographically varying 'mobile' NAO, which is obtained from sea-level pressure data by taking into account the migration of the AH nodal points. Other techniques also exist, such as optimally interpolated patterns, trend empirical orthogonal functions (EOFs; Hannachi 2007a, 2008) and cluster analysis (Cheng and Wallace 1993; Hannachi 2007b, 2010).

Regression of the NAO on near-surface winds (Fig. 2.2) illustrates the well-known fact that the positive NAO phase is accompanied by stronger than average westerlies in the mid-latitudes right across the North Sea region into Scandinavia (Hurrell and Deser 2009), thus contributing to enhanced precipitation in the northern mid-latitudes.

2.2.4 Other Modes of Variability

The NAO is essentially a signal of variations in the Atlantic eddy-driven jet stream, but one pattern is not sufficient to fully describe the jet variability. The eddy-driven jet stream variability and regimes can, in fact, be described by at least two modes of variability—the NAO and the East Atlantic Pattern (EA; Wallace and Gutzler 1981; Woollings et al. 2010; Hannachi et al. 2012). The latter is defined as the second prominent mode of atmospheric low frequency variability over the North Atlantic. It appears throughout the year, but is more prominent in winter. Comprising a north-south dipole of anomalies, the EA pattern[1] resembles the NAO, but with anomaly centres displaced south-eastward and thus is sometimes interpreted as a 'southward shifted' NAO (e.g. Barnston and Livezey 1987). The positive phase of the pattern is associated with wetter-than-average conditions over northern Europe and Scandinavia. The EA pattern has particularly strong fluctuations in the low frequency component showing a consistent positive trend over recent decades. However, this is indicative of trends over the Mediterranean region rather than the North Sea region (Woollings and Blackburn 2012). Trouet et al. (2012) introduced a 'summer NAO' pattern with a blocking high over the British Isles and a low over south-eastern Europe in its positive phase which is most pronounced on interannual timescales and resembles the EA.

A third pattern that has some impact on the North Sea and Scandinavia is the Scandinavian pattern[1] (Wallace and Gutzler 1981), characterised primarily by a centre over Scandinavia and weaker centres of opposite polarity over western Europe. The positive phase of the Scandinavian pattern is frequently linked to the occurrence of atmospheric blocking over northern Europe (Barriopedro et al. 2006) and is therefore characterised by below-average precipitation in this region, as well as by large interannual and decadal variability over the past 50 years (Croci-Maspoli et al. 2007; Tyrlis and Hoskins 2008), which may be related to longer term variability of blocking across the Atlantic Ocean

[1] www.cpc.ncep.noaa.gov/data/teledoc/telecontents.shtml.

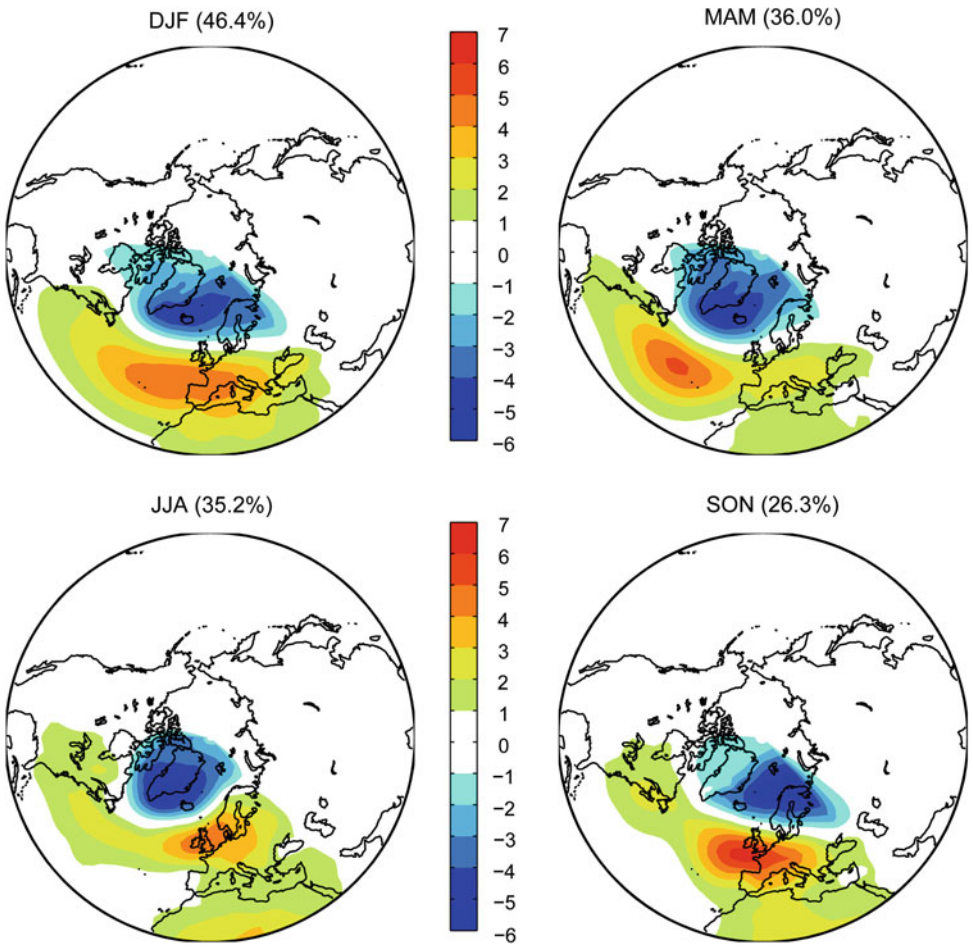

Fig. 2.1 Leading EOF of seasonal mean sea-level pressure (SLP) anomalies over the North Atlantic (20°–0°N, 90°W–40°E for the period 1948–2014. The percentage of explained variance is given above each panel

(Häkkinen et al. 2011). Before the 1980s the positive phase was dominant, this was followed by a negative phase between 1980 and 2000. The pattern amplitude has weakened over the past decade compared to the earlier part of the record.

Finally, on longer timescales, atmospheric conditions in the North Sea region are significantly influenced by the Atlantic Multidecadal Oscillation (AMO—more correctly termed Atlantic Multidecadal Variability, as there is no temporal regularity), which describes basin-wide variations in the temperature of the North Atlantic (Knight et al. 2005a, b) on the order of decades. These are particularly important in summer (Sutton and Hodson 2005) when the atmospheric response resembles a pattern termed the 'summer NAO' (Folland et al. 2009; Ionita et al. 2012b), see also Fig. 2.1. Warm periods were observed prior to 1880, between 1930 and 1965 and after 1995, and cool periods between 1900 and 1930 and between 1965 and 1995.

2.2.5 Summary

The NAO is the dominant mode of near-surface pressure variability over the North Atlantic and Europe, including the North Sea region. Amplitude and explained variance are largest in winter, but the NAO impacts the North Sea region throughout the year. Despite its apparent long-term irregularity, the NAO exhibits extended periods of positive or negative index values. It is therefore important to quantify the fraction of interannual NAO variance that cannot be explained by random forcing and so is likely to be influenced by external forcing. There is no consensus on the size of this fraction, or on the possible external forcing mechanisms.

2.3 Atmospheric Pressure and Wind

A typical characteristic of the climatology of the North Sea region is the large variability in meteorological variables on multiple time scales. The strong increase in wave height and storminess between the 1970s and the 1990s over the North Sea and North Atlantic (Carter and Draper 1988; Hogben 1994) raised public concern about a roughening wind climate and speculations about whether global warming might have an impact on storminess (Schmidt and von Storch 1993). With the availability of many more observations and gridded

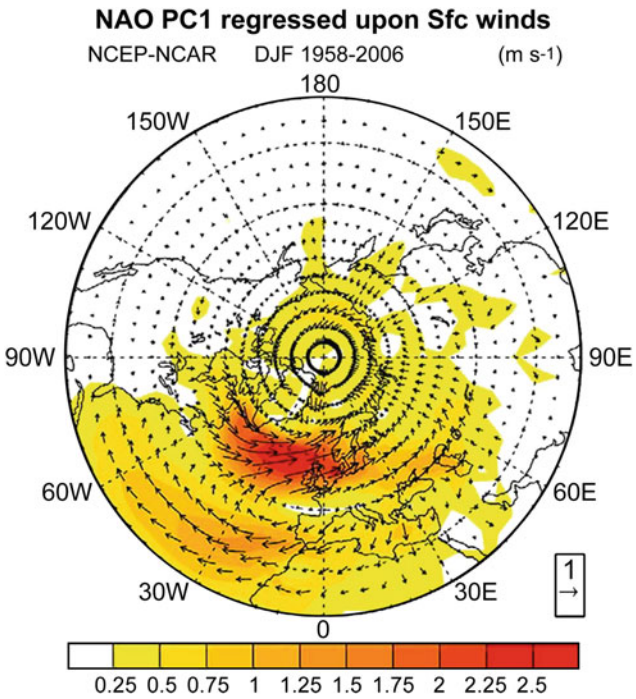

Fig. 2.2 Wind speed and direction associated with a 1 standard deviation change in the NAO index. The index is obtained from an EOF analysis of NCEP/NCAR sea-level pressure data (1958–2006) over the North Atlantic sector. Colour scale: m s^{-1}, unit vectors: 1 m s^{-1} (Hurrell and Deser 2009)

reanalysis data sets, detailed studies have significantly improved understanding of the atmospheric circulation and related winds over the North Atlantic and North Sea.

Owing to the large climate variability, results regarding changes or trends in the wind climate are strongly dependent on the period and region considered (Feser et al. 2015b). Through the strong link to large-scale atmospheric variability over the North Atlantic, conclusions about changes over the North Sea region are best understood in a wider spatial context. The following sections summarise studies on variations and trends in pressure and wind for recent decades and place these in the context of studies about changes over the last roughly 200 years.

2.3.1 Atmospheric Circulation and Wind Since Around 1950

The period since about 1950 is relatively well covered by observational data. The beginning of the satellite period in 1979 led to further substantial improvements in global data coverage, especially over the oceans and in data-sparse regions. Although in situ wind observations allow direct analysis of this variable, in particular over the sea (e.g. International Comprehensive Ocean-Atmosphere Data Set, ICOADS; Woodruff et al. 2011), the information is often predominantly local and inhomogeneities make the straightforward use of these data difficult, even for recent decades (Annex 1). Examples include an increase in roughness length over time due to growing vegetation or building activities, inhomogeneous wind data over the German Bight from 1952 onwards (Lindenberg et al. 2012) or 'atmospheric stilling' in continental surface wind speeds due to widespread changes in land use (Vautard et al. 2010).

Most studies therefore do not use direct wind observations, but instead rely on reanalysis products such as NCEP/NCAR (from 1948 onwards; Kalnay et al. 1996; Kistler et al. 2001), ERA40 (from 1958 onwards; Uppala et al. 2005) or, more recently, ERA-Interim, starting in 1979 (Dee et al. 2011) and the 20th Century Reanalysis 20CR (from 1871 onwards; Compo et al. 2011) and other reanalysis products, see Electronic (E-)Supplement Sect. S2.2. Making use of all available observations, a frozen scheme for the data assimilation of observations into state-of-the-art climate models is used to minimise inhomogeneities caused by changes in the observational record over time. However, studies indicate that these inhomogeneities cannot be fully eliminated (see E-Supplement S2). In addition, systematic differences between the underlying forecast models, such as due to their different spatial resolutions (Trigo 2006; Raible et al. 2008) and differences in detection and tracking algorithms (Xia et al. 2012) may affect cyclone statistics (for example changes in their intensity, number and position). Apart from these differences and inhomogeneities, the number of detected cyclones and their intensities show very high correlations between reanalyses (Weisse et al. 2005; Raible et al. 2008).

Three recent studies cover a continental-scale area. Franke (2009) manually counted the number of strong low pressure systems (central pressure below 950 hPa) over the North Atlantic (north of 30°N) from weather maps of the Maritime Department of the German Weather Service ('Seewetteramt'), see Fig. 2.3, which shows generally weak activity prior to 1988 and enhanced activity for the following decade, followed by a decrease to 2006.

Since then, the number of deep cyclones has again increased despite the predominantly negative NAO (Fig. A1.1 in Annex 1), and the maximum value with 18 such cyclones was observed in 2013/2014. Despite large decadal variations, there is still a positive trend in the number of deep cyclones over the last six decades, which is consistent with results based on NCEP reanalyses since 1958 over the northern North Atlantic Ocean (Lehmann et al. 2011). Using an analogue-based field reconstruction of daily pressure fields over central to northern Europe (Schenk and Zorita 2012), the increase in deep lows over the region might be unprecedented since 1850 (Schenk 2015). Barredo (2010) investigated adjusted storm losses in the period 1970–2008 on a European scale but did not find any trends despite a roughened wind climate. Based on the CoastDat2 reanalysis

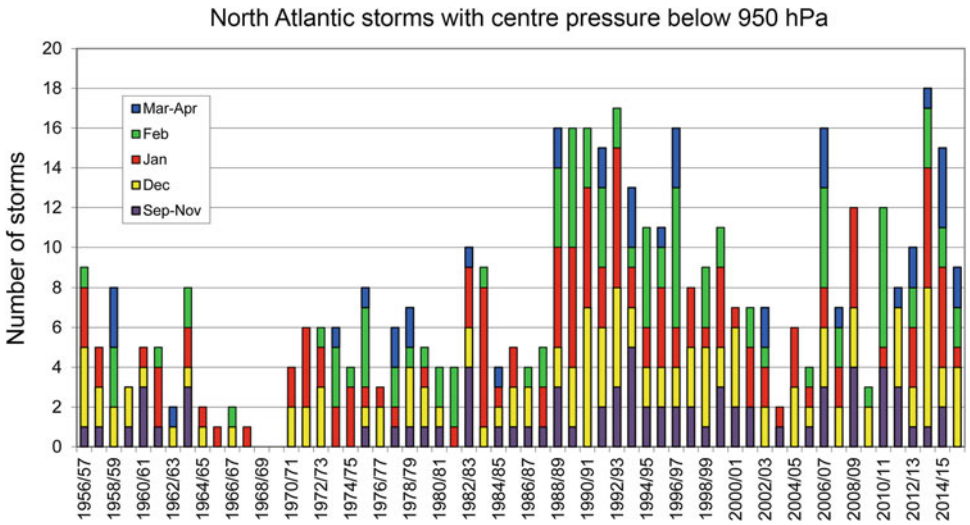

Fig. 2.3 Number of low pressure systems on the North Atlantic with a core pressure of 950 hPa or below, 1956/57–2015/16 (after Franke 2009, updated)

(Geyer 2014) and using E-OBS pressure data (van den Besselaar et al. 2011), von Storch et al. (2014) did not find robust evidence for supporting claims that the intensity of the two strong storms in late 2013 would be beyond historical occurrences and that the recent clustering of storms should be related to anthropogenic influence.

2.3.1.1 North Sea Region

Different studies based on reanalyses confirm the strong increase in wind speeds and wave heights observed over the North Sea region since the 1970s. Covering the period since about 1950, a positive trend is visible in annual storm activity in the NCEP, ERA40 and 20CR datasets, although the most recent decade shows a decrease in wind speed (e.g. Matulla et al. 2007; Donat et al. 2011) with no notable trend in mean wind speed for the period as a whole (1948–2014) over the North Sea (Fig. 2.4).

Siegismund and Schrum (2001) analysed decadal changes in wind forcing over the North Sea based on the NCEP reanalysis for the period 1958–1997 (Fig. 2.4). Over the 40 years, mean annual wind speeds increased by 10 %, mainly due to an increase in autumn and winter (ONDJ) after the 1960s and in late winter (FM) since the mid-1980s, but no trend was found for summer. Increased wind speeds are accompanied by an increase in WSW wind directions in autumn and winter (ONDJ) over the last three decades compared to the first (1958–1967). The enhanced mean winter wind speeds agree with an increase in the mean winter NAO index with a correlation of 0.69 for the year-to-year variations (Fig. 2.4). An update of the graphic for 1948–2014 shows a return to average wind conditions in the last decade with no notable trend remaining. The updated correlation with the NAO is 0.73.

Weisse et al. (2005) compared an NCEP-driven regional climate simulation (50 km resolution) with wind speeds from marine stations and found relatively good agreement. For the period 1958–2001, they found increasing storminess over most marine areas north of 45°N with a small, but significant positive trend over the North Sea and Norwegian Sea. The relative increase in storm frequency is largest over the southern North Sea across Denmark towards the Baltic Sea (1–2 % per year). The number of storms was lowest during the 1970s (with some notable exceptions, in particular the 'Capella' storm in January 1976) and peaked around 1990–1995. However, since then, a decrease in storm frequency has been observed which is confirmed by other studies (e.g. Matulla et al. 2007). Based on a high-resolution model hindcast forced by NCEP reanalyses for the storm season (November to March) 1958–2002, simulated storm-related sea-level variations confirm a significant positive trend for the Frisian and Danish coast (Weisse and Plüß 2006) while insignificant changes in mean and 90th percentile water levels are found for the UK, the Dutch coast and the German Bight. However, Weisse and Plüß also noted that positive trends in observations are higher than those in the NCEP-driven hindcast (see Chap. 3).

In contrast to the strong increase in wind speed in the NCEP reanalysis, Smits et al. (2005) found no increase in geostrophic wind speeds and even a decrease in homogenised wind observations for inland stations in the Netherlands for the period 1962–2002, while coastal stations show an increase consistent with NCEP. Smits et al. (2005) claimed that this is due to inconsistencies in the NCEP data, but it might also be that the 'atmospheric stilling' postulated by Vautard et al. (2010; see E-Supplement Sect. S2.1) can explain these differences.

2.3.1.2 Northern North Atlantic Region

As variations in atmospheric circulation and the wind climate over the North Sea show a high co-variability with

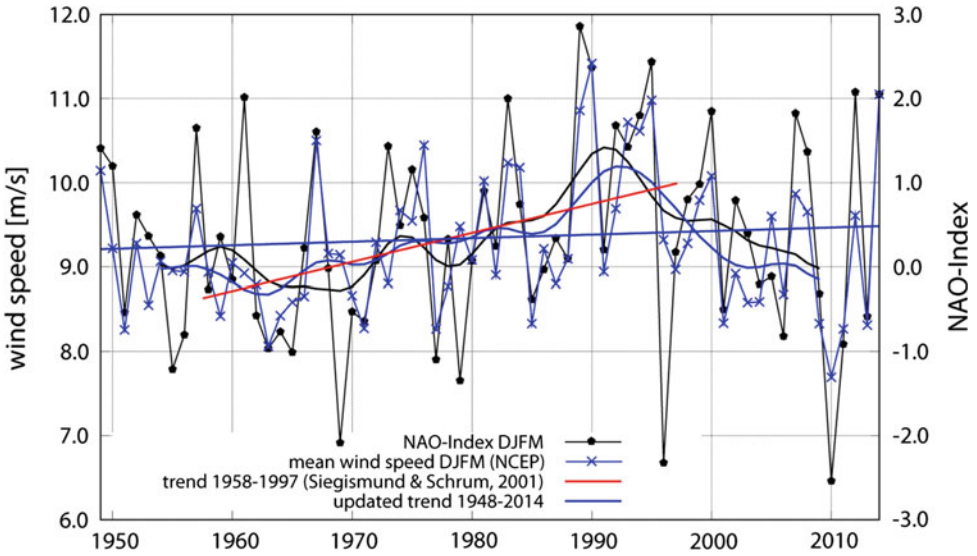

Fig. 2.4 Time series of mean seasonal wind speed derived from NCEP/NCAR reanalysis over the North Sea (*blue*) and the NAO index (*black*) for winter (DJFM) 1948–2014 recalculated and updated as in Siegismund and Schrum (2001), by F. Schenk. The positive trend (*red linear fit*) from this study has ended due to more average wind conditions in the last decade (*blue linear fit*). *Smoothed lines* are shown to highlight decadal-scale variations (11-year Hamming window)

large-scale variations and cyclonic activity over the North Atlantic, the majority of studies focus on the whole Euro-Atlantic region rather than on the North Sea alone. These studies show that the increase in wind speed or storminess is related to a general intensification of storm tracks over the North Atlantic north of about 55°N.

Based on NCEP reanalyses, Chang and Fu (2002) found a significant increase of about 30 % in decadal mean winter (DJF) storm track intensity for the period 1948–1998, with values about 30 % higher in the 1990s than during the late 1960s and early 1970s. The strengthening of storm track intensity is most pronounced over the North Atlantic albeit the trend compared to the few available conventional measurements seems to be overestimated in the NCEP reanalysis (Chang and Fu 2002; Harnik and Chang 2003; see E-Supplement Sect. S2.2). Geng and Sugi (2001) also found a significant increase in the number of North Atlantic cyclones and a significant intensifying trend for the cyclone central pressure gradient.

Similar results were found by Raible et al. (2008) based on ERA40 and NCEP for the period 1958–2001. The authors highlighted seasonal differences and reported a slight increase in number and a significant increase in intensity in winter (DJF) for the northern North Atlantic including the North Sea region (55°N–70°N, 45°W–15°E), a negative tendency in summer (JJA) and a non-significant increase in autumn (SON). The intensification in winter is stronger in NCEP than in ERA40 and also includes spring (MAM) in agreement with a similar increase in the number of deep lows (<980 hPa) in both seasons (Lehmann et al. 2011). The number of deep lows shows a minimum in the 1970s, followed by a strong increase.

The general enhancement in winter storm track intensity is accompanied by a northward shift in the storm track of 2–5° (depending on the data set) for NCEP (1948–1997; Chang and Fu 2002), ERA15 (1979–1997; Sickmoeller et al. 2000) and ERA40 (1958–2001; Wang et al. 2006), in agreement with a shift and intensification of deep lows (<980 hPa) towards the NE over the North Atlantic in the period 1948–2008 (Lehmann et al. 2011).

2.3.1.3 Southern North Atlantic Region

The general increase in the number of deep cyclones and storminess over the northern North Atlantic and North Sea is accompanied by partly opposing tendencies for the mid-latitudes south of 55–60°N (Gulev et al. 2001), suggesting a general northward shift in the cyclone tracks, consistent with findings of McCabe et al. (2001).

The north-south contrast in the sign of trends was also confirmed by Trigo (2006) who applied an objective detection and tracking algorithm to NCEP and ERA40 for winter (DJFM) 1958–2000 to produce a storm-track database for different stages in the cyclone lifecycle over the North Atlantic and Europe (20°–70°N; 85°W–70°E). On a seasonal basis, the trend is generally positive at higher latitudes (mostly due to an increased frequency of moderate and intense storms) and negative in the subtropical belt. Wang et al. (2006) and Raible et al. (2008) also drew similar

conclusions. All these results consistently show a northward shift in mean storm track position since about 1950 (Feser et al. 2015a).

2.3.2 Regional Variations in Pressure and Wind Since Around 1800

Observed changes in cyclone characteristics and winds over the last 40–60 years pose the question as to whether these changes merely reflect (multi-)decadal variations or whether they reflect long-term change. This section summarises current knowledge about the historical evolution of pressure and wind in the last 200 years over the Euro-Atlantic region.

Information about long-term variations in pressure and wind rely on multiple direct and indirect observations. They provide qualitative to semi-quantitative historical descriptions (the latter quite far back in time), such as storm surge-related damage on the Dutch coast since the 15th century (de Kraker 1999) or daily weather diaries like those at the observatory of Armagh (Ireland) since 1798 (Hickey 2003). Direct measurements such as surge levels at Liverpool since 1768 (Woodworth and Blackman 2002) and Cuxhaven since 1843 (Dangendorf et al. 2014) or wind records in the Dublin region since 1715 (Sweeney 2000) also provide important information on variations in the storm climate. The difficulty with these observations is that they often represent local conditions and so often exhibit inhomogeneities to an unknown extent.

As recommended by WASA Group (1998), most studies use pressure observations (which are more homogeneous over time than wind measurements) to derive wind and storm indices (e.g. WASA Group 1998; Klein Tank et al. 2002). The usefulness of typically-used pressure-based indices has recently been re-assessed and confirmed. Even single-station pressure indices such as strong pressure changes over 6- or 24-h periods or the annual number of deep lows provide useful information about long-term variations in the wind and storm climate (Krueger and von Storch 2011). The information content to describe long-term variations in the statistics of pressure and wind is even higher for indices of geostrophic wind speeds calculated from triangles of daily pressure observations (Krueger and von Storch 2012). The correlation of geostrophic wind speeds calculated from station triplets with real model wind speeds is especially high over open terrain and sea areas (i.e. regions that often lack conventional observations). Although pressure-based indices provide only an indirect link to real wind speeds or storminess, they can be considered a valid approach for assessing long-term statistics of pressure and wind (Krueger and von Storch 2011, 2012).

As historical information on pressure and wind mostly relates to regional or local scale rather than gridded fields, the studies presented in the following sections are discussed by region. Figure 2.5 provides an overview of potential long-term trends in the wind and storm climate.

2.3.2.1 North Atlantic and Iceland

The region north of around 55–60°N is of special interest regarding changes in the intensity or position of the main storm tracks. Historical information here is limited to the Shetland, Orkney and Faroe Islands as well as Iceland. The longest pressure-based wind index, the annual mean of absolute pressure changes over 24 h, suggests a significant positive trend over Iceland in the period 1823–2006 (Hanna et al. 2008), but no robust trend exists over the Norwegian Sea (since 1833) or the North Sea (since 1874). The latter is consistent with the result of Schmith et al. (1998) who found no significant trend for absolute daily pressure tendencies for stations around the NE Atlantic for winter 1871–1997. Analysis of high annual geostrophic wind speed percentiles over the NE Atlantic also indicates no significant change since the late 19th century (WASA Group 1998; Alexandersson et al. 2000; Matulla et al. 2007; Wang et al. 2009a, 2011). For the shorter period 1923–2008, positive trends exist over the northern NE Atlantic for spring (Wang et al. 2009a) which is in agreement with the intensification and northeast shift in cyclone activity in the last 60 years.

A positive trend also exists for the annual frequency of zonal weather types in the winter half-year 1881–1992 (Schiesser et al. 1997). As this weather type (Großwetterlagen) classification (Baur 1937; Hess and Brezowsky 1952, 1977; Hoy et al. 2012) relies on historical weather maps over the North Atlantic and Europe, the trend should be viewed with caution due to an improvement over time in detecting smaller lows (E-Supplement S2).

2.3.2.2 British Isles

There are many historical wind and wind-related documents and records for Great Britain and Ireland. Although robust trend estimates have not been undertaken, available information suggests large multi-decadal variations but no overall long-term trends (e.g. Sweeney 2000 for the number of storms per decade from historical reports of the Dublin region 1715–1999). For the shorter period 1903–1999, however, adjusted wind observations do show a decrease in the decadal number of storms exceeding 50 knots (25.7 m s^{-1}). The record of storms from a daily weather diary of Armagh (Ireland) 1798–1999 (Hickey 2003) also indicates similarly large variations to those of recent decades, although observer bias reduces reliability over time. Anemometer readings at the station show no obvious trend in the number of gale days per year for the period 1883–1999.

For the Irish Sea, tide gauge records at Liverpool provide an indirect estimate of long-term variations in storms. These show a negative tendency for the annual maximum surge at

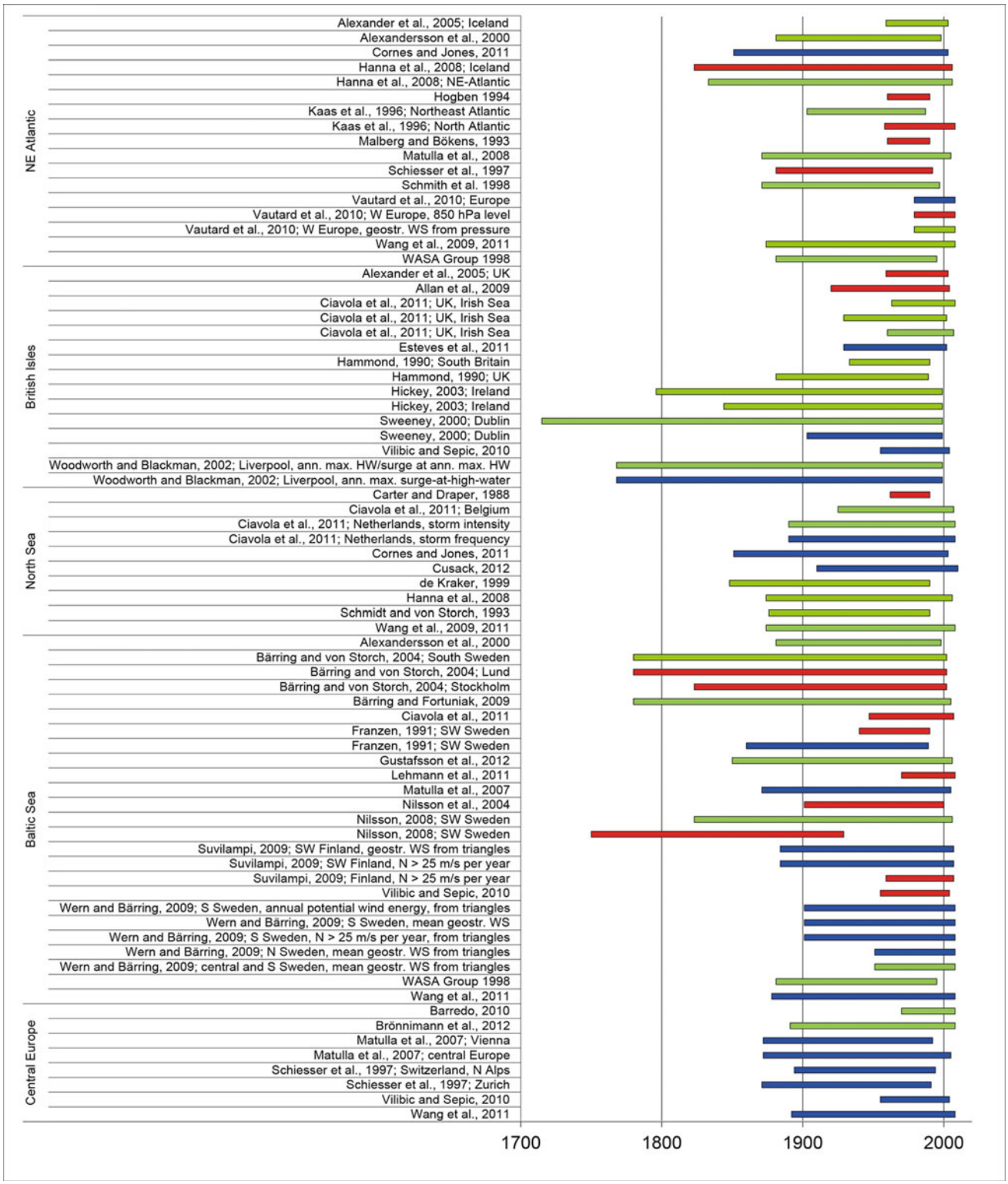

Fig. 2.5 Long-term trends for storminess over the Euro-Atlantic region based on different historical and observational sources (Feser et al. 2015a). *Red*, *blue* and *green colours* indicate positive, negative or no trend, respectively

high water for the period 1768–1999 (Woodworth and Blackman 2002) but no trend in the annual maximum high water level or the surges at annual maximum high water for this period. For shorter periods, no trends are found for maximum monthly wind speed observations for the Irish Sea 1929–2002 (Ciavola et al. 2011) while Esteves et al. (2011) found a weak but significant negative trend for monthly mean wind speeds at the Bidston observatory on the northern Irish Sea coast over the same period.

For southern England, Hammond (1990) used different stations to calculate an annual windiness index taking the annual average of monthly mean wind speeds for the Boscombe Down area. For the period 1881–1989, the annual windiness index does not show any long-term trend. For the end of the 17th and the first half of the 18th century (Late Maunder Minimum), wind indices were derived from ship logbooks for the Øresund region (Frydendahl et al. 1992) and the English Channel (Wheeler et al. 2009). Ship logbooks offer a unique source of information about past wind climates, as discussed for example by Küttel et al. (2009). Wind indices based on these logbooks suggest a generally stationary wind climate with large decadal variations. For the period 1920–2004, the 1930s show another period of more severe storms for the British Isles based on extreme three-hourly pressure changes (Allan et al. 2009).

2.3.2.3 North Sea Region

Limited historical information about dike repair costs for northern Flanders indicates no obvious visible long-term trend for the period 1488–1609 (de Kraker 1999). However, storm-related damage does appear to reflect similarly large multi-decadal variations as for storm observations over recent decades. An update of the historical index using water level observations at Flushing at the mouth of the Western Scheldt estuary for 1848–1990 shows a notable increase in spring tides in the 1990s which at least partly reflects the 30 cm rise in sea level over this period.

Other datasets do not indicate long-term trends in storm intensity. Surge information for the Netherlands shows a decrease in storm frequency over the period 1890–2008 (Ciavola et al. 2011). Also, Cusack (2012) found a weak negative tendency for the decadal running mean of the annual number of damaging storms and a related storm loss index calculated from homogenised wind observations of the Netherlands for 1910–2010, but did find large decadal variations for stormy conditions in the 1920s and 1990s. Storm intensity estimates derived from wind, wave and surge observations from Belgium for the period 1925–2007 show no trend (Hossen and Akhter 2015).

An analysis of geostrophic wind speeds for the German Bight shows no robust trends for the period 1876–1990 (Schmidt and von Storch 1993). But when the record is extended to include the period up to 2012 (Fig. 2.6) a tendency for decreasing wind speed in the upper percentiles becomes visible, corroborating direct wind, surge and wave observations from Belgium and the Netherlands, and findings by Rosenhagen et al. (2011). Analogue-based storminess shows a good correlation with the German Bight index and indicates no long-term trend since 1850 (Schenk 2015). Wang et al. (2011) found significant negative trends over the North Sea and surrounding land areas for the 99th percentile of geostrophic wind in summer, but no robust trends in other seasons. Direct wind observations from Skagen in northern Denmark also suggest decreasing overall storminess for the period 1860–2012 with extremely high storminess prior to 1875 (Clemmensen et al. 2014).

2.3.2.4 Northern Alps and Central Europe

Although not directly linked to the North Sea wind climate, observations from further south are also useful to help understand variations in large-scale atmospheric circulation and give indications about a northward displacement in storm tracks. For Vienna, the number of gale days (above 8 Bft, 17.2 m s^{-1}) show a clear decrease for the period 1872–1992 (Matulla et al. 2007), however based on non-homogenised observations. This is corroborated by significant negative trends in the number of days exceeding 7, 8 and 9 Bft (>13.9, 17.2 and 20.8 m s^{-1}, respectively) in northern Switzerland for the period 1894–1994 (Schiesser et al. 1997). The duration of strong winds (>7 Bft) also shows a negative trend for Zürich for 1871–1991 except in winter (Brönnimann et al. 2012). Negative trends are also found for central Europe (Matulla et al. 2007; Wang et al. 2011). In contrast, Stucki et al. (2014) found no clear trends, but large interdecadal variability, over Switzerland.

2.3.3 Trends in the 20th Century Reanalysis Since 1871

As shown in Fig. 2.5, the majority of studies using observational storm proxies find no robust trends, some even a negative tendency, for the wind and storm climate in historical pressure and wind observations. In contrast, 20CR (Compo et al. 2011) suggests significant upward trends for storminess over data-sparse regions like the NE Atlantic (Donat et al. 2011) while Bett et al. (2013) did not find a clear trend over Europe. Closer inspection reveals that the agreement of 20CR and wind observations over land like Zürich is reasonable (Brönnimann et al. 2012), but there are discrepancies over sea (Krueger et al. 2013; Schenk 2015). This is because 20CR, like other reanalyses, assimilates all available pressure observations at a given time step which leads to a strong increase in assimilated land pressure observations (and to a lesser extent also sea pressure observations) over time. Following Krueger et al. (2013),

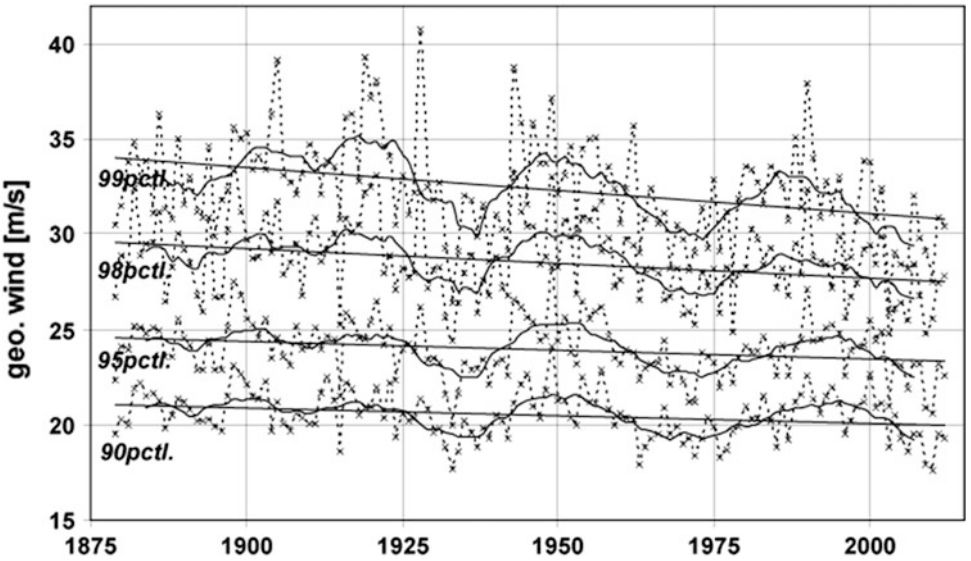

Fig. 2.6 High annual percentiles of geostrophic wind speeds over the German Bight after Schmidt and von Storch (1993) updated and reproduced for 1879–2012. Running 11-year means and linear trends are displayed to highlight long-term variations (data by G. Rosenhagen, figure by F. Schenk)

inconsistencies between 20CR and pressure-based storm indices over data-sparse regions increase back in time as the number of assimilated stations by 20CR, mainly over sea areas, decreases. Spurious pressure trends in data-sparse regions, identified in the NCEP/NCAR reanalysis (Hines et al. 2000) might also affect 20CR (E-Supplement Sect. S2.3).

2.3.4 Summary

Different studies mainly based on reanalysis data show positive trends in storm activity over the NE Atlantic and North Sea together with a northeast shift in the position of storm tracks over the last 40–60 years. This is also reflected in a roughened wind and wave climate, although a return to average conditions beginning at the end of the 20th century has clearly reduced trends from earlier publications. As summarised in Fig. 2.5 direct or indirect historical records of long-term variations in pressure, wind or wind-related proxies mostly show no robust long-term trends for the last 100 years or more. Large decadal variations seem to dominate for centuries.

While the increase in wind speeds and storminess in the latter half of the 20th century does not seem unprecedented in the context of historical observations, the northeast shift in storm tracks in this period may be a new phenomenon. The long-term decrease north of the Alps mainly results from a less stormy period during the 1990s compared to the North Sea and North Atlantic while the period at the end of the 19th century is comparably windy. The less stormy 1990s further south are consistent with the northeast shift in storm tracks and the decrease in winter cyclone activity in the mid-latitudes. This northeast shift together with the trend pattern of decreasing cyclone activity for southern mid-latitudes and increasing trends north of 55–60°N after around 1950 seems consistent with scenario simulations to 2100 under increasing greenhouse gas concentrations (e.g. Ulbrich et al. 2009; Feser et al. 2015a; see Chap. 5). This corroborates the findings by Wang et al. (2009b) that combined anthropogenic and natural forcing had a detectable influence on this pattern of atmospheric circulation, storminess and ocean wave heights during boreal winter 1955–2004 while an analysis for the first half of the 20th century is less likely to be dominated by external forcing.

Uncertainties remain not only for long historical wind and pressure observations (e.g. Lindenberg et al. 2012; Wang et al. 2014), but also for 20CR that to a large extent relies on these observations (Brönnimann et al. 2013; Krueger et al. 2013; Dangendorf et al. 2014; Schenk 2015). These are discussed in detail in E-Supplement S2. As a better understanding of long-term variations versus trends, and their link to atmospheric circulation is crucial for any regional climate change analysis, data rescue initiatives and digitisation initiatives such as data.rescue@home (www.data-rescue-at-home.org) or oldWeather (www.oldweather.org) are essential for further improvements towards the homogenisation of observations and reanalyses prior to about 1950. Such data can then be used in reanalysis projects such as ACRE (Atmospheric Circulation Reconstructions over the Earth; www.met-acre.org). However, in the light of problems apparently introduced into the WASA dataset during the digitisation step (see E-Supplement Sect. S2.3), it is also essential to thoroughly quality-check this type of data.

2.4 Surface Air Temperature

Despite the large variability in temperature, the warming trend of recent decades is strong enough to be discernible in local temperature observations, and it is larger than the warming trend simulated by state-of-the-art climate models. The principal drivers for this 'excess warming' appear to be changes in atmospheric circulation, mainly in winter and spring, and feedbacks involving soil moisture and cloud cover, mainly in summer and autumn (Van Oldenborgh et al. 2009).

The data sources for near-surface air temperature are different over land and sea. Terrestrial measurements are made at fixed locations, with typically standardised installations (WMO 2010) and at a reference height of 2 m (e.g. Klein Tank et al. 2002). In contrast, marine air temperature observations are typically made aboard moving ships (ICOADS; Woodruff et al. 2011), adjusted to a common reference height of 10 m (necessary because the typical observation height has increased by about 20 m over the period of record; Kent et al. 2013). Only a few fixed station measurements exist, such as on oil platforms. Observations of marine air temperature from ships are affected by daytime heating biases, and to avoid these problems datasets (for example from the Hadley Centre) are constructed using night-time observations only. Alternatively, both day and night observations, with adjustments for daytime heating following Berry et al. (2004), can be used. The North Sea region is relatively well sampled, but observations are sparse in the 19th Century and, more recently, during the Second World War.

2.4.1 Terrestrial Surface Air Temperature

The first decade of the 21st century was characterised by some extreme seasons. The hot summer of 2003 was probably unprecedented for at least 500 years in western Europe (Luterbacher et al. 2004), but was even surpassed in extremity by the East European summer of 2010 (Barriopedro et al. 2011). Summer and autumn 2006 and winter 2006/2007 were also exceptionally warm (Luterbacher et al. 2007; Cattiaux et al. 2009). On the other hand, winter 2010/2011 had a very negative NAO index (see Sect. 2.2), but was much warmer than comparable winters with a similarly negative NAO index (Cattiaux et al. 2010). Figure 2.7 shows time series of annually averaged land air temperature for the North Sea region, defined here as the area between 48°N and 62°N and 6°W and 10°E, for various data sets. The graphic shows 2014 to be unprecedentedly warm, even though none of the four seasons was the warmest on record (winter ranks 2nd after 2006/2007, spring 3rd after 2007 and 2011, summer 14th and autumn 2nd after 2006), and the previous maximum from 2011 was exceeded by almost 0.5°C. The datasets used are the CRUTEM4v (from UEA/CRU; Jones et al. 2012), GHCN-M version 3 (NOAA/NCDC, Peterson and Vose 1997; Jones and Moberg 2003), GISTEMP (NASA/GISS; Hansen et al. 2010) and BerkeleyEarth (http://berkeleyearth.org/), which have been subject to a homogeneity adjustment, supplemented by the E-OBS daily dataset version 10.0 (Haylock et al. 2008). To compare the different datasets, the grids of the global datasets are regridded to match that of the E-OBS grid (0.5° × 0.5°; van der Schrier et al. 2013).

The similarity between these estimates of temperature over the North Sea region is evident, with only minor differences in trend values (Table 2.1). Over the period 1980–2010, the trend in annual averaged daily mean temperature is approximately 0.38 °C decade^{-1}. Trend values are based on a linear least-square approximation to the data. Table 2.1 also gives temperature change for the whole of Europe (30°–75°N, 12°W–45°E plus Iceland, based on E-OBS), the northern hemisphere land and the global land area, both based on CRUTEM4. For 1980–2010, the warming trend in the North Sea region is smaller than that of Europe as a whole, but larger than the average over the northern hemisphere and global land areas.

In all datasets the period from the early 1990s onwards is warmest. Figure 2.8 highlights annual temperatures of the past few decades, averaged over the North Sea region and relative to the 1961–1990 climatology, based on the E-OBS dataset. The grey bars in Fig. 2.8 indicate the estimated uncertainties which take into account both errors introduced by spatial interpolation over areas without observations, by inhomogeneities in the temperature data that result from station relocations or instrument changes etc., and by urbanisation, as documented by van der Schrier et al. (2013) and Chrysanthou et al. (2014). The uncertainties indicate that although it is not possible to be 100 % certain about the ranking of individual years, the positive overall trend since the 1980s is very pronounced and 2014 stands out, even taking the uncertainties into account.

Ionita et al. (2012b) examined the connection between diurnal temperature range (DTR) and atmospheric circulation. They found that modes of interannual winter DTR variability are strongly related to the NAO and, to a lesser extent, the AMO, whereas in summer DTR variability is mainly influenced by a blocking pattern over Europe.

2.4.2 Number of Frost Days and Summer Days

According to Della-Marta et al. (2007), the length of western European heat waves has doubled since 1880 and Europe's climate has seen more warm extremes. This is illustrated in Fig. 2.9 which shows the difference in the annual number of frost days (minimum temperature <0 °C) and summer days

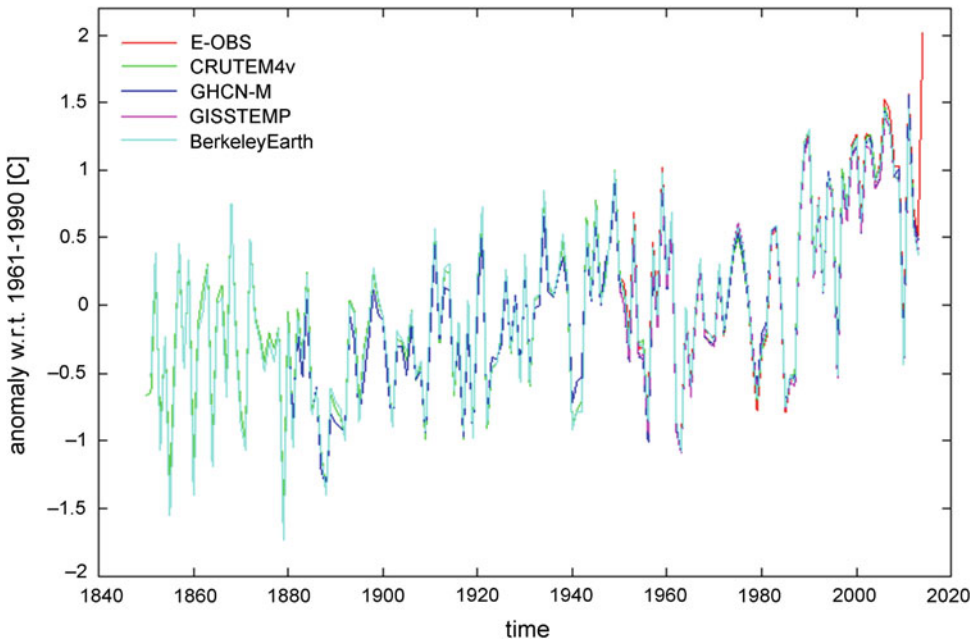

Fig. 2.7 Land-based annual mean air temperatures averaged over the North Sea region (48°–62°N, 6°W–10°E) with respect to the 1961–1990 climatology as calculated by E-OBS (*red*), CRUTEM4v (*green*), GHCN-M (*blue*), GISTEMP (*purple*) and the Berkeley Earth dataset (*light blue*)

Table 2.1 Linear temperature trends (°C decade^{-1}) over 1950–2010 and 1980–2010 for the North Sea region for CRUTEM4v, GHCN-D, GISTEMP, BerkeleyEarth and E-OBS

	CRUTEM4v	GHCN-D	GISTEMP	Berkeley Earth	E-OBS	Europe	NH land	Global land
1950–2010	0.210	**0.174**	0.228	**0.157**	0.204	**0.179**	**0.199**	**0.172**
1980–2010	**0.383**	**0.389**	**0.389**	**0.353**	**0.408**	**0.414**	**0.337**	**0.267**

The last three columns give trends for Europe (based on E-OBS), the northern hemisphere land and global land temperatures (based on CRUTEM4), respectively. Numbers in bold indicate that the trend is statistically significant at the 5 % level based on a t-test accounting for the reduced degrees of freedom due to autocorrelation (von Storch and Zwiers 1999)

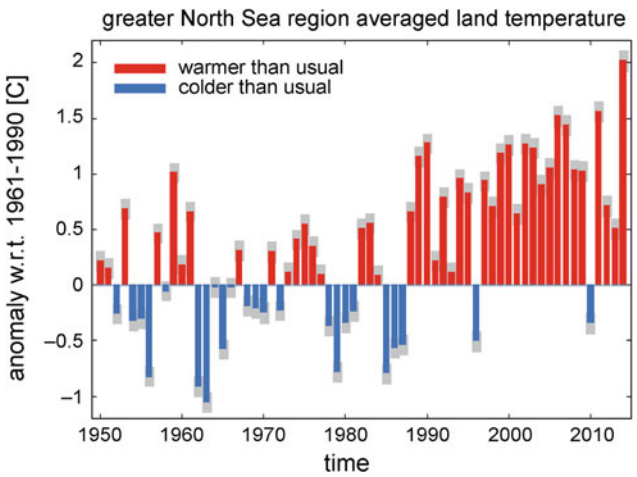

Fig. 2.8 Annual averages for land-based air temperature over the North Sea region with respect to the 1961–1990 climatology as calculated by the E-OBS dataset. The uncertainty estimate for the E-OBS data is included as *grey boxes*

(maximum temperature ≥25 °C) between 1981–2010 and 1951–1980 (based on E-OBS data). The change in these indices is not spatially consistent (in contrast to the increase in annual averaged temperature—not shown). All differences are statistically significant at the 5 % level using a one-sided Student t-test. The figure shows that the number of frost days has declined almost everywhere, with the strongest decreases found in the northern and eastern parts of the domain. The number of summer days has also increased almost everywhere, with the smallest increases in Scotland, northern England and Scandinavia and the largest in northern France.

2.4.3 Night Marine Air Temperature

As for land-based temperatures, the night marine air temperature (NMAT) also increased over the period 1856–2010 (Fig. 2.10). Two datasets were used, an uninterpolated 5° monthly mean dataset for 1880–2010 (HadNMAT2; Kent et al. 2013) and an interpolated (using a large-scale

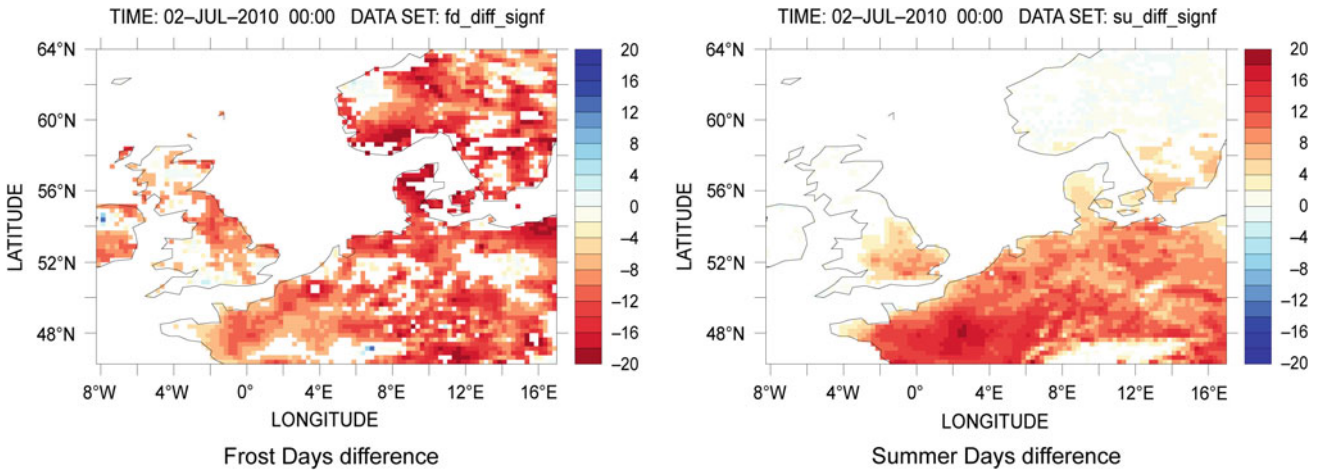

Fig. 2.9 Difference between the 1981–2010 and 1951–1980 climatological values of the annual number of frost days (*left*, daily minimum temperature <0 °C) and summer days (*right*, daily maximum temperature ≥25 °C). Grid squares with missing data or where the difference did not pass the 95 % significance level using a Student t-test, are white. Calculations based on E-OBS data

reconstruction technique; Rayner et al. 2003) 5° monthly mean dataset for 1856–2001. Differences between these datasets are larger than for land temperatures, especially around 1900 and during and just after the Second World War. In the latter period, sampling is sparse and non-standard observing practices necessitated adjustments to the observations (Kent et al. 2013). After about 1950, agreement improves. Linear trends in air temperature, adjusted for day-time heating biases (Berry and Kent 2009) show similar values.

Figure 2.10 also indicates that for marine air temperature the values in the most recent decade are likely to be the warmest on record, although uncertainty is large in the early part of the record due to sparse sampling.

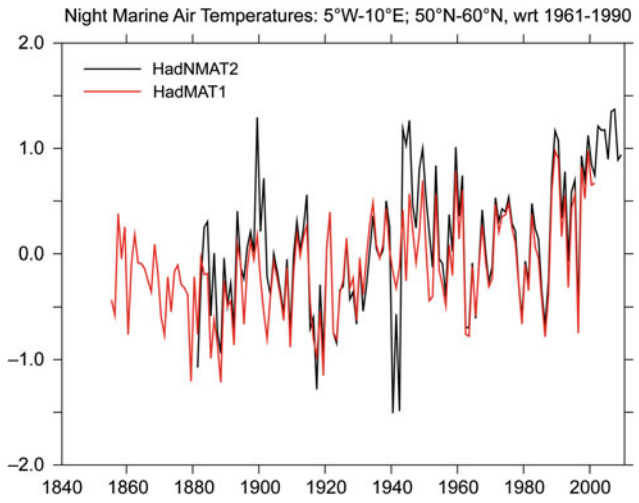

Fig. 2.10 Annual average night marine air temperature anomalies (°C) for the region 50°–60°N, 5°W–10°E from 5° monthly mean datasets: HadNMAT2 (*black*) and HadMAT1 (*red*)

Seasonal time series of the marine air temperature data sets show broadly similar variability to land-based temperatures (Fig. 2.11), but with a smaller amplitude. Very recently, the differences again increase, but this seems to be due to sparse observations and changes in the marine observing system (Kent et al. 2007, 2013).

2.4.4 Comparison of Land and Marine Air Temperatures

A comparison of land and marine temperatures (Fig. 2.12) shows general agreement. The lower plot in each panel depicts three estimates of the land-marine air temperature difference over the North Sea region based on E-OBS data for the land component and three different marine air temperature datasets: the NOCv2.0 dataset (Berry and Kent 2009, 2011), the HadNMAT2 dataset and the HadMAT1 dataset. Due to the much larger heat capacity of water, the difference series between the land and marine air temperature shows a residual positive trend over the last few decades of the record.

2.4.5 Summary

There is generally good agreement between the different temperature data sets over the oceans and over land. While temperatures have clearly increased over land, the NMAT shows there has also been an increase over the North Sea, even though the variability on seasonal timescales is smaller than for the land temperatures. Furthermore, due to the large heat capacity of water it takes much longer to warm the ocean than the land. In addition, heat is transported away

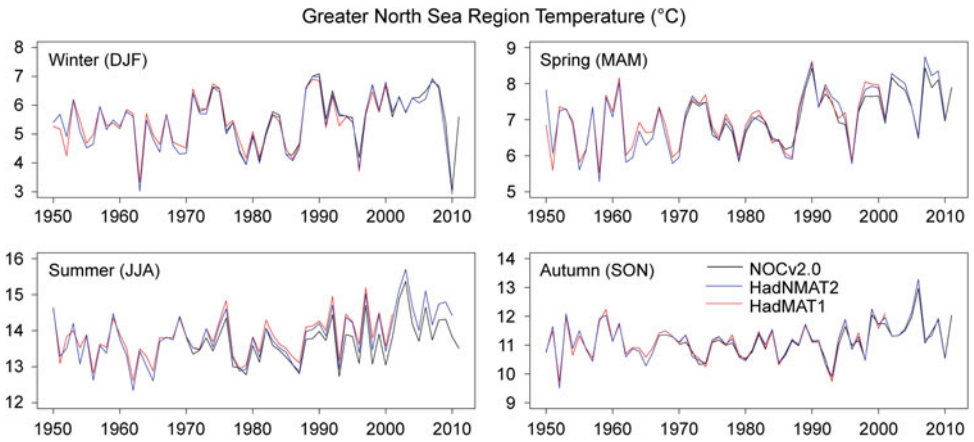

Fig. 2.11 Seasonal mean night marine air temperature (°C) from NOCv2.0 (1970–2010), HadNMAT2 (1950–2010) and HadMAT1 (1950–2001). HadNMAT2 and HadMAT1 were averaged to the same 1° grid as NOCv2.0 and masked to the NOCv2.0 land mask

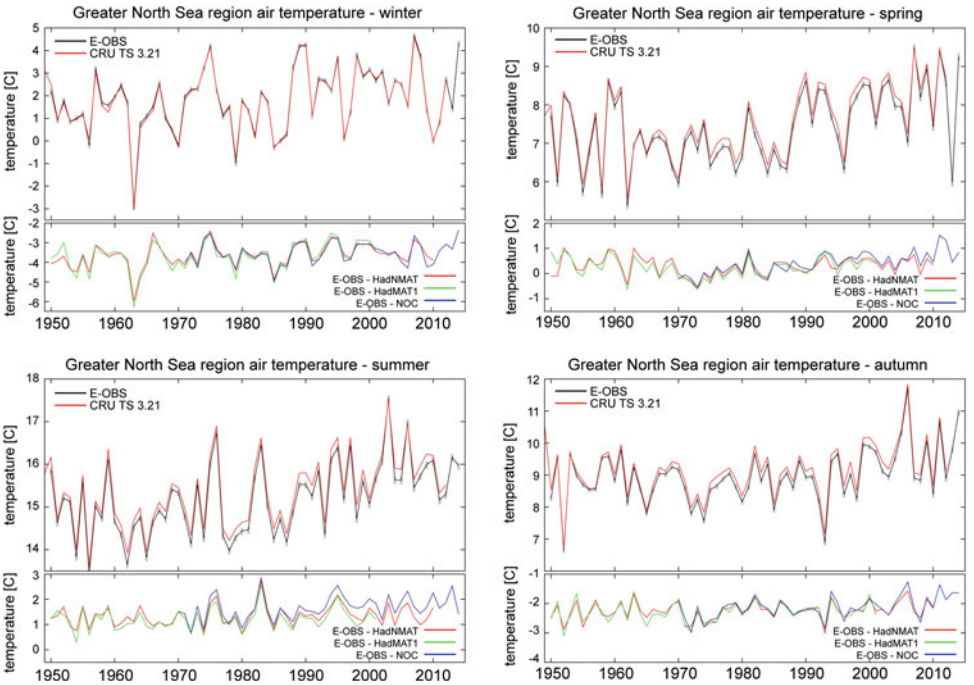

Fig. 2.12 Land-based air temperature over the North Sea region for winter (*upper left*), spring (*upper right*), summer (*lower left*) and autumn (*lower right*) based on the CRU TS 3.10 (Harris et al. 2014; *red*) and E-OBS (*black*) datasets. The uncertainty estimate for the E-OBS data is included as *grey boxes*. The *lower plots* show the difference between land-based air temperature and marine air temperature for this region, for three marine air temperature datasets

from the surface into deeper waters, where it cannot be directly measured. Thus, it would be expected that the land warms faster than the sea as long as the radiative forcing is positive. This is exactly the situation being observed, and according to the datasets, the imbalance is up to several tenths of a degree.

2.5 Precipitation

2.5.1 Precipitation Over Land in the North Sea Region

In a warmer climate, the atmospheric water vapour content is likely to rise due to the increase in saturation water vapour pressure with air temperature, as described by the Clausius-Clapeyron relation, and to result in an intensification of rainfall (Held and Soden 2006; O'Gorman and Schneider 2009). Evidence of higher amounts and more extreme precipitation has already been reported (e.g. Groisman et al. 2005; Moberg et al. 2006; Donat et al. 2013; Hartmann et al. 2013). Even though floods are a recurring event in Europe, attempts have been made to link increased flood risk to changes in the frequency of atmospheric blocking events (Lavers et al. 2012) or to anthropogenic climate change (Pall et al. 2011).

In a global study, Donat et al. (2013) showed a weak increase in the number of days exceeding 10 mm of precipitation (R10 mm) over the northern parts of Europe (but statistically significant only over eastern Europe at the 96 %

level). Over the Iberian Peninsula, a non-significant decrease in this metric is observed. A non-significant increase in the contribution of extreme precipitation events to the total precipitation amount (R95pTOT) is also observed over Great Britain and Scandinavia.

The European Climate Assessment and Dataset (ECA&D, Klein Tank et al. 2002) is a collection of daily station observations of 12 elements (of which five are gridded) and contains (as of March 2014) data from nearly 8000 stations across Europe and the Mediterranean. The station time series are updated on a regular basis using data provided by the national meteorological and hydrological services (NMHSs), universities or, before updates from these institutions are available, synoptic messages from the Global Telecommunication System (GTS). ECA&D receives time series from 61 data providers for 62 countries (as of March 2014).

Figure 2.13 compares precipitation for three stations with data since the beginning of the 20th century; Cambridge (UK), Stromsfoss Sluse (Norway) and De Bilt (Netherlands). The time series show strong interannual and decadal variability. A general upward trend is visible in the Dutch and Norwegian time series with trends of 14.52 mm decade^{-1} in the annual data over the 1901–2014 period for De Bilt and 28.81 mm decade^{-1} over the 1901–1950 period for Stromsfoss Sluse. Both trends are (just) statistically significant at the 5 % level following a t-test accounting for autocorrelation in the time series (von Storch and Zwiers 1999). A long-term trend in the UK time series is less pronounced. The Norwegian time series exhibits an enhanced trend since the mid-1990s, especially in summer. A weak drying trend since the 1990s, although not unprecedented, is visible in the UK series. It is also clear that, under certain circumstances, the entire area is influenced by high pressure for extended periods (e.g. in 1921) such that the whole North Sea area remains very dry.

Trends in annual land precipitation are positive almost everywhere over the North Sea region for the period 1951–2012 (Fig. 2.14, top panel). The greatest increase in precipitation is observed in winter (Fig. 2.14, lower left), especially along the west coast of Norway, over southern Sweden, parts of Scotland and the Netherlands and Belgium. Further inland, trends are much smaller and statistically non-significant almost everywhere. In summer, there is no evidence of increasing precipitation trends along the coast of western Norway, while the contrast between trends in coastal regions and more inland regions of the European mainland increases considerably as the latter show negative trends in summer (Fig. 2.14, lower right).

Winter and spring in northern Europe (defined as the land area north of 48°N) show an overall decreasing trend in return periods of extreme precipitation (van den Besselaar et al. 2013), which is indicative of increasing precipitation extremes. The trend is most pronounced in the 5-day precipitation amount in northern Europe during spring. The 5-day amount which is statistically a 20-year event over the 1951–1970 period becomes an approximately 8-year event in the 1991–2010 period.

For annual 5-day and 10-day precipitation amounts in the UK, Fowler and Kilsby (2003) found significant decadal-level changes in many regions. For the 10-day precipitation amount, the 50-year event during 1961–1990 became an 8-, 11- and 25-year event in eastern, southern and

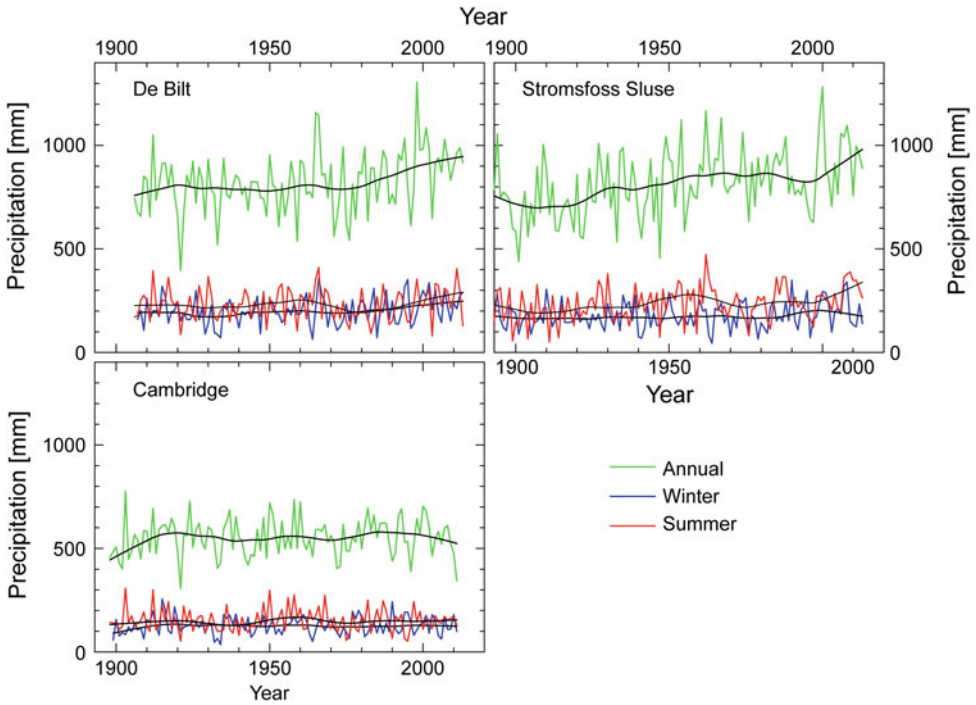

Fig. 2.13 Annual, winter and summer precipitation series for three stations from the ECA&D dataset; De Bilt (Netherlands, *top left*), Stromsfoss Sluse (Norway, *top right*) and Cambridge (UK, *lower left*). A low-pass filter is applied for the *black curves*

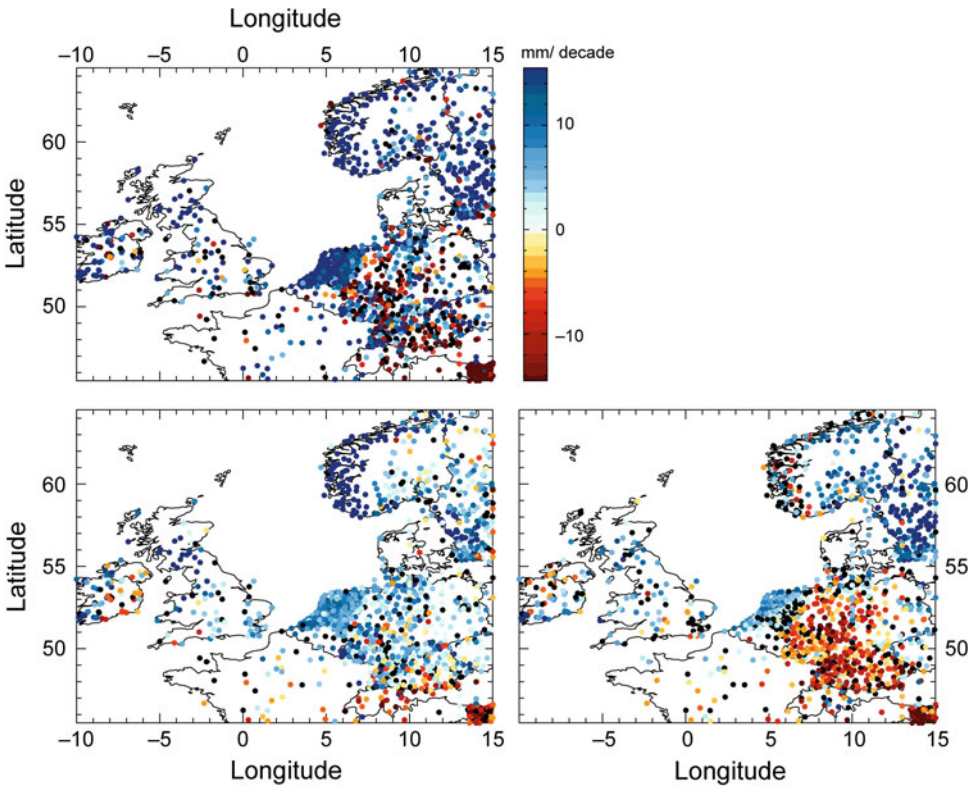

Fig. 2.14 Linear least-squares fit trends in annual (*top*), winter (*lower left*) and summer (*lower right*) precipitation over the period 1951–2012 in mm decade^{-1}. *Blue circles* denote a trend towards wetter conditions, while *orange* and *red circles* denote a trend towards drier conditions, both significant at the 5 % level ($p \leq 0.05$). *Black circles* fail to be significant at the 25 % level ($p \leq 0.25$) and are added to the figure to illustrate areas without any significant trend. *Source* ECA&D

northern Scotland, respectively, during the 1990s. In northern England the average return period has also halved.

Cortesi et al. (2012) analysed the precipitation concentration index, which is a measure of the amount of precipitation on a day with precipitation. The north-western coast of Europe shows relatively low values for this index (i.e. evenly distributed precipitation) compared to more Mediterranean climate types. No clear spatial pattern was detected in the trends in the index.

Groisman et al. (2005) studied total precipitation and frequency of intense precipitation in several regions of the world, including Fennoscandia. They found a significant increase in the annual totals and in the frequency of very heavy annual and summer precipitation events, where 'very heavy' precipitation events are defined by counting the upper 0.3 % of daily rainfall events (relating to a daily event that occurs once every 3–5 years).

There is temporal variability in trends when studying precipitation indices of extremes. For example, the trend in precipitation fraction due to very wet days, related to the 95th percentile in daily sums (R95pTOT), shows a different picture when the trends are determined over the period 1951–1978 compared to 1979–2012 (Fig. 2.15). Along the coasts of south-eastern England and the Netherlands, there is no trend apparent for the period 1951–1978, while the period 1979–2012 has an increasing trend for several stations in these areas.

Care should be taken if the precipitation fraction exceeding the 95th percentile (R95pTOT) is determined over a climatological period of several decades, since extremes may have increased disproportionally and thus the shape of the distribution may have changed. For example, an index S95pTOT, using the Weibull shape parameter instead of an explicit estimate of the 95th percentile, can be used (Leander et al. 2014). Northern Europe shows a (significant) increase in R95pTOT, but this is far less pronounced for S95pTOT. Since R95pTOT cannot distinguish between a shift in the median of the probability distribution for precipitation and a change in only the tail of the distribution, trends are generally 'more negative' for S95pTOT, especially over southern Scandinavia, the Netherlands, Germany and the UK.

Zolina et al. (2009) introduced a new index for R95pTOT, making use of a gamma distribution for wet day precipitation amounts and the associated theoretical distribution of the fractional contribution of the wettest days to the seasonal or annual total. The trend results for their new index are similar to R95pTOT.

Another way of analysing changes in precipitation is by counting the number of wet days. An example of this is the index CWD (maximum number of consecutive wet days, here defined as the number of days with precipitation ≥1 mm). Trends in the station records for the period 1951–2012 are shown in Fig. 2.16, which indicates that most of the stations in the North Sea region show a slight increasing

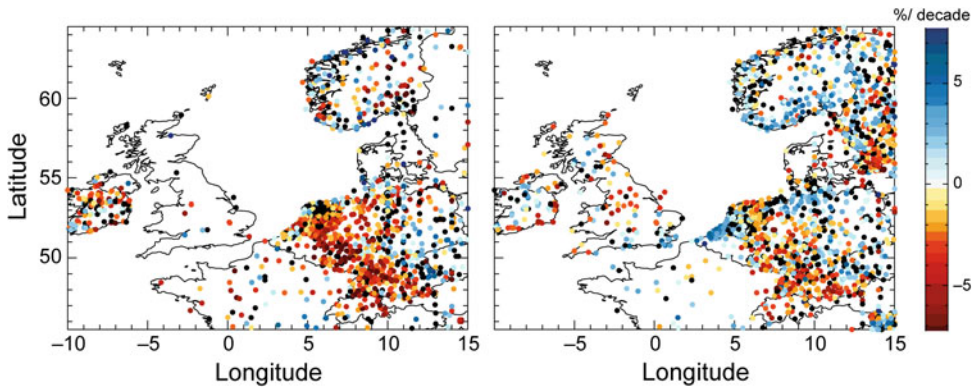

Fig. 2.15 Linear trends in the precipitation fraction due to very wet days (R95pTOT) in winter over the periods 1951–1978 (*left*) and 1979–2012 (*right*). *Blue circles* denote a trend towards wetter conditions, while *orange* and *red circles* denote a trend towards drier conditions, both significant at the 5 % level ($p \leq 0.05$). *Black circles* fail to be significant at the 25 % level ($p \leq 0.25$) and are added to the figure to illustrate areas without any significant trend. *Source* ECA&D

trend in the annual number of consecutive wet days. A similar map for trends in the maximum number of consecutive dry days (CDD) does not indicate a coherent change in the region. The majority of stations show trend values that do not meet even the 25 % significance level.

An example of interaction between North Sea waters and coastal climate was documented by Lenderink et al. (2009) for a month with extreme precipitation in the coastal region of the Netherlands (August 2006), where precipitation amounts were four times higher than the climatological average. Preceded by an extremely warm July (see Sect. 2.4) with very high sea surface temperatures in the North Sea at the end of July, favourable atmospheric flow conditions transported large amounts of moisture onto land, producing excessive rainfall in an area less than 50 km from the coastline. This phenomenon seems to be a robust finding since the positive trend in the difference between coastal and inland precipitation observed in the Netherlands is not sensitive to the period analysed.

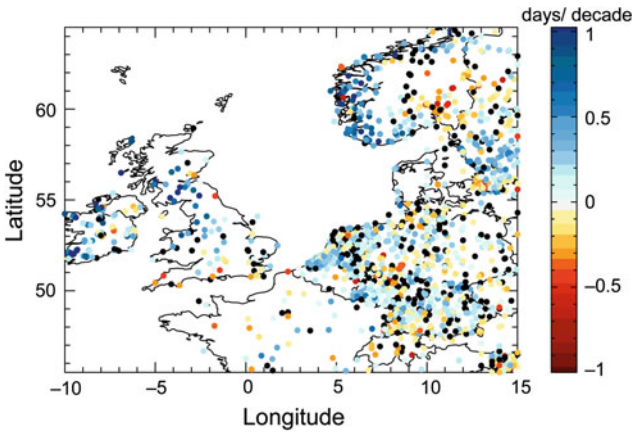

Fig. 2.16 Linear trend in annual maximum number of consecutive wet days (CWD) over the period 1951–2012. *Blue circles* denote a trend towards wetter conditions, while *orange* and *red circles* denote a trend towards drier conditions, both significant at the 5 % level ($p \leq 0.05$). *Black circles* fail to be significant at the 25 % level ($p \leq 0.25$) and are added to the figure to illustrate areas without any significant trend. *Source* ECA&D

2.5.2 Precipitation Over the North Sea

Only limited information is available for precipitation over oceans in general and the North Sea in particular. Almost no in situ measurements exist, which means it is necessary to rely on satellite observations using passive microwave detectors. HOAPS (Hamburg Ocean-Atmosphere Parameters and Fluxes) is one such dataset (Andersson et al. 2010, 2011). This covers the period 1988–2008 and is the only generally available satellite-based dataset for which fields of precipitation and evaporation over the oceans are consistently derived (Andersson et al. 2011). Over land, the dataset is gauge-based. Figure 2.17 shows the geographical distribution of annual average precipitation for the North Sea region (Fennig et al. 2012). Over most of the North Sea, the mean annual precipitation is between 600 and 800 mm, although values below 600 mm are also found off the east coast of England. Most coastal regions receive more than 800 mm, and in some mountainous regions (Scotland, Norway) more than 2000 mm are observed. While land stations in the south of the region have most rain in winter with a weak secondary summer maximum, further north and generally over the sea, there is only a maximum in winter, and May and June are the driest months.

Table 2.2 shows annual precipitation totals over the central North Sea region (54°–58°N, 1.5°–5.5°E) from the few available datasets.

There are considerable differences between the various estimates of precipitation, even in reasonably data-rich regions like the North Sea. There are also large differences

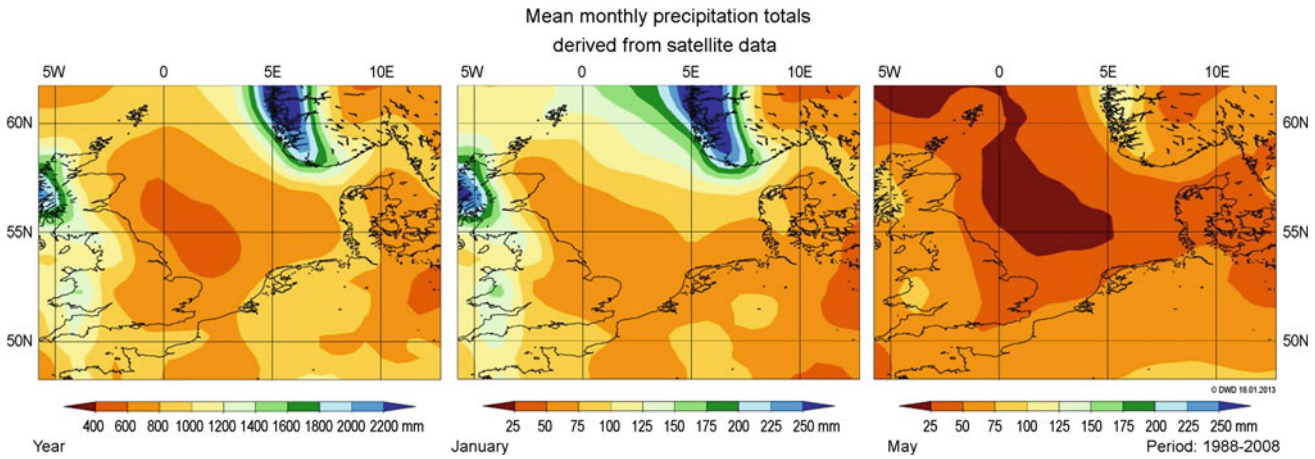

Fig. 2.17 Precipitation over the North Sea area. Ocean: HOAPS dataset (Fennig et al. 2012), land: gauge-based. Annual sum (*left*), monthly sum for January (*centre*), and monthly sum for May (*right*) for the period 1988–2008. All data in mm

Table 2.2 Estimates of annual average precipitation over the North Sea region from different reanalyses and satellite-based datasets

Dataset	1979–2001	1988–2008	Source
HOAPS	–	643	Andersson et al. (2010)
ERA-Interim	812	800	Simmons et al. (2010) and Berrisford et al. (2009)
ERA40	691		Uppala et al. (2005)
Coastdat2 (cDII.00)	853	861	Geyer (2014)
NCEP-CFSR	966	1000	Saha et al. (2010)
MERRA	754	772	Rienecker et al. (2011)

All units in mm

between periods, highlighting the problems in deriving trends in precipitation (Bengtsson et al. 2004). Precipitation in reanalyses depends on the moisture flux divergence, a rather weakly constrained quantity, which in turn does not depend on direct observations, but on the assimilation of satellite radiances (see e.g. Lorenz and Kunstmann 2012).

2.5.3 Summary

An assessment of temporal variability shows that precipitation over land and, but somewhat weaker, over sea is positively correlated with the NAO. Winters with strong positive NAO anomalies show distinct peaks in precipitation and amounts up to twice the average over the North Sea region (Andersson et al. 2010). On longer time scales, drought conditions over central Europe are also connected to the AMO (Atlantic Multidecadal Oscillation; Ionita et al. 2012a). Generally speaking, precipitation is more variable than temperature, and agreement between datasets is less. Nevertheless, there are indications of an increase in precipitation to the north of the North Sea region and a decrease to the south, in agreement with the projected north-eastward shift in the storm tracks. In many regions, there are also indications that extreme precipitation events have become more extreme and that return periods have decreased.

2.6 Radiative Properties

Meteorological observations aboard ships usually do not include measurements of sunshine duration and radiation. As a result there are few data available, and these are mainly from isolated field campaigns on research vessels. In contrast, cloud parameters are often observed routinely, although the quality of observations varies widely. The following discussion of clouds, solar radiation and sunshine duration therefore relies mainly on studies concerning a wider area, but these data should also be valid for the North Sea region.

2.6.1 Clouds

Clouds have a significant impact on the Earth's radiation budget. They affect incoming solar shortwave (SW) radiation (by reflecting this back to space) as well as outgoing thermal longwave (LW) radiation (by reducing its emission

to space). The difference between the actual radiative flux and that under clear sky conditions is referred to as cloud radiative forcing (CRF). The largest contribution to LW CRF is made by high clouds, whereas the largest contribution to SW CRF is from optically thick clouds due to their higher albedo compared to the clear sky surface albedo. Thus, variations in cloudiness are of great interest in relation to rising global temperatures. The Extended Edited Cloud Report Archive (EECRA; Warren et al. 1986, 1988, 2006) consists of quality controlled climatologies of total cloud cover and cloud type amounts over land and ocean, respectively, based on surface synoptic cloud observations.

Few analyses of changes in cloud cover exist, and even less for the North Sea region. A decrease has been observed in global high cloud cover over almost all land regions since 1971 and most ocean regions since 1952. Norris (2008) analysed global mean time series from gridded surface observations of low-, mid- and upper-level clouds as well as total cloud cover and satellite cloud observations over land and ocean based on EECRA, other surface synoptic cloud reports from land since 1971, the ship-based ICOADS which includes observations since 1952, and satellite observations available from July 1983 in the International Satellite Cloud Climatology Project (ISCCP). Norris (2008) found inconsistencies for the overlapping period of in situ and satellite data except for high clouds.

Over Europe, variability in total winter cloud cover is strongly connected to the NAO. Because the NAO was undergoing a positive trend during a study by Warren et al. (2006), there is a strong positive trend in total cloud cover over Norway at this time (Fig. 2.18). No clear trend is visible further south in the North Sea region (Thompson et al. 2000; Hense and Glowienka-Hense 2008).

Warren et al. (2006) also analysed cloud types observed at European land stations in relation to the NAO/AO signal in winter for the period 1971–1996. Not surprisingly, the strongest correlation was for nimbostratus (Fig. 2.19). Across the western parts of Europe correlations are negative, but high positive correlations exist in the northern part of the North Sea region from northern Scotland to Norway.

2.6.2 Solar Radiation

Time series of measured solar radiation data at various sites around the globe show decreasing irradiances on the order of 6–9 W m^{-2} (corresponding to a decline of 4–6 % over 30 years) after the mid-1950s ('global dimming'; Gilgen et al. 1998; Stanhill and Cohen 2001; Liepert and Tegen 2002) and mainly over land, and subsequent increases since the mid-1980s ('global brightening'; Wild et al. 2005; Norris and Wild 2007) which cannot be explained by variations in solar irradiance or cloudiness alone (Wild 2009), but are largely due to marked changes in the amount of anthropogenic aerosol particles after the Second World War (Stanhill and Cohen 2001; Liepert and Tegen 2002; Streets et al. 2006; Norris and Wild 2007). Since the 1980s, air-quality regulations have led to a decline in air pollution, as can be seen from time series of optical depth (Mishchenko et al. 2007; Ruckstuhl et al. 2008). More recent studies (e.g. Granier et al. 2011; Lee et al. 2013; Myhre et al. 2013; Shindell et al. 2013) corroborate these findings.

For Europe, Norris and Wild (2007) examined changes in SW downward radiation and total cloud cover to distinguish the effects of cloud variability from long-term aerosol influences in the period 1971–2002 (Fig. 2.20). Their 'cloud cover radiative effect' (CCRE), defined as the radiative effects of changes in cloud cover, is derived from daytime synoptic surface observations and ISCCP data, subtracted from the downward radiation obtained from the Global

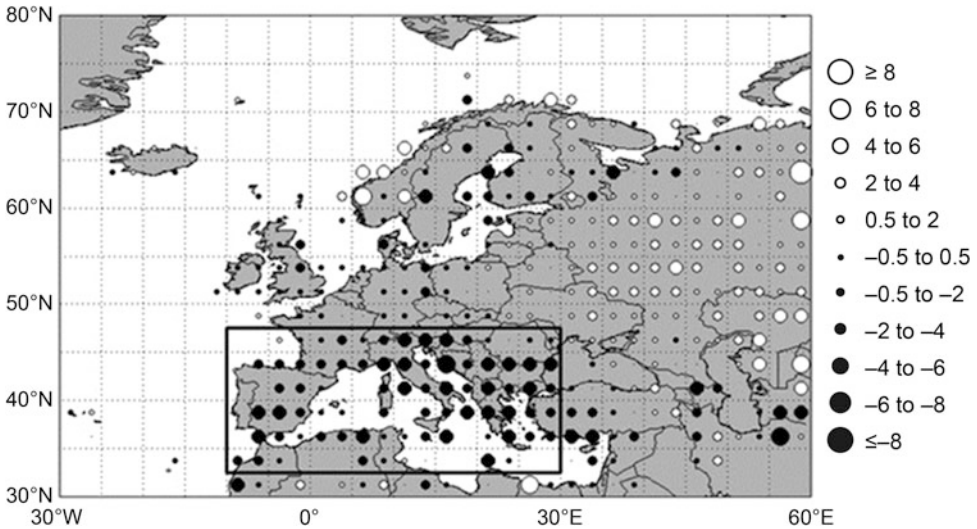

Fig. 2.18 Linear trends in total cloud cover in percent per decade for 2.5° × 2.5° boxes in Europe and North Africa in winter (DJF) for the period 1971–1996. The size of each *dot* indicates the magnitude of the trend (Warren et al. 2006)

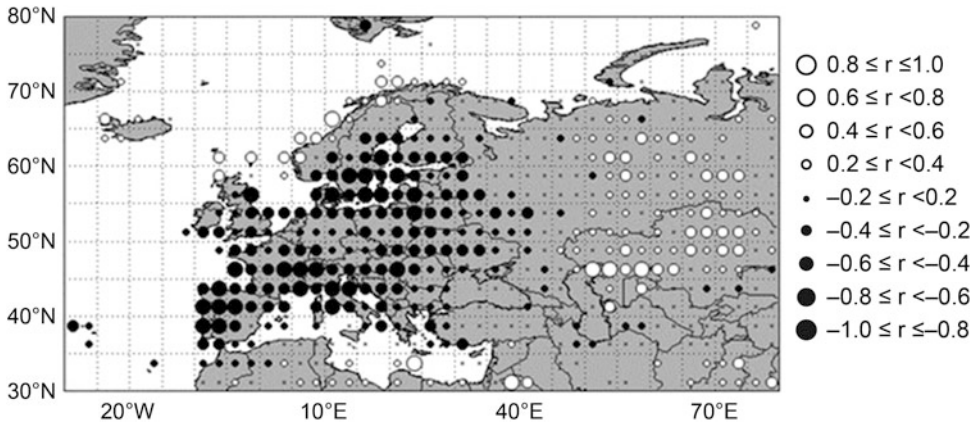

Fig. 2.19 Correlation of nimbostratus anomalies with the Arctic Oscillation index, for 2.5° × 2.5° boxes in Europe and North Africa in winter (DJF) for the period 1971–1996. The size of each *dot* indicates the magnitude of the correlation coefficient (Warren et al. 2006)

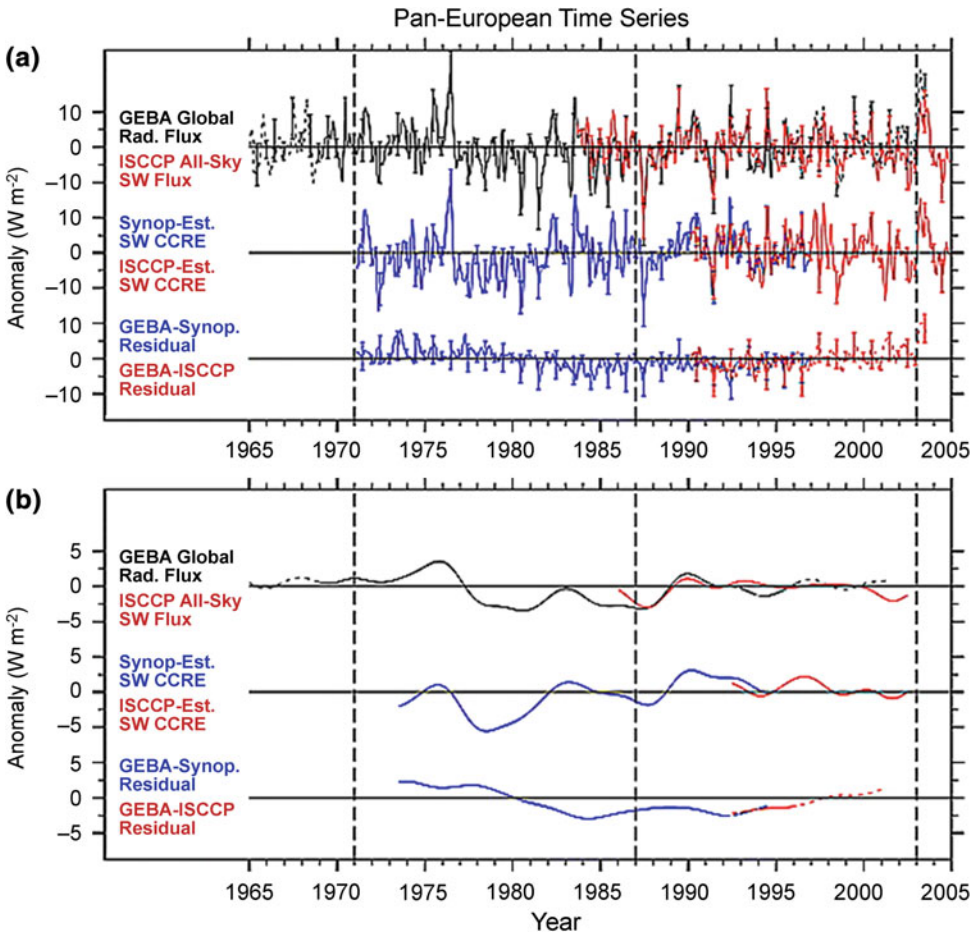

Fig. 2.20 Time series of monthly anomalies averaged over grid boxes covering most of Europe with **a** a 1-2-1 filter and **b** a 61-point 5-year Lanczos low-pass filter for GEBA global radiation flux (*upper, black*), ISCCP all-sky downward SW radiation flux (*upper, red*), SW cloud cover radiation effect (CCRE) estimated from synoptic reports of total cloud cover (*middle, blue*), SW CCRE estimated from ISCCP total cloud cover amount (*middle, red*), residual anomalies after removing synoptic-estimated SW CCRE from GEBA global radiation (*lower, blue*) and residual anomalies after removing ISCCP-estimated SW CCRE from GEBA global radiation (*lower, red*). *Dashed values* indicate where less than 75 % of the grid boxes contributed to the GEBA time series. *Small vertical bars* denote 95 % confidence intervals for June and December anomalies, and *vertical dashed lines* mark the start and end times for trend calculations (Norris and Wild 2007)

Energy Balance Archive (GEBA). The resulting time series comprises variations in clear-sky solar flux as well as radiative effects of changes in cloud albedo that are not linearly correlated to the cloud cover. They found a high correlation (r = 0.88) between global radiation anomalies and the estimated cloud cover radiative effect on monthly and sub-decadal timescales, but the time series of differences show dimming and brightening as well as low frequency trends with minima related to the volcanic eruptions of El Chichón (Mexico) and Pinatubo (Philippines). Decreasing trends for the period 1971–1986 and then increasing trends for 1987–2002 are found for coastal areas of the North Sea region (not shown), but these are mostly not statistically significant (Ruckstuhl et al. 2008, Ruckstuhl and Norris 2009).

Aerosol particles influence the radiation budget and hence air temperature in two ways. The direct aerosol radiative effect refers to clear-sky cases, when solar radiation is directly scattered (mainly by sulphate) or absorbed (mainly by black carbon), while the indirect aerosol effect enhances cloud albedo via an increase in the number of aerosol particles that act as condensation nuclei creating smaller droplets and prolonging cloud lifetime due to a decrease in droplet size and less precipitation loss.

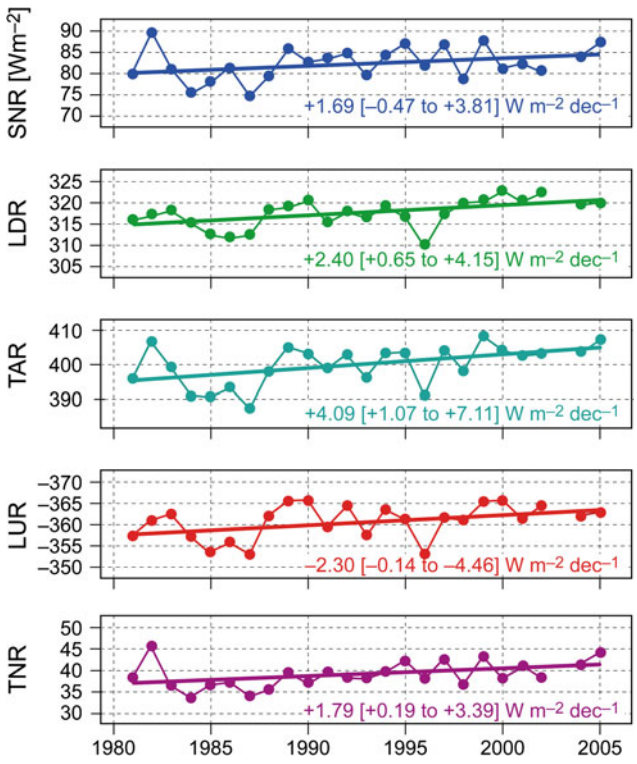

Fig. 2.21 Radiation budget and surface forcing. Annual mean values (W m^{-2}) for the individual components of the surface radiation budget for eight stations in northern Germany: SW net radiation (SNR), LW downward radiation (LDR), total absorbed radiation (TAR), LW upward radiation (LUR) and total net radiation (TNR) from 1981 to 2005 (missing 2003 data). Downward fluxes are positive and upward fluxes negative. Trends in W m^{-2} $decade^{-1}$ with the 95 % confidence interval in brackets. TNR, the balance between downward and upward fluxes at the surface representing the energy available for sensible and latent energy fluxes increases primarily due to the increase of water vapour in the atmosphere (Philipona et al. 2009)

For the period 1981–2005, Ruckstuhl et al. (2008) estimated the direct and indirect aerosol effects by determining the SW downward radiation for cloud-free and cloudy conditions from eight sites in northern Germany. Excluding the sunny year 2003, the net LW forcing under cloud-free skies is 0.84 W m^{-2} $decade^{-1}$ (range: 0.49–1.20), whereas the SW net forcing from changes in cloudiness is 0.56 W m^{-2} $decade^{-1}$ (range: −0.91 to 2.00), resulting in a total cloud forcing of 0.16 W m^{-2} $decade^{-1}$ (range: −0.26 to 0.57). Thus, the direct aerosol effect has a much larger impact on climate forcing than the indirect aerosol and other cloud effects.

Philipona et al. (2009) found an increase in LW downward radiation over Germany, based on observations for 1981–2005, due to rising temperature and humidity and to the increase in greenhouse gas concentration, but found no effect of changes in cloudiness (Fig. 2.21). The total net LW radiation (the difference between incoming and outgoing radiation at the surface) depends on temperature and absolute humidity, which itself is dependent on temperature.

For northern Germany, the LW forcing due to greenhouse gases including water vapour resulted in 0.95 W m^{-2} $decade^{-1}$ (range: 0.26–1.64), while the part due to water vapour feedback alone is 0.60 W m^{-2} $decade^{-1}$ (range: 0.16–1.04) (Philipona et al. 2009). Thus, the total SW forcing is three times larger than the LW forcing from rising atmospheric levels of anthropogenic greenhouse gases.

2.6.3 Sunshine Duration

Operational measurements of sunshine duration started at most weather stations in the 1930s or 1940s, mainly using the Campbell-Stokes heliograph. However, over recent decades, new electronic–optical equipment has increasingly been used, causing data quality issues and thus consistency problems within the time series of sunshine duration data (Augter 2013). As the existing sunshine duration database for the open sea is insufficient for climate analyses, the results presented in this chapter are based on coastal or island stations only. Sunshine duration depends on three factors: daylength (which is a function of latitude and season), amount of daytime clouds, and atmospheric opacity. Cloudiness and opacity are influenced by meteorological conditions and the latter also by aerosol concentration, which can be very different over land and sea. For Germany, Schönwiese and Janoschitz (2005) analysed changes in sunshine duration for the periods 1951–2000 and 1971–

2000 and found no obvious trends. It is not clear whether the increase in global radiation is related to an increase in sunshine duration.

2.6.4 Summary

From the few available datasets on radiative properties, it may be concluded that there are non-negligible trends together with potential uncertainties and land-sea inhomogeneities which make it difficult to assess these quantities in detail.

2.7 Summary and Open Questions

It is not obvious how atmospheric circulation has changed in the North Sea region over the last roughly 200 years. Further research is therefore necessary to understand climate change versus climate variability. One open research question is the extent to which circulation over the North Sea region is controlled by distant factors. In particular, whether there is a link between changes in the Arctic cryosphere and atmospheric circulation further south, including over the North Sea region. Overland and Wang (2010) highlighted a connection between the recent decrease in Arctic sea ice and cold winters in several areas of Europe. With the ongoing decline in sea ice in the Arctic, any such effect on circulation patterns would be important for climate in the North Sea region. Rahmstorf et al. (2015) proposed a proxy-based connection between the observed cooling in the North Atlantic south of Greenland and a weakening of the Atlantic Meridional Overturning Circulation (AMOC) partly due to increased melting of the Greenland Ice Sheet and subsequent freshening of the surface waters. Changes in the strength of the AMOC, however, are still debated and Zhang (2008) and more recently, Tett et al. (2014) have stated that its strength has actually increased.

Owing to large internal variability, it is unclear which part of the observed atmospheric changes is due to anthropogenic activities and which is internally forced. Slowly varying natural factors with an effect on European climate, such as the AMO (Petoukhov and Semenov 2010), may superimpose long-term trends and therefore be difficult to distinguish from the anthropogenic climate change signal.

There are signs of an increase in the number of deep cyclones (but not in the total number of cyclones). There are also indications that the persistence of circulation types has increased over the last century or so (Della-Marta et al. 2007). It is an open question whether this is also related to the decline in Arctic sea ice.

Another open question is whether there have been changes in extreme weather events. However, most studies rely on small datasets covering relatively short time periods, which makes it is difficult to draw statistically significant conclusions. As short time series and a lack of homogeneous data make it impossible to obtain reliable trend estimates, it is important to make available and homogenise the large number of data from past decades that have not yet been digitised. However, shown by the case of the erroneous pressure digitisations in the WASA dataset (see E-Supplement Sect. S2.3), it is essential for data to be thoroughly quality-checked. Experience from the WASA data suggests that this step requires human expertise and cannot be fully automated. On the other hand, further reanalyses, which may be considered a 'best-possible' time-space interpolator for observed data, can be useful as long as any bias that is potentially introduced through new instruments, station relocations etc. is properly addressed. The same is true for existing reanalyses, as it is unclear how homogeneous reanalyses can be that rely only on surface observations such as 20CR (Compo et al. 2011).

Temperature has increased in the North Sea region, and there is a clear signal in the annual number of frost days or summer days. While there is a clear winter and spring warming signal over the Baltic Sea region (Rutgersson et al. 2014), this is not as clear for the North Sea region. For precipitation, it is difficult to deduce long-term trends; however, there are indications of longer precipitation periods and 'more extreme' extreme events.

Other quantities, such as clouds, radiation or sunshine duration, are difficult to judge owing to a general lack of data.

References

Alexandersson H, Tuomenvirta H, Schmith T, Iden K (2000) Trends of storms in NW Europe derived from an updated pressure data set. Clim Res 14:71–73

Allan R, Tett S, Alexander L (2009) Fluctuations in autumn-winter severe storms over the British Isles: 1920 to present. Int J Climatol 29:357–371

Ambaum MHP, Hoskins BJ, Stephenson DB (2001) Arctic Oscillation or North Atlantic Oscillation? J Clim 14:3495–3507

Andersson A, Bakan S, Graßl H (2010) Satellite derived precipitation and freshwater flux variability and its dependence on the North Atlantic Oscillation. Tellus A 62:453–468
Andersson A, Klepp C, Bakan S, Graßl H, Schulz J (2011) Evaluation of HOAPS-3 ocean freshwater flux components. J Appl Meteor Climatol 50:379–398
Augter G (2013) Vergleich der Referenzmessungen des Deutschen Wetterdienstes mit automatisch gewonnenen Messwerten [Comparison of reference measurements of the German Weather Service with automatically obtained measurements]. Berichte des Deutschen Wetterdienstes 238
Barnes EA, Hartmann DL (2010) Dynamical feedbacks and the persistence of the NAO. J Atmos Sci 67:851–865
Barnston AG, Livezey RE (1987) Classification, seasonality and persistence of low frequency atmospheric circulation patterns. Mon Wea Rev 115:1083–1126
Barredo JI (2010) No upward trend in normalised windstorm losses in Europe: 1970–2008. Nat Hazard Earth Syst Sci 10:97–104
Barriopedro D, Garcìa-Herrera R, Lupo AR, Hernández E (2006) A climatology of northern hemisphere blocking. J Climate 19:1042–1063
Barriopedro D, Fischer EM, Luterbacher J, Trigo RM, Garcia-Herrera R (2011) The hot summer of 2010: Redrawing the temperature record map of Europe. Science 332:220–224
Baur F (1937) Einführung in die Großwetterforschung [Introduction to Grosswetter research; in German]. Verlag BG Teubner, Leipzig
Benedict JJ, Lee S, Feldstein SB (2004) Synoptic view of the North Atlantic Oscillation. J Atmos Sci 61:121–144
Bengtsson L, Hagemann S, Hodges KI (2004) Can climate trends be calculated from reanalysis data? J Geophys Res 109:D11111 doi:10.1029/2004JD004536
Berrisford P, Dee DK, Fuentes M, Kållberg P, Kobayashi S, Uppala S (2009). The ERA-Interim archive. ERA-40 Report Series No. 1. European Centre for Medium-Range Weather Forecasts, UK
Berry DI, Kent EC (2009) A new air-sea interaction gridded dataset from ICOADS with uncertainty estimates. Bull Am Met Soc 90:645–656
Berry DI, Kent EC (2011) Air-sea fluxes from ICOADS: The construction of a new gridded dataset with uncertainty estimates. Int J Climatol 31:987–1001
Berry DI, Kent EC, Taylor PK (2004) An analytical model of heating errors in marine air temperatures from ships. J Atmos Ocean Technol 21:1198–1215
Bett PE, Thornton HE, Clark RT (2013) European wind variability over 140 yr. Adv Sci Res 10:51–58
Blessing S, Fraedrich K, Junge M, Kunz T, Linkheit F (2005) Daily North Atlantic Oscillation (NAO) index: statistics and its stratospheric polar vortex dependence. Meteorol Z 14:763–769
Brönnimann S, Martius O, von Waldow H, Welker C, Luterbacher J, Compo G, Sardeshmukh PD, Usbeck T (2012) Extreme winds at northern mid-latitudes since 1871. Meteorol Z 21:13–27
Brönnimann S, Martius O, Franke J, Stickler A, Auchmann R (2013) Historical weather extremes in the "Twentieth Century Reanalysis". In: Brönnimann S, Martius O (eds) (2013) Weather Extremes During the Past 140 Years. Geographica Bernensia G89:7–17
Budikova D (2009) Role of Arctic sea ice in global atmospheric circulation: A review. Global Plan Change 68:149–163
Budikova D (2012) Northern Hemisphere climate variability: Character, forcing mechanisms, and significance of the North Atlantic/Arctic Oscillation. Geogr Compass 6:401–422
Carter DJ, Draper L (1988) Has the north-east Atlantic become rougher? Nature 332:494
Cassou C (2008) Intraseasonal interaction between the Madden-Julian Oscillation and the North Atlantic Oscillation. Nature 455:523–527
Cattiaux J, Vautard R, Yiou P (2009) Origins of the extremely warm European fall of 2006. Geophys Res Lett 36:L06713 doi:10.1029/2009GL037339
Cattiaux J, Vautard R, Cassou C, Yiou P, Masson-Delmotte V, Codron F (2010) Winter 2010 in Europe: A cold extreme in a warming climate. Geophys Res Lett 37:L20704 doi:10.1029/2010GL044613
Chang EK, Fu Y (2002) Interdecadal variations in Northern Hemisphere winter storm track intensity. J Climate 15:642–658
Cheng X, Wallace JM (1993) Cluster analysis of the Northern Hemisphere wintertime 500 hPa height field: Spatial patterns. J Atmos Sci 50:2674–2696
Chrysanthou A, van der Schrier G, van den Besselaar EJM, Klein Tank AMG, Brandsma T (2014) The effects of urbanization on the rise of the European temperature since 1960. Geophys Res Lett 41:7716–7722 doi:10.1002/2014GL061154
Ciavola P, Ferreira O, Haerens P, van Koningsveld M, Armaroli C, Lequeux Q (2011) Storm impacts along European coastlines. Part 1: The joint effort of the MICORE and ConHaz Projects. Environ Sci Policy 14:912–923
Clemmensen LB, Hansen KWT, Kroon A (2014) Storminess variation at Skagen, northern Denmark since AD 1860: Relations to climate change and implications for coastal dunes. Aeolian Res 15:101–112
Cohen J, Barlow M (2005) The NAO, the AO, and global warming: How closely related? J Climate 18:4498–4513
Compo GP, Whitaker JS, Sardeshmukh PD, Matsui N, Allan RJ, Yin, X, Gleason BE, Vose RS, Rutledge G, Bessemoulin P, Brönnimann S, Brunet M, Crouthamel RI, Grant AN, Groisman PY, Jones PD, Kruk M, Kruger AC, Marshall GJ, Maugeri M, Mok HY, Nordli Ø, Ross TF, Trigo RM, Wang XL, Woodruff SD, Worley SJ (2011) The twentieth century reanalysis project. Q J Roy Met Soc 137:1–28
Cortesi N, Gonzalez-Hidalgo JC, Brunetti M, Martin-Vide J (2012) Daily precipitation concentration across Europe 1971–2010. Nat Hazards Earth Syst Sci 12:2799–2810
Croci-Maspoli M, Schwierz C, Davies H (2007) Atmospheric blocking: Space-time links to the NAO and PNA. Clim Dyn 29:713–725
Cusack S (2012) A 101 year record of windstorms in the Netherlands. Clim Change 116:693–704
Dangendorf S, Müller-Navarra S, Jensen J, Schenk F, Wahl T, Weisse R (2014) North Sea storminess from a novel storm surge record since AD 1843. J Climate 27:3582–3595
de Kraker A (1999) A method to assess the impact of high tides, storms and storm surges as vital elements in climatic history - the case of stormy weather and dikes in the northern part of Flanders, 1488 to 1609. Clim Change 43:287–302
de Viron O, Dickey JO, Ghil M (2013) Global models of climate variability. Geophys Res Lett 40:1832–1837
Dee DP, Uppala SM, Simmons AJ, Berrisford P, Poli P, Kobayashi S, Andrae U, Balmaseda MA, Balsamo G, Bauer P, Bechtold P, Beljaars ACM, van de Berg L, Bidlot J, Bormann N, Delsol C, Dragani R, Fuentes M, Geer AJ, Haimberger L, Healy SB, Hersbach H, Hólm EV, Isaksen L, Kållberg P, Köhler M, Matricardi M, McNally AP, Monge-Sanz BM, Morcrette JJ, Park BK, Peubey C, de Rosnay,Tavolato C, Thépaut JN, Vitart F (2011) The ERA-Interim reanalysis: configuration and performance of the data assimilation system. Quart J Roy Met Soc 137:553–597
Della-Marta PM, Haylock MR, Luterbacher J, Wanner H (2007) Doubled length of western European summer heat waves since 1880. J Geophys Res 112:D15103 doi:10.1029/2007JD008510
Delworth TL, Knutson TR (2000) Simulation of early 20th century global warming. Science 287:2246–2250
Donat MG, Renggli D, Wild S, Alexander LV, Leckebusch GC, Ulbrich U (2011) Reanalysis suggests long-term upward trends in European storminess since 1871. Geophys Res Lett 38:L14703 doi:10.1029/2011GL047995
Donat MG, Alexander LV, Yang H, Durre I, Vose R, Dunn RJH, Willett KM, Aguilar E, Brunet M, Caesar J, Hewitson B, Jack C, Klein Tank AMG, Kruger AC, Marengo J, Peterson TC, Renom M,

Oria Rojas C, Rusticucci M, Salinger J, Elrayah AS, Sekele SS, Srivastava AK, Trewin B, Villarroel C, Vincent LA, Zhai P, Zhang X, Kitching S (2013) Updated analyses of temperature and precipitation extreme indices since the beginning of the twentieth century: The HadEX2 dataset. J Geophys Res 118:2098–2118

Esteves LS, Williams JJ, Brown JM (2011) Looking for evidence of climate change impacts in the eastern Irish Sea. Nat Hazards and Earth System Sci 11:1641–1656

Feldstein SB (2000) Teleconnection and ENSO: The timescale, power spectra, and climate noise properties. J Climate 13:4430–4440

Feldstein SB (2002) The recent trend and variance increase of the annular mode. J Climate 15:88–94

Fennig K, Andersson A, Bakan S, Klepp C, Schroeder M (2012) Hamburg Ocean Atmosphere Parameters and Fluxes from Satellite Data - HOAPS 3.2 - Monthly means / 6-hourly composites. Satellite Application Facility on Climate Monitoring. doi:10.5676/EUM_SAF_CM/HOAPS/V001

Feser F, Barcikowska M, Krueger O, Schenk F, Weisse R, Xia L (2015a) Storminess over the North Atlantic and Northwestern Europe – A Review. Q J Roy Met Soc. 141:350–382

Feser F, Barcikowska M, Haeseler S, Lefebvre C, Schubert-Frisius M, Stendel M, von Storch H, Zahn M (2015b) Hurricane Gonzalo and its extratropical transition to a strong European storm. In: Explaining Extreme Events of 2014 from a Climate Perspective. Bull Amer Met Soc 96:S51–S55

Fischer EM, Luterbacher J, Zorita E, Tett SFB, Casty C, Wanner H (2007) European climate response to tropical volcanic eruptions over the last half millennium. Geophys Res Lett 34:L05707 doi:10.1029/2006GL027992

Folland CK, Knight J, Linderholm HW, Fereday D, Ineson S, Hurrell JW (2009) The summer North Atlantic Oscillation: Past, present, and future. J Climate 22:1082–1103

Fowler H, Kilsby C (2003) A regional frequency analysis of United Kingdom extreme rainfall from 1961 to 2000. Int J Climatol 23:1313–1334

Franke R (2009) Die nordatlantischen Orkantiefs seit 1956. Naturwissenschaftliche Rundschau 62:349–356

Franzke C, Woollings T (2011) On the persistence and predictability properties of North Atlantic climate variability. J Climate 24:466–472

Franzke C, Lee S, Franzke SB (2004) Is the North Atlantic Oscillation a breaking wave? J Atmos Sci 61:145–160

Frydendahl K, Frich P, Hansen C (1992) Danish weather observations 1685–1715. Danish Met Inst Tech Rep 92-3

Furevik T, Nilsen JEØ (2005) Large-scale atmospheric circulation variability and its impacts on the Nordic Seas ocean climate - a review. In Drange H, Dokken T, Furevik T, Gerdes R, Berger W (eds.) The Nordic Seas: An Integrated Perspective. Geophys Mon Ser 158.

Geng Q, Sugi M (2001) Variability of the North Atlantic cyclone activity in winter analyzed from NCEP-NCAR reanalysis data. J Climate 14:3863–3873

Geyer B (2014) High-resolution atmospheric reconstruction for Europe 1948–2012: coastDat2. Earth Syst Sci Data 6:147–164

Gilgen H, Wild M, Ohmura A (1998) Means and trends of shortwave irradiance at the surface estimated from Global Energy Balance Archive data. J Climate 11:2042–2061

Gillett NP (2005) Climate modelling: Northern Hemisphere circulation. Nature 437:496

Gillett NP, Zwiers FW, Weaver AJ, Stott PA (2003) Detection of human influence on sea-level pressure. Nature 422:292–294

Gönnert G (2003) Sturmfluten und Windstau in der Deutschen Bucht, Charakter, Veränderungen und Maximalwerte im 20. Jahrhundert. Die Küste 67

Granier C, Bessagnet B, Bond T, d'Angiola A, van der Gon HD, Frost GJ, Heil A, Kaiser JW, Kinne S, Klimont Z, Kloster S, Lamarque J-F, Liousse C, Masui T, Meleux F, Mieville A, Ohara T, Raut J-C, Riahi K, Schultz MG, Smith SJ, Thompson A, van Aardenne J, van der Werf GR, van Vuuren DP (2011) Evolution of anthropogenic and biomass burning emissions of air pollutants at global and regional scales during the 1980–2010 period. Clim Change 109:163–190

Groisman P, Knight R, Easterling D, Karl T, Hegerl G, Razuvaev V (2005) Trends in intense precipitation in the climate record. J Climate 18:1326–1350

Gulev SK, Zolina O, Grigoriev S (2001) Extratropical cyclone variability in the Northern Hemisphere winter from the NCEP/NCAR reanalysis data. Clim Dyn 17:795–809

Häkkinen S, Rhines PB, Worthen DL (2011) Atmospheric blocking and Atlantic multidecadal ocean variability. Science 334:655–659

Hammond JM (1990). Storm in a teacup or winds of change? Weather 45:443–448

Hanna E, Cappelen J, Allan R, Jónsson T, LeBlancq F, Lillington T, Hickey K (2008) New insights into North European and North Atlantic surface pressure variability, storminess, and related climatic change since 1830. J Climate 21:6739–6766

Hannachi A (2007a): Pattern hunting in climate: a new method for trends in gridded climate data. Int J Climatol 27:1–15

Hannachi A (2007b) Tropospheric planetary wave dynamics and mixture modeling: Two preferred regimes and a regime shift. J Atmos Sci 64:3521–3541

Hannachi A (2008) A new set of orthogonal patterns in weather and climate: Optimally interpolated patterns. J Climate 21:6724–6738

Hannachi A (2010) On the origin of planetary-scale extratropical circulation regimes. J Atmos Sci 67:1382–1401

Hannachi A, Woollings T Fraedrich K (2012) The North Atlantic jet stream: a look at preferred positions, paths and transitions. Q J Roy Met Soc 138:862–877

Hansen, J, Ruedy R, Sato M, Lo K (2010) Global surface temperature change. Rev Geophys 48:RG4004 doi:10.1029/2010RG000345

Harnik N, Chang EK (2003) Storm track variations as seen in radiosonde observations and reanalysis data. J Climate 16:480–495

Harris I, Jones PD, Osborn TJ, Lister DH (2014) Updated high-resolution grids of monthly climatic observations - the CRU TS 3.10 dataset. Int J Climatol 34:623–642

Hartmann DL, Klein Tank AMG, Rusticucci M, Alexander LV, Brönnimann S, Charabi Y, Dentener FJ, Dlugokencky EJ, Easterling DR, Kaplan A, Soden BJ, Thorne PW, Wild M, Zhai PM (2013) Observations: atmosphere and surface. In: Climate Change 2013: The Physical Science Basis. Contribution of Working Group I to the Fifth Assessment Report of the Intergovernmental Panel on Climate Change. Stocker TF, Qin D, Plattner G-K, Tignor M, Allen SK, Boschung J, Nauels A, Xia Y, Bex V, Midgley PM (eds) Cambridge University Press

Haylock MR, Hofstra N, Klein Tank AMG, Klok EJ, Jones PD, New M (2008) A European daily high-resolution gridded dataset of surface temperature and precipitation for 1950–2006. J Geophys Res 113: D20119 doi:10.1029/2008JD10201

Held IM, Soden BJ (2006) Robust responses of the hydrological cycle to global warming. J Climate 19:5686–5699

Hense A, Glowienka-Hense R (2008) Auswirkungen der Nordatlantischen Oszillation. [Climate impact of the North Atlantic Oscillation; in German]. Promet 34:89–94

Hess P, Brezowsky H (1952) Katalog der Großwetterlagen Europas [Catalogue of European Grosswetterlagen; in German]. Ber Dt Wetterd in der US-Zone 33:39

Hess P, Brezowsky H (1977) Katalog der Großwetterlagen Europas 1881–1976 (3. verb. u. erg. Aufl.), Ber. Dt. Wetterd. 15(113)

Selbstverlag des Deutschen Wetterdienstes, Offenbach am Main, Germany
Hickey KR (2003) The storminess record from Armagh Observatory, Northern Ireland, 1796–1999. Weather 58:28–35
Hines KM, Bromwich DH, Marshall G J (2000) Artificial surface pressure trends in the NCEP–NCAR Reanalysis over the Southern Ocean and Antarctica. J Climate 13:3940–3952
Hoerling MP, Hurrell JW, Xu T (2001) Tropical origins for recent North Atlantic climate change. Science 292:90–92
Hogben N (1994) Increases in wave heights over the North Atlantic: A review of the evidence and some implications for the naval architect. Trans R Inst Naval Arch 5:93–101
Hossen MA, Akhter F (2015) Study of the wind speed, rainfall and storm surges for the Scheldt Estuary in Belgium. Int J Sci Tech Res 4:130–134
Hoy A, Sepp M, Matschullat J (2012) Atmospheric circulation variability in Europe and northern Asia (1901 to 2010). Theor Appl Climatol 113:105–126
Hurrell JW (1995) Decadal trends in the North Atlantic Oscillation, regional temperatures and precipitation. Science 269:676–679
Hurrell JW, Deser C (2009) North Atlantic climate variability: The role of the North Atlantic Oscillation. J Mar Sys 78:28–41
Hurrell JW, Kushnir Y, Ottersen G, Visbeck M (2003) An overview of the North Atlantic Oscillation. In: The North Atlantic Oscillation: Climatic significance and environmental impact. Geoph Monog Series 134:1–36
Ineson S, Scaife AA, Knight JR, Manners JC, Dunstone NJ, Gray LJ, Haigh JD (2011) Solar forcing of winter climate variability in the northern hemisphere. Nature Geosci 4:753–757
Ionita M, Lohmann G, Rimbu N, Chelcea S, Dima M (2012a) Interannual to decadal summer drought variability over Europe and its relationship to global sea surface temperature. Clim Dyn 38:363–377
Ionita M, Lohmann G, Rimbu N, Scholz P (2012b) Dominant modes of diurnal temperature range variability over Europe and their relationship with large-scale atmospheric circulation and sea surface temperature anomaly patterns. J Geophys Res 117:D15111, doi:10.1029/2011JD016669
Johannessen OM, Bengtsson L, Miles MW, Kuzmina SI, Semenov VA, Alekseev GV, Nagurnyi AP, Zakharov VF, Bobylev LP, Pettersson LH, Hasselmann K, Cattle HP (2004) Arctic climate change: Observed and modelled temperature and sea-ice variability. Tellus A 56:328–341
Jones PD, Moberg A (2003) Hemispheric and large-scale surface air temperature variations: An extensive revision and an update to 2001. J Climate 16:206–223
Jones PD, Jonsson T, Wheeler D (1997) Extension to the North Atlantic Oscillation using early instrumental pressure observations from Gibraltar and south-west Iceland. Int J Climatol 17:1433–1450
Jones, PD, Lister DH, Osborn TJ, Harpham C, Salmon M, Morice CP (2012) Hemispheric and large-scale land surface air temperature variations: An extensive revision and an update to 2010. J Geophys Res 117:D05127 doi:10.1029/2011JD017139
Joshi MM, Charlton AJ, Scaife AA (2006) On the influence of stratospheric water vapor changes on the tropospheric circulation. Geophys Res Lett 33:L09806. doi:10.1029/2006GL025983
Jung T, Vitart F, Ferranti L, Morcrette JJ (2011) Origin and predictability of the extreme negative NAO winter of 2009/10. Geophys Res Lett 38:L07701 doi:10.1029/2011GL046786
Kalnay E, Kanamitsu M, Kistler R, Collins W, Deaven D, Gandin L, Iredell M, Saha S, White G, Woollen J, Zhu Y, Leetmaa A, Reynolds R, Chelliah M, Ebisuzaki W, Higgins W, Janowiak J, Mo KC, Ropelewski C, Wang J, Jenne R, Joseph D (1996) The NCEP/NCAR 40-Year Reanalysis Project. Bull Am Met Soc 77:437–471
Keeley SPE, Sutton RT, Shaffrey, LC (2009) Does the North Atlantic Oscillation show unusual persistence on intraseasonal timescales? Geophys Res Lett 36:L22706. doi:10.1029/2009GL040367
Kent, EC, Woodruff SD, Berry DI (2007) Metadata from WMO Publication No. 47 and an Assessment of Voluntary Observing Ships Observation Heights in ICOADS. J Atmos Ocean Tech 24:214–234
Kent EC, Rayner NA, Berry DI, Saunby M, Moat BI, Kennedy JJ, Parker DE (2013) Global analysis of night marine air temperature and its uncertainty since 1880, the HadNMAT2 Dataset. J Geophys Res 118:1281–1298
Kistler R, Collins W, Saha S, White G, Woollen J, Kalnay E, Chelliah M, Ebisuzaki W, Kanamitsu M, Kousky V, van den Dool H, Jenne R, Fiorino M (2001) The NCEP-NCAR 50-Year Reanalysis: Monthly Means CD-ROM and Documentation. Bull Am Met Soc 82:247–267
Klein Tank AMG, Wijngaard JB, Können GP, Böhm R, Demarée G, Gocheva A, Mileta M, Pashiardis S, Hejkrlik L, Kern-Hansen C, Heino R, Bessemoulin P, Müller-Westermeier G, Tzanakou M, Szalai S, Pálsdóttir T, Fitzgerald D, Rubin S, Capaldo M, Maugeri M, Leitass A, Bukantis A, Aberfeld R, van Engelen AFV, Forland E, Mietus M, Coelho F, MaresC, Razuvaev V, Nieplova E, Cegnar T, Antonio López J, Dahlström B, Moberg A, Kirchhofer W, Ceylan A, Pachaliuk O., Alexander LV, Petrovic P (2002) Daily dataset of 20th-century surface air temperature and precipitation series for the European Climate Assessment. Int J Climatol 22:1441–1453
Knight JR, Folland CK, Scaife AA (2005a) Climate impacts of the Atlantic Multidecadal Oscillation. Geophys Res Lett 33:L17706. doi:10.1029/2006GL026242
Knight JR, Allan RJ, Folland CK, Vellinga M, Mann ME (2005b) A signature of persistent natural thermohaline circulation cycles in observed climate. Geophys Res Lett 32:L20708. doi:10.1029/2005GL024233
Kravtsov S, Robertson AW, Ghil M (2006) Multiple regimes and low‐frequency oscillations in the Northern Hemisphere's zonal-mean flow. J Atmos Sci 63:840–860
Krueger O, von Storch H (2011) Evaluation of an air pressure‐based proxy for storm activity. J Climate 24:2612–2619
Krueger O, von Storch H (2012) The informational value of pressure-based single-station proxies for storm activity. J Atmos Ocean Technol 29:569–580
Krueger O, Schenk F, Feser F, Weisse R (2013) Inconsistencies between long-term trends in storminess derived from the 20CR reanalysis and observations. J Climate 26:868–874
Kucharski F, Molteni F, Bracco A (2006) Decadal interactions between the western tropical Pacific and the North Atlantic Oscillation. Clim Dyn 26:79–91
Küttel M, Xoplaki E, Gallego D, Luterbacher J, García-Herrera R, Allan R, Barriendos M, Jones PD, Wheeler D, Wanner H (2009) The importance of ship log data: reconstructing North Atlantic, European and Mediterranean sea level pressure fields back to 1750. Clim Dyn 34:1115–1128
Lavers DA, Villarini G, Allan RP, Wood EF, Wade AJ (2012) The detection of atmospheric rivers in atmospheric reanalyses and their links to British winter floods and the large-scale climatic circulation. J Geophys Res 117:D20106. doi:10.1029/2012JD018027
Leander R, Buishand TA, Klein Tank AMG (2014) An alternative index for the contribution of precipitation on very wet days to the total precipitation. J Climate 27:1365–1378

Lee YH, Lamarque J-F, Flanner MG, Jiao C, Shindell DT, Berntsen T, Bisiaux MM, Cao J, Collins WJ, Curran M, Edwards R, Faluvegi G, Ghan S, Horowitz LW, McConnell JR, Ming J, Myhre G, Nagashima T, Naik V, Rumbold SDT, Skeie RB, Sudo K, Takemura T, Thevenon F, Xu B, Yoon J-H (2013) Evaluation of preindustrial to present-day black carbon and its albedo forcing from Atmospheric Chemistry and Climate Model Intercomparison Project (ACCMIP). Atmos Chem Phys 13:2607–2634

Lehmann A, Getzlaff K, Harlaß J (2011) Detailed assessment of climate variability in the Baltic Sea area for the period 1958 to 2009. Clim Res 46:185–196

Lenderink G, van Meijgaard E, Selten F (2009) Intense coastal rainfall in the Netherlands in response to high sea surface temperatures: analysis of the event of August 2006 from the perspective of a changing climate. Clim Dyn 32:19–33

Liepert B, Tegen I (2002) Multidecadal solar radiation trends in the United States and Germany and direct tropospheric aerosol forcing. J Geophys Res 107:L02806. doi:10.1029/2001JD000760

Lindenberg J, Mengelkamp HT, Rosenhagen G (2012) Representativity of near surface wind measurements from coastal stations at the German Bight. Meteorol Z 21:99–106

Lorenz E (1951) Seasonal and irregular variations of the Northern Hemisphere sea-level pressure profile. J. Meteor 8:52–59

Lorenz C, Kunstmann H (2012) The hydrological cycle in three state-of-the-art reanalyses: Intercomparison and performance analysis. J Hydromet 13:1397–1420

Luo D, Cha J, Feldstein SB (2012) Weather regime transitions and the interannual variability of the North Atlantic Oscillation. Part I: A likely connection. J Atmos Sci 69:2329–2346

Luterbacher J, Dietrich D, Xoplaki E, Grosjean M, Wanner H (2004) European seasonal and annual temperature variability, trends, and extremes since 1500. Science 303:1499–1503

Luterbacher J, Liniger, MA, Menzel A, Estrella N, Della-Marta PM, Pfister C, Rutishauser T, Xoplaki E (2007) Exceptional European warmth of autumn 2006 and winter 2007: Historical context, the underlying dynamics, and its phenological impacts. Geophys Res Lett 34:L12704. doi:10.1029/2007GL029951

Marshall AG, Scaife AA (2009) Impact of the QBO on surface winter climate. J Geophys Res 114:D18110. doi:10.1029/2009JD011737

Marshall J, Johnson H, Goodman J (2001) A study of the interaction of the North Atlantic Oscillation with the ocean circulation. J Climate 14:1399–1421

Matulla C, Schöner W, Alexandersson H, von Storch H, Wang X (2007) European storminess: late nineteenth century to present. Clim Dyn 31:125–130

McCabe GJ, Clark MP, Serreze MC (2001) Trends in Northern Hemisphere surface cyclone frequency and intensity. J Climate 14:2763–2768

Mishchenko MI, Geogdzhayev IV, Rossow WB, Cairns B, Carlson BE, Lacis AA, Liu L, Travis LD (2007) Long-term satellite record reveals likely recent aerosol trend. Science 315:1543

Moberg A, Jones PD, Lister D, Walther A, Brunet M, Jacobeit J, Alexander LV, Della-Marta PM, Luterbacher J, Yiou P, Chen D, Klein Tank AMG, Saladié O, Sigró J, Aguilar E, Alexandersson H, Almarza C,Auer I, Barriendos M, Begert M, Bergström H, Böhm R, Butler C. J. Caesar J, Drebs A, Founda D, Gerstengarbe F-W, Micela G, Tolasz R, Tuomenvirta H, Werner PC, Linderholm,H, Philipp A, Wanner H, Xoplaki E (2006) Indices for daily temperature and precipitation extremes in Europe analyzed for the period 1901–2000. J Geophys Res 111:2156–2202

Myhre G, Samset BH, Schulz M, Balkanski Y, Bauer S, Berntsen TK, Bian H, Bellouin N, Chin M, Diehl T, Easter RC, Feichter J, Ghan SJ, Hauglustaine D, Iversen T, Kinne S, Kirkevåg A, Lamarque J-F, Lin G, Liu X, Lund MT, Luo G, Ma X, van Noije T, Penner JE, Rasch PJ, Ruiz A, Seland Ø, Skeie RB, Stier P, Takemura T, Tsigaridis K, Wang P, Wang Z, Xu L, Yu H, Yu F, Yoon J-H, Zhang K, Zhang H, Zhou C (2013) Radiative forcing of the direct aerosol effect from AeroCom Phase II simulations. Atmos Chem Phys 13:1853–1877

Norris JR (2008) Observed interdecadal changes in cloudiness: real or spurious. In: Brönnimann S, Luterbacher J, Ewen T, Diaz HF, Stolarski RS, Neu U (eds) Climate Variability and Extremes During the Past 100 Years. Springer

Norris JR, Wild M (2007) Trends in aerosol radiative effects over Europe inferred from observed cloud cover, solar "dimming" and solar "brightening". J Geophys Res 112:D08214 doi:10.1029/2006JD007794

O'Gorman PA, Schneider T (2009) The physical basis for increases in precipitation extremes in simulations of 21st century climate change. Proc Natl Acad Sci USA 106:14773–14777

Overland JE, Wang M (2010) Large-scale atmospheric circulation changes are associated with the recent loss of Arctic sea ice. Tellus A 62:1–9

Pall P, Stone DA, Stott PA, Nozawa T, Hilberts AGJ, Lohmann D, Allen MR (2011) Anthropogenic greenhouse gas contribution to flood risk in England and Wales in autumn 2000. Nature 470:382–385

Peterson TC, Vose RS (1997) An overview of the global historical climatology network temperature data base. Bull Am Met Soc 78:2837–2849

Petoukhov V, Semenov VA (2010) A link between reduced Barents-Kara sea ice and cold winter extremes over northern continents. J Geophys Res 115:D21111 doi:10.1029/2009JD013568

Philipona R, Behrens K, Ruckstuhl C (2009) How declining aerosols and rising greenhouse gases forced rapid warming in Europe since the 1980s. Geophys Res Lett 36:L02806 doi:10.1029/2008GL036350

Pinto JG, Raible CC (2012) Past and recent changes in the North Atlantic oscillation. Clim Change 3:79–90

Portis DH, Walsh JE, El-Hamly M, Lamb PJ (2001) Seasonality of the North Atlantic Oscillation. J Climate 14:2069-2078

Rahmstorf S, Box JE, Feulner G, Mann ME, Robinson A, Rutherford S, Schaffernicht EJ (2015) Exceptional twentieth-century slowdown in Atlantic Ocean overturning circulation. Nature Clim Change 5:475–480

Raible C, Della-Marta PM, Schwierz C, Blender R (2008) Northern Hemisphere extratropical cyclones: a comparison of detection and tracking methods and different reanalyses. Mon Wea Rev 136:880–897

Rayner NA, Parker DE, Horton EB, Folland CK, Alexander LV, Rowell DP, Kent EC, Kaplan A (2003) Global analyses of sea surface temperature, sea ice, and night marine air temperature since the late nineteenth century. J Geophys Res 108:4407 doi:10.1029/2002JD002670

Rennert KJ, Wallace JM (2009) Cross-frequency coupling, skewness, and blocking in the Northern Hemisphere winter circulation. J Climate 22:5650–5666

Rienecker MR, Suarez MJ, Gelaro R, Todling R, Julio Bacmeister EL, Bosilovich MG, Schubert SD, Takacs L, Kim G-K, Bloom S, Chen J, Collins D, Conaty A, da Silva A, Gu W, Joiner J, Koster RD, Lucchesi R, Molod A, Owens T, Pawson S, Pegion P, Redder CR, Reichle R, Robertson FR, Ruddick AG, Sienkiewicz M, Woollen J (2011) MERRA: NASA's modern-era retrospective analysis for research and applications. J. Climate 24:3624–3648

Ripesi O, Ciciulla F, Maimone F, Pelino V (2012) The February 2010 Arctic Oscillation Index and its stratospheric connection. Q J Roy Met Soc 138:1961–1969

Rodwell MJ, Rowell DP, Folland CK (1999) Oceanic forcing of the wintertime North Atlantic Oscillation and European climate. Nature 398:320–323

Rosenhagen G, Schatzmann M, Schrön A (2011) Das Klima der Metropolregion auf Grundlage meteorologischer Messungen und Beobachtungen. In: v Storch H, Claussen M (eds) Klimabericht für die Metropolregion Hamburg

Ruckstuhl C, Norris JR (2009) How do aerosol histories affect solar "dimming" and "brightening" over Europe? IPCC-AR4 models versus observations. J Geophys Res 114:D00D04 doi:10.1029/2008JD011066

Ruckstuhl C, Philipona R, Behrens K, Coen MC, Dürr B, Heimo A, Mätzler C, Nyeki S, Ohmura A, Vuilleumier L, Weller M, Wehrli C, Zelenka A (2008) Aerosol and cloud effects on solar brightening and recent rapid warming. Geophys Res Lett 35:L12708 doi:10.1029/2008GL034228

Rutgersson A, Jaagus J, Schenk F, Stendel M (2014) Observed changes and variability of atmospheric parameters in the Baltic Sea region during the last 200 years. Clim Res 61:177–190

Saha S, Moorthi S, Pan H-L, Wu X, Wang J, Nadiga S, Tripp P, Kistler R, Woollen J, Behringer D, Liu H, Stokes D, Grumbine R, Gayno G, Wang J, Hou Y-T, Chuang H-Y, Juang H-MH, Sela J, Iredell M, Treadon R, Kleist D, van Delst P, Keyser D, Derber J, Ek M, Meng J, Wei H, Yang R, Lord S, van den Dool H, Kumar A, Wang W, Long C, Chelliah M, Xue Y, Huang B, Schemm J-K, Ebisuzaki W, Lin R, Xie P, Chen M, Zhou S, Higgins W, Zou C-Z, Liu Q, Chen Y, Han Y, Cucurull L, Reynolds RW, Rutledge G, Goldberg M (2010) The NCEP climate forecast system reanalysis. Bull Amer Meteor Soc 91:1015–1057

Scaife AA, Knight JR, Vallis G, Folland CK (2005) A stratospheric influence on the winter NAO and north Atlantic surface climate. Geophys Res Lett 32:L18715 doi:10.1029/2005GL023226

Scaife AA, Kucharski F, Folland CK, Kinter J, Brönnimann S, Fereday D, Fischer AM, Grainger S, Jin EK, Kang IS, Knight JR, Kusunoki S, Lau NC, Nath MJ, Nakaegawa T, Pegion P, Schubert S, Sporyshev P, Syktus J, Yoon JH, Zeng N, Zhou T (2009) The CLIVAR C20C project: selected twentieth century climate events. Clim Dyn 33:603–614

Schenk F (2015) The analog-method as statistical upscaling tool for meteorological field reconstructions over Northern Europe since 1850. Dissertation Univ Hamburg

Schenk F, Zorita E (2012) Reconstruction of high resolution atmospheric fields for Northern Europe using analog-upscaling. Clim Past 8:1681–1703

Schiesser HH, Pfister C, Bader J (1997) Winter storms in Switzerland north of the Alps 1864/1865–1993/1994. Theor Appl Climatol 58:1–19

Schmidt H, von Storch H (1993) German Bight storms analysed. Nature 365:791

Schmith T, Kaas E, Li TS (1998) Northeast Atlantic winter storminess 1875-1995 re-analysed. Clim Dyn 14:529–536

Schönwiese CD, Janoschitz R (2005) Klima-Trendatlas Deutschland, 1901-2000. Berichte Inst Atmosph Umwelt Univ Frankfurt 4

Selten FM, Branstator GW, Dijkstra HA, Kliphuis M (2004) Tropical origins for recent and future Northern Hemisphere climate change. Geophys Res Lett 31:L21205 doi:10.1029/2004GL020739

Semenov VA, Latif M, Jungclaus JH, Park W (2008) Is the observed NAO variability during the instrumental record unusual? Geophys Res Lett 35:L11701 doi:10.1029/2008GL033273

Shindell DT, Schmidt GA, Mann ME, Rind D, Waple A (2001) Solar forcing of regional climate change during the Maunder minimum. Science 294:2149–2152

Shindell DT, Lamarque J-F, Schulz M, Flanner M, Jiao C, Chin M, Young PJ, Lee Y.H, Rotstayn L, Mahowald N, Milly G, Faluvegi G, Balkanski Y, Collins WJ, Conley AJ, Dalsoren S, Easter R, Ghan S, Horowitz L, Liu X, Myhre G, Nagashima T, Naik V, Rumbold ST, Skeie R, Sudo K, Szopa S, Takemura T, Voulgarakis A, Yoon J-H, Lo F (2013) Radiative forcing in the ACCMIP historical and future climate simulations. Atmos Chem Phys 13:2939–2974

Sickmoeller M, Blender R, Fraedrich K (2000) Observed winter cyclone tracks in the Northern Hemisphere in re-analysed ECMWF data. Q J Roy Met Soc 126:591–620

Siegismund F, Schrum C (2001) Decadal changes in the wind forcing over the North Sea. Clim Res 18:39–45

Simmons AJ, Willett KM, Jones PD, Thorne PW, Dee DP (2010) Low-frequency variations in surface atmospheric humidity, temperature, and precipitation: Inferences from reanalyses and monthly gridded observational data sets. J Geophys Res 115:D01110 doi:10.1029/2009JD012442

Slonosky VC, Jones PD, Davies TD (2000) Variability of the surface atmospheric circulation over Europe, 1774–1995. Int J Climatol 20:1875–1897

Slonosky VC, Jones PD, Davies TD (2001) Atmospheric circulation and surface temperature in Europe from the 18th century to 1995. Int J Climatol 21:63–75

Smits A, Klein Tank AM, Können GP (2005) Trends in storminess over the Netherlands, 1962–2002. Int J Climatol 25:1331–1344

Spangehl T, Cubasch U, Raible CC, Schimanke S, Korper J, Hofer D (2010) Transient climate simulations from the Maunder minimum to present day: role of the stratosphere. J Geophys Res 115:D00110 doi:10.1029/2009JD012358

Stanhill G, Cohen S (2001) Global dimming: A review of the evidence for a widespread and significant reduction in global radiation with discussion of its probable causes and possible agricultural consequences. Agric for Meteorol 107:255–278

Stephenson DB, Pavan V, Bojariu R (2000) Is the North Atlantic Oscillation a random walk? Int J Climatol 20:1–18

Streets DG, Wu Y, Chin M (2006) Two-decadal aerosol trends as a likely explanation of the global dimming/brightening transition. Geophys Res Lett 33:L15806 doi:10.1029/2006GL026471

Strong C, Magnusdottir G (2011) Dependence of NAO variability on coupling with sea ice. Clim Dyn 36:1681–1689

Stucki P, Brönnimann S, Martius O, Welker C, Imhof M, von Wattenwyl N, Philipp N (2014) A catalogue of high-impact windstorms in Switzerland since 1859. Nat Haz Earth Syst Sci Discuss 2:3821–3862

Sutton RT, Hodson DLR (2005) Atlantic Ocean forcing of North American and European summer climate. Science 309:115–118

Sweeney J (2000) A three-century storm climatology for Dublin 1715–2000. Irish Geogr 33:1–14

Takahashi T, Sutherland SC, Sweeney C, Poisson A, Metzl N, Tilbrook B, Bates N, Wanninkhof R, Feely RA, Sabine C (2002) Global sea-air CO_2 flux based on climatological surface ocean pCO_2, and seasonal biological and temperature effects. Deep Sea Res II 49:1601–1622

Tett SFB, Sherwin TJ, Shravat A, Browne O (2014) How much has the North Atlantic Ocean overturning circulation changed in the last 50 years? J Climate 27:6325–6342

Thompson DWJ, Wallace JM (1998) The Arctic oscillation signature in the wintertime geopotential height and temperature fields. Geophys Res Lett 25:1297–1300

Thompson DWJ, Wallace JM, Hegerl GC (2000) Annual modes in the extratropical circulation: Part II: Trends. J Climate 13:1018–1036

Trigo IF (2006) Climatology and interannual variability of storm-tracks in the Euro-Atlantic sector: a comparison between ERA-40 and NCEP/NCAR reanalyses. Clim Dyn 26:127–143

Trouet V, Panayotov MP, Ivanova A, Frank D (2012) A pan-European summer teleconnection mode recorded by a new temperature

reconstruction from the northeastern Mediterranean (ad 1768–2008). The Holocene 22:887–898
Tyrlis E, Hoskins BJ (2008) Aspects of a Northern Hemisphere atmospheric blocking climatology. J Atmos Sci 65:1638–1652
Ulbrich U, Leckebusch GC, Pinto JG (2009) Extra-tropical cyclones in the present and future climate: a review. Theor Appl Climatol 96:117–131
Uppala SM, Kållberg PW, Simmons AJ, Andrae U, Da Costa Bechtold V, Fiorino M, Gibson JK, Haseler J, Hernandez A, Kelly GA, Li X, Onogi K, Saarinen S, Sokka N, Allan RP, Andersson E, Arpe K, Beljaars ACM, Van De Berg L, Bidlot J, Bormann N, Caires S, Chevallier F, Dethof A, Dragosavac M, Fisher M, Fuentes M, Hagemann S, Hólm E, Hoskins BJ, Isaksen L, Janssen PAEM, Jenne R, McNally AP, Mahfouf J-F, Morcrette J-J, Rayner NA, Saunders RW, Simon P, Sterl A, KE Trenberth, Untch A, Vasiljevic D, Viterbo P, Woollen J (2005) The ERA-40 re-analysis. Q J ROY METEOR SOC 131, Issue 612, 2961–3012. J (2005) The ERA-40 re-analysis. Q J Roy Met Soc 131:2961–3012
van den Besselaar EJM, Haylock MR, Klein Tank AMG, van der Schrier G (2011) A European daily high-resolution observational gridded data set of sea level pressure. J Geophys Res 116:D11110 doi:10.1029/2010JD015468
van den Besselaar EJM, Klein Tank AMG, Buishand TA (2013) Trends in European precipitation extremes over 1951–2010. Int J Climatol 33:2682–2689
van der Schrier G, van den Besselaar, EJM, Klein Tank AMG,Verver G (2013) Monitoring European averaged temperature based on the E-OBS gridded dataset. J Geophys Res 118:5120–5135
van Oldenborgh GJ, Drijfhout SS, van Ulden A, Haarsma R, Sterl A, Severijns C, Hazeleger W, Dijkstra H (2009) Western Europe is warming much faster than expected. Clim Past 5:1–12
Vautard RJ, Yiou P, Thépaut J-N, Ciais P (2010) Northern Hemisphere atmospheric stilling partly attributed to an increase in surface roughness. Nat Geosci 3:756–761
von Storch H, Reichardt H (1997) A scenario of storm surge statistics for the German Bight at the expected time of doubled atmospheric carbon dioxide concentration. J Climate 10:2653–2662
von Storch H, Zwiers FW (1999) Statistical analysis in climate research. Cambridge University Press
von Storch H, Feser F, Haeseler S, Lefebvre C, Stendel M (2014) A violent mid-latitude storm in Northern Germany and Denmark, 28 October 2013. Special Supplement to the Bull Am Met Soc 95:76–78
Wallace JM, Gutzler DS (1981) Teleconnections in the geopotential height field during the Northern Hemisphere winter. Mon Wea Rev 109:784–812
Wang XL, Swail VR, Zwiers FW (2006) Climatology and changes of extratropical cyclone activity: comparison of ERA40 with NCEP-NCAR reanalysis for 1958-2001. J Climate 19:3145–3166
Wang XL, Zwiers F, Swail V, Feng Y (2009a) Trends and variability of storminess in the Northeast Atlantic region, 1874–2007. Clim Dyn 33:1179–1195
Wang XL, Swail V, Zwiers F, Zhang X, Feng Y (2009b) Detection of external influence on trends of atmospheric storminess and northern oceans wave heights. Clim Dyn 32:189–203
Wang XL, Wan H, Zwiers FW, Swail VR, Compo GP, Allan RJ, Vose RS, Jourdain S, Yin X (2011) Trends and low-frequency variability of storminess over western Europe, 1878–2007. Clim Dyn 37:2355–2371
Wang XL, Feng Y, Compo GP, Zwiers FW, Allan RJ, Swail VR, Sardeshmukh PD (2014) Is the storminess in the Twentieth Century Reanalysis really inconsistent with observations? A reply to the comment by Krueger at al. (2013b). Clim Dyn 42:1113–1125
Wanner H, Brönnimann S, Casty C, Gyalistras D, Luterbacher J, Schmutz C, Stephenson DB, Xoplaki E (2001) North Atlantic Oscillation - concepts and studies. Surv Geophys 22:321–381
Warren SG, Hahn CJ, London J, Chervin RM, Jenne RL (1986) Global distribution of total cloud cover and cloud type amounts over land. NCAR Tech. Note TN-273 + STR
Warren SG, Hahn CJ, London J, Chervin RM, Jenne RL (1988) Global distribution of total cloud cover and cloud type amounts over the ocean. NCAR Tech. Note TN-317 + STR
Warren SG, Eastman RM, Hahn CJ (2006) A survey of changes in cloud cover and cloud types over land from surface observations, 1971-96. J Climate 20:717–738
WASA Group (1998) Changing waves and storms in the Northeast Atlantic? Bull Am Met Soc 79:741–760
Weisse R, Plüß A (2006) Storm-related sea level variations along the North Sea coast as simulated by a high-resolution model 1958–2002. Ocean Dyn 56:16–25
Weisse R, von Storch H, Feser F (2005) Northeast Atlantic and North Sea storminess as simulated by a regional climate model during 1958–2001 and comparison with observations. J Climate 18:465–479
Wheeler D, Garcia-Herrera R, Wilkinson CW, Ward C (2009) Atmospheric circulation and storminess derived from Royal Navy logbooks: 1685 to 1750. Clim Change 110:257–280
Wild M (2009) Global dimming and brightening: A review. J Geophys Res 114:D00D16 doi:10.1029/2008JD011470
Wild M, Gilgen H, Roesch A, Ohmura A, Long CN, Dutton EG, Forgan B, Kallis A, Russak V, Tsvetkov A (2005) From dimming to brightening: Decadal changes in solar radiation at Earth's surface. Science 308:847–850
WMO (2010) WMO Guide to Meteorological Instruments and Methods of Observation, World Meteorological Organisation Publication No. 8, WMO, Geneva
Woodruff SD, Worley SJ, Lubker SJ, Ji Z, Freeman JE, Berry DI, Brohan P, Kent EC, Reynolds RW, Smith SR, Wilkinson C (2011) ICOADS Release 2.5 and Data Characteristics. Int J Climatol 31:951–967
Woodworth PL, Blackman DL (2002) Changes in extreme high waters at Liverpool since 1768. Int J Climatol 22:697–714
Woollings TJ, Blackburn M (2012) The North Atlantic jet stream under climate change and its relation to the NAO and EA patterns. J Climate 25:886–902
Woollings TJ, Hoskins BJ, Blackburn M, Berrisford P (2008) A New Rossby wave-breaking interpretation of the North Atlantic oscillation. J Atmos Sci 65:609–626
Woollings TJ, Hannachi A, Hoskins B, Turner A (2010) A regime view of the North Atlantic Oscillation and its response anthropogenic forcing. J Climate 23:1291–1307
Xia L, Zahn M, Hodges KI, Feser F (2012) A comparison of two identification and tracking methods for polar lows. Tellus A 64:17196
Zhang R (2008) Coherent surface-subsurface fingerprint of the Atlantic meridional overturning circulation. Geophys Res Lett 35:L20705 doi:10.1029/2008GL035463
Zolina O, Simmer C, Belyaev K, Kapala A, Gulev S (2009) Improving estimates of heavy and extreme precipitation using daily records from European rain gauges. J Hydromet 10:701–716

Recent Change—North Sea

3

John Huthnance, Ralf Weisse, Thomas Wahl, Helmuth Thomas, Julie Pietrzak, Alejandro Jose Souza, Sytze van Heteren, Natalija Schmelzer, Justus van Beusekom, Franciscus Colijn, Ivan Haigh, Solfrid Hjøllo, Jürgen Holfort, Elizabeth C. Kent, Wilfried Kühn, Peter Loewe, Ina Lorkowski, Kjell Arne Mork, Johannes Pätsch, Markus Quante, Lesley Salt, John Siddorn, Tim Smyth, Andreas Sterl and Philip Woodworth

Electronic supplementary material Supplementary material is available in the online version of this chapter at 10.1007/978-3-319-39745-0_3.

J. Huthnance (✉) · A.J. Souza · P. Woodworth
National Oceanography Centre, Liverpool, UK
e-mail: jmh@noc.ac.uk

A.J. Souza
e-mail: ajso@noc.ac.uk

P. Woodworth
e-mail: plw@noc.ac.uk

R. Weisse (✉) · J. van Beusekom · F. Colijn · M. Quante
Institute of Coastal Research, Helmholtz-Zentrum Geesthacht, Geesthacht, Germany
e-mail: ralf.weisse@hzg.de

J. van Beusekom
e-mail: Justus.Beusekom@hzg.de

F. Colijn
e-mail: franciscus.colijn@hzg.de

M. Quante
e-mail: markus.quante@hzg.de

T. Wahl
College of Marine Science, University of South Florida, St. Petersburg, USA

T. Wahl
University of Southampton, Southampton, UK
e-mail: t.wahl@soton.ac.uk

H. Thomas
Department of Oceanography, Dalhousie University, Halifax, Canada
e-mail: helmuth.thomas@posteo.org

J. Pietrzak
Environmental Fluid Mechanics Section, Delft University of Technology, Delft, The Netherlands
e-mail: J.D.Pietrzak@tudelft.nl

S. van Heteren
Department of Geomodeling, TNO-Geological Survey of the Netherlands, Utrecht, The Netherlands
e-mail: sytze.vanheteren@tno.nl

N. Schmelzer · J. Holfort
Federal Maritime and Hydrographic Agency (BSH), Rostock, Germany
e-mail: natalija.schmelzer@bsh.de

J. Holfort
e-mail: juergen.holfort@bsh.de

I. Haigh
Ocean and Earth Science, University of Southampton, Southampton, UK
e-mail: I.D.Haigh@soton.ac.uk

S. Hjøllo · K.A. Mork
Institute of Marine Research (IMR), Bergen, Norway
e-mail: solfrid.hjollo@imr.no

K.A. Mork
e-mail: kjell.arne.mork@imr.no

E.C. Kent
National Oceanography Centre, Southampton, UK
e-mail: eck@noc.ac.uk

W. Kühn · J. Pätsch
Institute of Oceanography, CEN, University of Hamburg, Hamburg, Germany
e-mail: wilfried.kuehn@uni-hamburg.de

J. Pätsch
e-mail: johannes.paetsch@uni-hamburg.de

P. Loewe · I. Lorkowski
Federal Maritime and Hydrographic Agency (BSH), Hamburg, Germany
e-mail: peter.loewe@bsh.de

I. Lorkowski
e-mail: ina.lorkowski@bsh.de

L. Salt
Royal Netherlands Institute for Sea Research, Texel, The Netherlands
e-mail: lesleyannesalt@gmail.com

M. Quante and F. Colijn (eds.), *North Sea Region Climate Change Assessment*, Regional Climate Studies, DOI 10.1007/978-3-319-39745-0_3

Abstract

This chapter discusses past and ongoing change in the following physical variables within the North Sea: temperature, salinity and stratification; currents and circulation; mean sea level; and extreme sea levels. Also considered are carbon dioxide; pH and nutrients; oxygen; suspended particulate matter and turbidity; coastal erosion, sedimentation and morphology; and sea ice. The distinctive character of the Wadden Sea is addressed, with a particular focus on nutrients and sediments. This chapter covers the past 200 years and focuses on the historical development of evidence (measurements, process understanding and models), the form, duration and accuracy of the evidence available, and what the evidence shows in terms of the state and trends in the respective variables. Much work has focused on detecting long-term change in the North Sea region, either from measurements or with models. Attempts to attribute such changes to, for example, anthropogenic forcing are still missing for the North Sea. Studies are urgently needed to assess consistency between observed changes and current expectations, in order to increase the level of confidence in projections of expected future conditions.

3.1 Introduction

John Huthnance, Ralf Weisse

Physical variables, most obviously sea temperature, relate closely to climate change and strongly affect other properties and life in the sea. This chapter discusses past and ongoing change in the following physical variables within the North Sea: temperature, salinity and stratification (Sect. 3.2), currents and circulation (Sect. 3.3), mean sea level (Sect. 3.4) and extreme sea levels, i.e. contributions from wind-generated waves and storm surges (Sect. 3.5). Also considered are carbon dioxide (CO_2), pH, and nutrients (Sect. 3.6), oxygen (Sect. 3.7), suspended particulate matter and turbidity (Sect. 3.8), coastal erosion, sedimentation and morphology (Sect. 3.9) and sea ice (Sect. 3.10). The distinctive character of the Wadden Sea is addressed in Sect. 3.11, with a particular focus on sediments and nutrients. The chapter covers the past 200 years. Chapter 1 described the North Sea context and physical process understanding, so the focus of the present chapter is on the historical development of evidence (measurements, process understanding and models), the form, duration and accuracy of the evidence available (further detailed in Electronic (E-) Supplement S3) and what the evidence shows in terms of the state and trends in the respective variables.

J. Siddorn
Met Office, Exeter, UK
e-mail: john.siddorn@metoffice.gov.uk

T. Smyth
Plymouth Marine Laboratory, Plymouth, UK
e-mail: tjsm@pml.ac.uk

A. Sterl
Royal Netherlands Meteorological Institute (KNMI), De Bilt, The Netherlands
e-mail: sterl@knmi.nl

3.2 Temperature, Salinity and Stratification

John Huthnance, Elizabeth C. Kent, Tim Smyth, Kjell Arne Mork, Solfrid Hjøllo, Peter Loewe

3.2.1 Historical Perspective

Observations of sea-surface temperature (SST) have been made in the North Sea since 1823, but were sparse initially. The typical number of observations per month (from ships, and moored and drifting buoys) increased from a few hundred in the 19th century to more than 10,000 in recent decades, despite the Voluntary Observing Ship (VOS) fleet declining from a peak of about 7700 ships worldwide in 1984/85 to about 4000 in 2009 (www.vos.noaa.gov/vos_scheme.shtml). Early SST observations used buckets (Kent et al. 2010); adjustments of up to ~0.3 °C in the annual mean, and 0.6 °C in winter, may be needed for these early data owing to sample heat loss or gain (Folland and Parker 1995; Smith and Reynolds 2002; Kennedy et al. 2011a, b). The adjustments depend on large-scale forcing and assumptions about measurement methods—local variations add uncertainty. Cooling water intake temperatures have been measured on ships since the 1920s but data quality is variable, sometimes poor (Kent et al. 1993). Temperature sensors on ships' hulls became more numerous in recent decades (Kent et al. 2010). About 70 % of in situ observations in 2006 came from moored and drifting buoys

(Kennedy et al. 2011b). Other modern shipboard methods include radiation thermometers, expendable bathythermographs (XBTs) and towed thermistors (Woodruff et al. 2011). Satellite estimates of SST are regularly available using Advanced Very High Resolution Radiometers (AVHRR; from 1981) and passive microwave radiometers (with little cloud attenuation; from 1997).

Below the sea surface, temperature was measured by reversing (mercury) thermometers until the 1960s. Since then, electronic instruments lowered from ships (conductivity-temperature-depth profilers; CTDs) enable near-continuous measurements. Since about 2005, multi-decadal model runs have become increasingly available and now provide useful information on temperature distribution to complement the observational evidence (see E-Supplement Sect. S3.1).

Early salinity estimates used titration-based chemical analysis of recovered water samples (from buckets and water intakes) and from lowered sample bottles. Titration estimates usually depended on assuming a constant relation between chlorinity and total dissolved salts (a subject of discussion since 1900), with typical error O(0.01 ‰). Since the 1960s–1970s lowered CTD conductivity cells enable near-continuous measurements, calibrated by comparing the conductivity of water samples against standardised sea water; typical error O(0.001 ‰). Consistent definition of salinity has continued to be a research topic (Pawlowicz et al. 2012).

Thermistors and conductivity cells as on CTDs now record temperature and salinity of (near-surface) intake water on ships. Since the late 1990s, CTDs on profiling 'Argo' floats have greatly increased available temperature and salinity data for the upper 2000 m of the open ocean (www.argo.ucsd.edu). Although not available for the North Sea, these data greatly improve estimates of open-ocean temperature and salinity and thereby North Sea model estimates by better specifying open-ocean boundary conditions.

The history of stratification estimates, based on profiles of temperature and salinity (or at least near-surface and near-bottom values), corresponds with that of subsurface temperature and salinity.

Detail on time-series evidence for coastal and offshore temperature and salinity variations is given in E-Supplement S3.1 and S3.2.

3.2.2 Temperature Variability and Trends

3.2.2.1 Northeast Atlantic

Most water entering the North Sea comes from the adjacent North Atlantic via Rockall Trough and around Scotland. The North Atlantic has had relatively cool periods (1900–1925, 1970–1990) and warm periods (1930–1960, since 1990; Holliday et al. 2011; Dye et al. 2013a; Ivchenko et al. 2010 using 1999–2008 Argo float data). Adjacent to the north-west European shelf, however, different Atlantic water sources make varying contributions (Holliday 2003). For Rockall Trough surface waters, the period 1948–1965 was about 0.8 °C warmer on average than the period 1876–1915 (Ellett and Martin 1973). Subsequently, temperatures of upper water (0–800 m) in Rockall Trough and Atlantic water on the West Shetland slope (Fig. 3.1) oscillated with little trend until around 1994. Temperatures then rose,

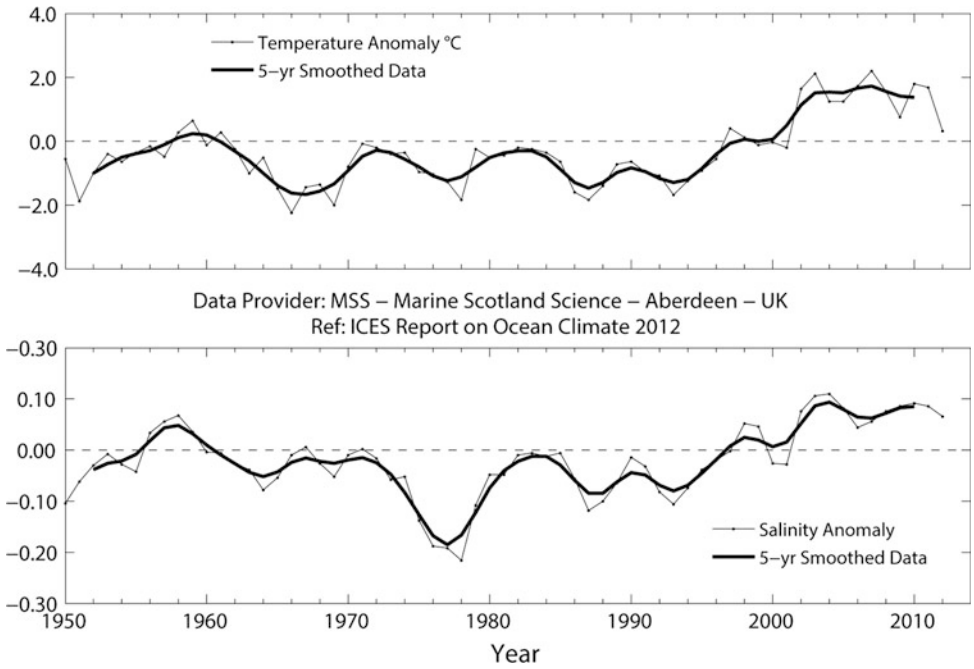

Fig. 3.1 Atlantic Water in the Faroe–Shetland Channel slope current. Temperature (*upper*) and salinity (*lower*) anomalies relative to the 1981–2010 average (Beszczynska-Möller and Dye 2013)

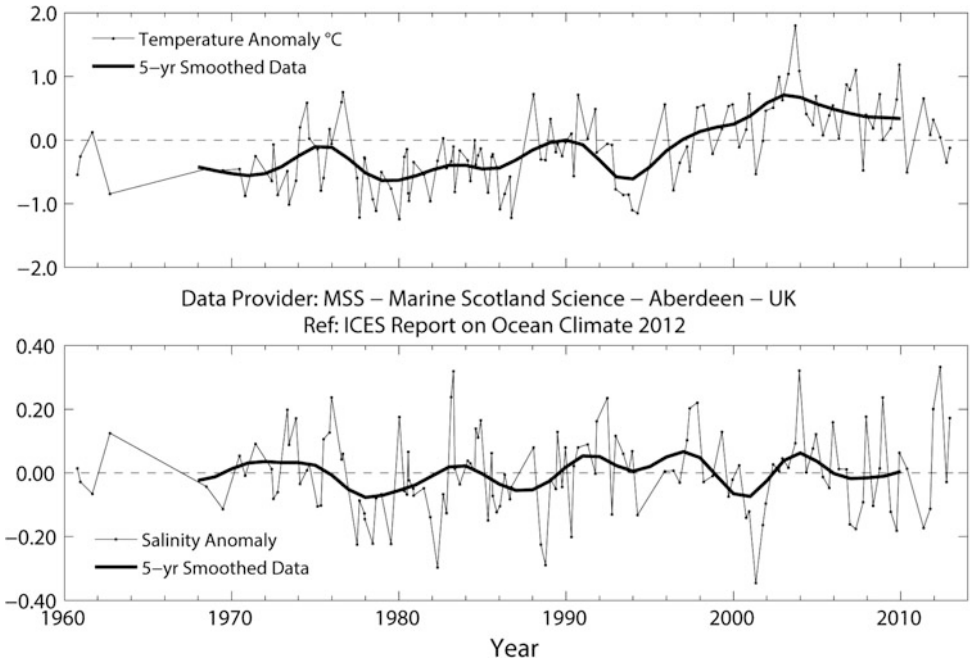

Fig. 3.2 Fair Isle Current entering the northern North Sea from the west and north of Scotland. Annual upper water temperature (*upper*) and salinity (*lower*) anomalies relative to the 1981–2010 average (Beszczynska-Möller and Dye 2013)

peaked in 2006, and subsequently cooled to early 2000s values (Berx et al. 2013; Beszczynska-Möller and Dye 2013; Holliday and Cunningham 2013).

West and north of Britain, the HadISST data set shows an SST trend of 0.2–0.3 °C decade^{-1} over the period 1983–2012, which is higher than the global average (Rayner et al. 2003; see Dye et al. 2013a among several references). Thus positive temperature anomalies exceeding one standard deviation (based on the period 1981–2010) were widespread in adjacent Atlantic Water and the northern North Sea during 2003–2012 (Beszczynska-Möller and Dye 2013). In fact, several authors suggest an inverse relation between Subpolar Gyre strength and the extent of warm saline water (e.g. Hátún et al. 2005; Johnson and Gruber 2007; Haekkinen et al. 2011).

3.2.2.2 North Sea

In Atlantic Water inflow to the North Sea at the western side of the Norwegian Trench (Utsira section, 59.3°N), 'core' temperature has risen by about 0.8 °C since the 1970s and about 1 °C near the seabed in the north-western part of the section (estimated from Holliday et al. 2009). Figure 3.2 shows long-term temperature variability in the Fair Isle Current flowing into the North Sea on the shelf.

For the North Sea as a whole, annual average SST derived from six gridded data sets (Fig. 3.3) shows relatively cool SST from 1870, especially in the early 1900s, 'plateaux' in the periods 1932–1939 and 1943–1950, and then overall decline to a minimum around 1988 (anomaly about −0.8 °C). This was followed by a rise to a peak in 2008 (anomaly about 1 °C) and subsequent fall. SST trends

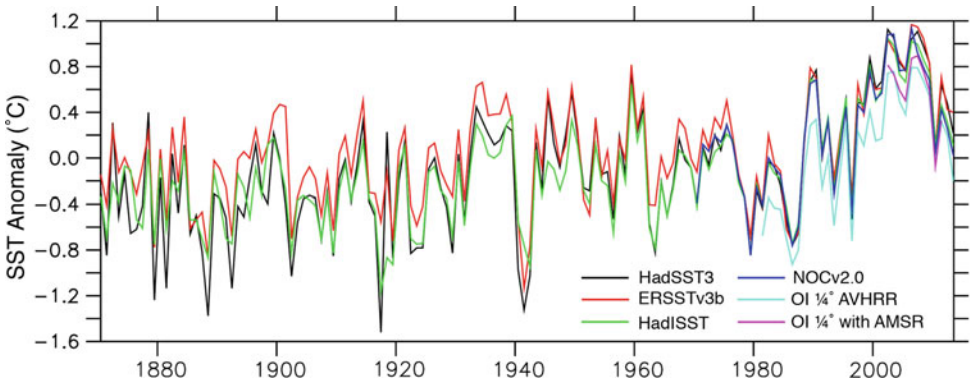

Fig. 3.3 North Sea region annual sea-surface temperature (SST) anomalies relative to the 1971–2000 average, for the datasets in E-Supplement Table S3.1 (figure by Elizabeth Kent, UK National Oceanography Centre)

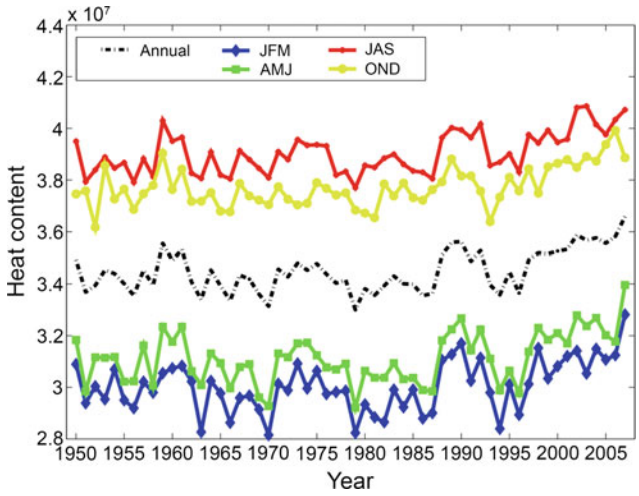

Fig. 3.4 Annual and seasonal mean North Sea heat content (10^7 J m^{-3}) (reprinted from Meyer et al. 2011)

generally show also in heat content (Hjøllo et al. 2009; Meyer et al. 2011) and in all seasons (Fig. 3.4), despite winter-spring variability exceeding summer-autumn variability. The increase in North Sea heat content between 1985 and 2007 was about 0.8×10^{20} J, much less than the seasonal range (about 5×10^{20} J) and comparable with interannual variability (Hjøllo et al. 2009).

Despite an inherent anomaly adjustment time-scale of just a few months (Fig. 3.5 and Meyer et al. 2011), the longer-term decline in SST from the 1940s to 1980s and subsequent marked rise to the early 2000s are widely reported. The basis is in observations, for example those shown by McQuatters-Gollop et al. (2007 using HADISST v1.1; see Fig. 3.6 and E-Supplement Table S3.1), Kirby et al. (2007), Holt et al. (2012, including satellite SST data, Fig. 3.7) and multi-decadal hindcasts, such as those of Meyer et al. (2011) and Holt et al. (2012). Particular features noted

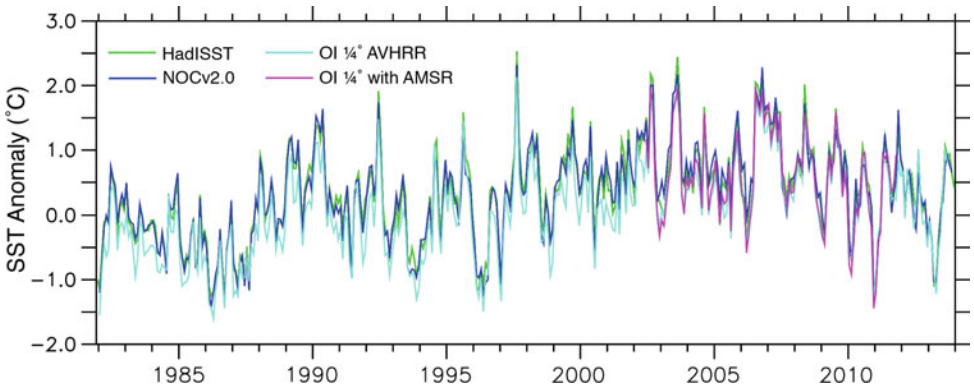

Fig. 3.5 North Sea region monthly sea-surface temperature (SST) anomalies relative to 1971–2000 monthly averages, for the gridded datasets in E-Supplement Table S3.1 with resolution of 1° or finer. Sharp month-to-month variability indicates an inherent anomaly 'adjustment' time of just a few months (figure by Elizabeth Kent, UK National Oceanography Centre)

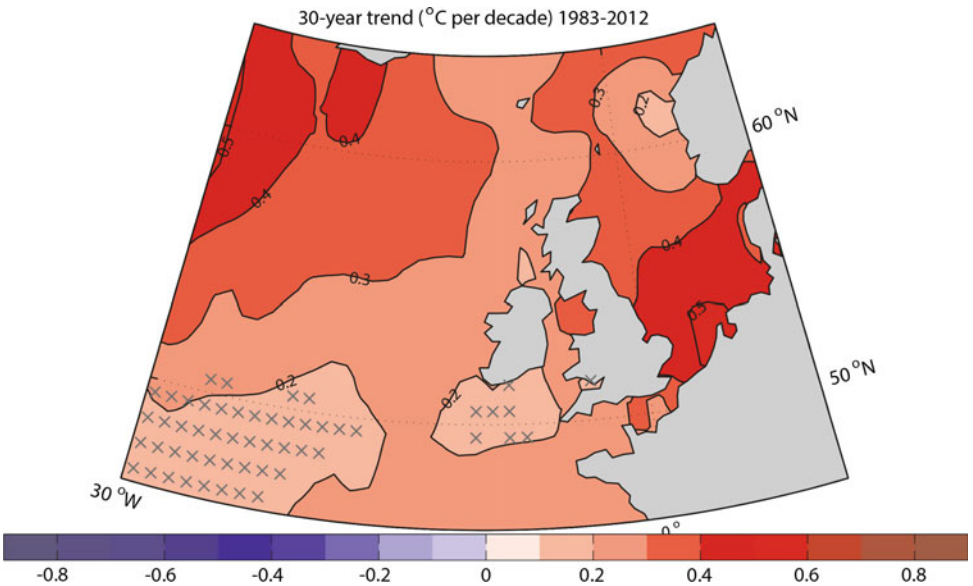

Fig. 3.6 Linear sea-surface temperature trends (°C $decade^{-1}$) in annual values for the period 1983–2012. From the HadISST1 dataset (Rayner et al. 2003). Hatched areas: trend not significantly different from zero at 95 % confidence level (Dye et al. 2013a, see Acknowledgement)

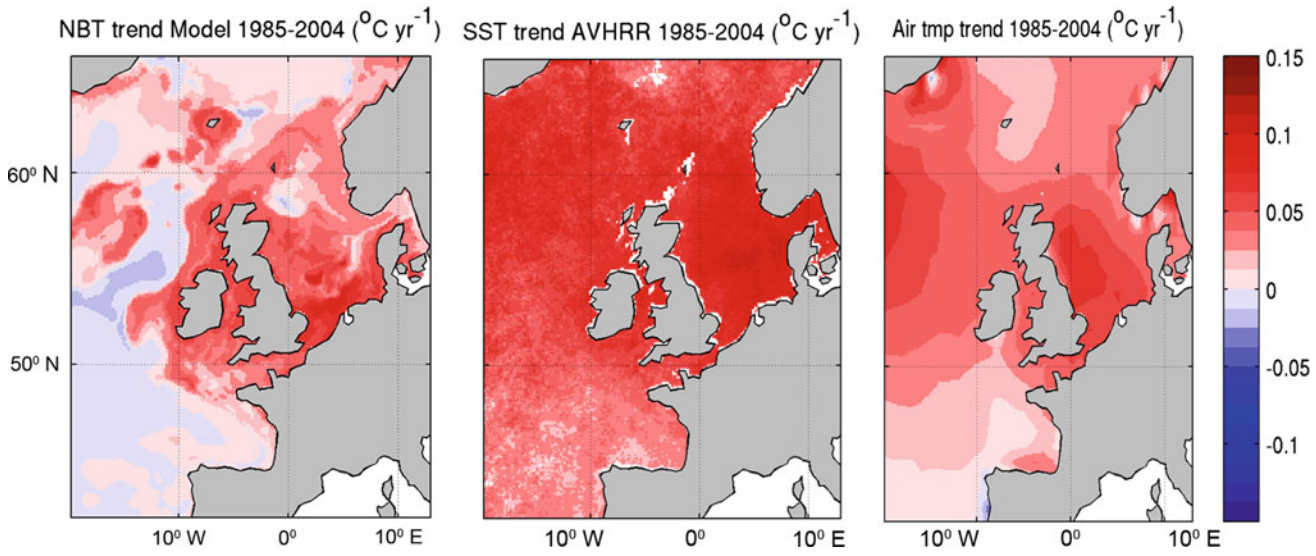

Fig. 3.7 Linear trends for the period 1985–2004 in model near-bed temperature (*left*), satellite sea-surface temperature (SST; *middle*) and 2-m ERA40 air temperature (*right*) (Holt et al. 2012)

are rapid cooling in the period 1960–1963, rapid warming in the late 1980s, followed by cooling again in the early 1990s and then resumed warming to about 2006. The warming trends of the 1980s to 2000s are widely reported to be significant (e.g. Holt et al. 2012) and are mainly but not entirely accounted for by trends in air temperature (see hindcasts of Meyer et al. 2011; Holt et al. 2012). Observed North Sea winter bottom temperature between 1983 and 2012 shows a typical trend of 0.2–0.5 °C decade^{-1} (Dye et al. 2013a) superimposed on by considerable interannual variability.

3.2.2.3 Regional Variations

The rise in North Sea SST since the 1980s increased from north (trend <0.2 °C decade^{-1}) to south (trend 0.8 °C decade^{-1}; Fig. 3.6; McQuatters-Gollop et al. 2007). Based on HadISST1 for the period 1987–2011, the EEA (2012) showed warming of 0.3 °C decade^{-1} in the Channel, 0.4 °C decade^{-1} off the Dutch coast, and less than 0.2 °C decade^{-1} at 60°N off Norway.

The German Bight shows the largest warming trend in recent decades (Fig. 3.6) with a rapid SST rise in the late 1980s (Wiltshire et al. 2008; Meyer et al. 2011). Variability is also large, between years O(1 °C) and longer term (Wiltshire et al. 2008; Meyer et al. 2011; Holt et al. 2012). At Helgoland Roads Station (54° 11′N, 7° 54′E) decadal SST trends since 1873 show the warming after the early 1980s was the strongest.

For southern North Sea SST, the 1971–2010 ferry data (Fig. 3.8) show a rise of O(2 °C) from 1985/6 to 1989; the five-year smoothing emphasises a late 1980s rise of about 1.5 °C followed by 5- to 10-year fluctuations superimposed on a slow decline from the early 1990s to about 1 °C above the 1971–1986 average (smoothed values). Model hindcast spatial averages between Dover Strait and 54.5°N (water column mostly well-mixed; Alheit et al. 2012 based on Meyer et al. 2011) also show cold winters for 1985 to 1987 but the 1990 winter as the warmest since 1948 (and winter 2007 as warmer again). Anomalies (observations and model results) became mainly positive from the late 1980s apart from a dip in the early 1990s. This all illustrates the late 1980s temperature rise.

The Dutch coastal zone shows a trend of rising SST since 1982 (van Aken 2010), despite a very cold winter in 1996 (January–March; about 4 °C below the 1969–2008 average; van Hal et al. 2010). Factors contributing to this rise are thermal inertia (seasonally), winds and cloudiness or bright sunshine (van Aken 2010). The 1956–2003 Marsdiep winter temperature (Tsimplis et al. 2006) and Wadden Sea winter and spring temperature (van Aken 2008) were significantly correlated with the winter North Atlantic Oscillation (NAO) index (see Annex 1). However, decadal to centennial temperature variations (a cooling of about 1.5 °C over the period 1860–1890 and a similar warming in the last 25 years) were not related to long-term changes in the NAO.

The western English Channel (50.03°N, 4.37°W) warmed in the 1920s and 1930s (Southward 1960); after a dip it warmed again in the 1950s, cooled in the 1960s and warmed over the full water column from the mid-1980s to the early 2000s (0.6 °C decade^{-1}, Smyth et al. 2010; see E-Supplement Fig. S3.2). The greatest (1990s) temperature rise coincided with a decrease in median wind speed (from 3.5 to 2.75 m s^{-1}) and an increase in surface solar irradiation (of about 20 %), both correlated with changes in the NAO (Smyth et al. 2010).

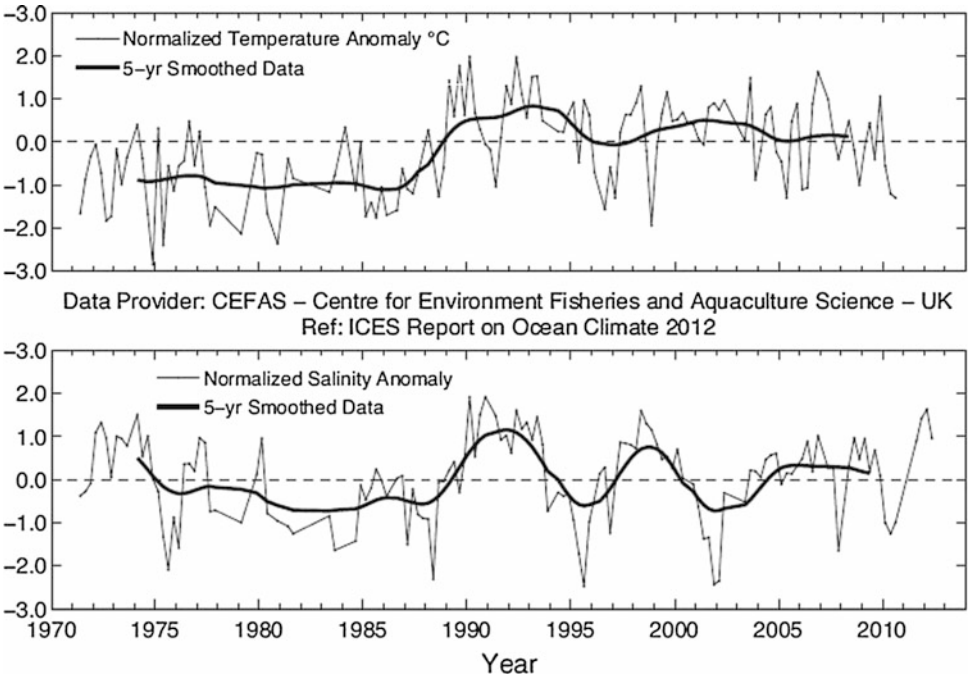

Fig. 3.8 Ferry-based sea-surface temperature (*upper*) and salinity (*lower*) anomalies relative to the 1981–2010 average, along 52°N at six standard stations. The graphic shows three-monthly averages (DJF, MAM, JJA, SON) (Beszczynska-Möller and Dye 2013)

Off northern Denmark and Norway, coastal waters in winter (JFM) were 0.8–1.3 °C warmer in the period 2000–2009 than the period 1961–1990 (Albretsen et al. 2012); the corresponding rise at 200 m depth was 0.55–0.8 °C. Winter–spring observed SST in the Kattegat and Danish Straits rose by about 1 °C between 1897–1901 and the 1980s, and again by about 1 °C to the 1990s–2006 period (Henriksen 2009). Summer–autumn trends were not as clear.

3.2.3 Salinity Variability and Trends

3.2.3.1 Northeast Atlantic

North Atlantic surface salinity shows pronounced interannual and multi-decadal variability. In the Subpolar Gyre salinity variations are correlated with SST such that high salinities usually coincide with anomalously warm water and vice versa (such as in Rockall Trough; Beszczynska-Möller and Dye 2013). On decadal time scales, upper-layer salinity is also positively correlated with the winter NAO, especially in the eastern part of the gyre (Holliday et al. 2011). Shelf-sea and oceanic surface waters to the north and west of the UK had a salinity maximum in the early 1960s and a relatively fresh period in the 1970s, associated with the so-called Great Salinity Anomaly (Dickson et al. 1988). In Rockall Trough the minimum occurred about 1975 (Dickson et al. 1988) and was followed by increasing salinities, interrupted by a mid-1990s minimum (Holliday et al. 2010; Hughes et al. 2012; Sherwin et al. 2012).

Correspondingly, the Fair Isle—Munken section (~2°W 59.5°N to 6°W 61°N across the Faroe-Shetland Channel) at 50–100 m depth showed an upward salinity trend of 0.075 decade^{-1} during the period 1994–2011 (Fig. 3.1; Berx et al. 2013). Likewise, the salinity of Atlantic water inflow to the Nordic Seas through Svinøy section (to the north-west off Norway through ~4°E 63°N) has increased by about 0.15 since the 1970s (Holliday et al. 2008; Beszczynska-Möller and Dye 2013), for example by 0.08 from 1992 to 2009 (Mork and Skagseth 2010).

3.2.3.2 North Sea

Salinity has shown a long-term (1958–2003) increase around northern Scotland (Leterme et al. 2008) and (1971–2012) in the northern North Sea (Fig. 3.9). This is confirmed by Hughes et al. (2012) who charted pentadal-mean upper-ocean salinity showing positive anomalies (relative to the 1971–2000 mean) since 1995 in the northern North Sea most influenced by the Atlantic. Linkage to more saline Atlantic inflow has been suggested (Corten and van de Kamp 1996).

On the western side of the Norwegian Trench and in the central northern North Sea (Utsira section, 59.3°N), influenced by Atlantic water, salinity has increased by about 0.05 since the late 1970s (when values were relatively stable after the Great Salinity Anomaly; Beszczynska-Möller and Dye 2013). On the other hand, salinity in the Fair Isle Current shows interannual variability and no clear long-term trend (Fig. 3.2), being influenced by the fresher waters of the Scottish Coastal Current from west of Scotland.

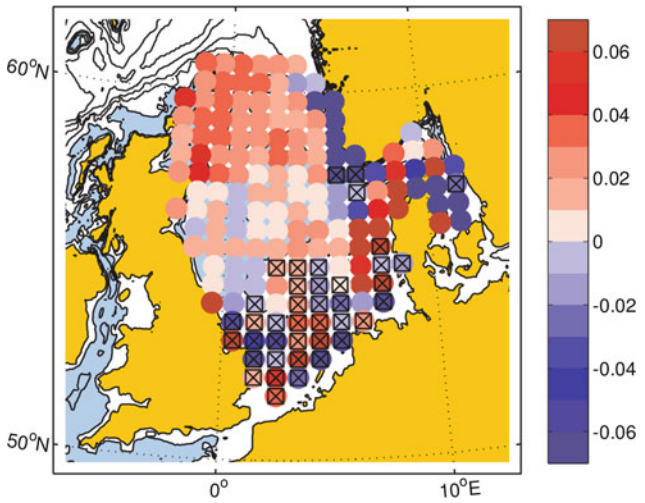

Fig. 3.9 Linear trend per decade in winter bottom salinity, from International Bottom Trawl Survey (IBTS) Quarter 1 data, 1971–2012. Values are calculated for ICES rectangles with more than 30 years of data (hatched areas: trend not significantly different from zero at 95 % confidence level, Dye et al. 2013b; see Acknowledgement, updated from UKMMAS 2010, courtesy of S. Hughes, Marine Scotland Science)

Coastal regions of the southern North Sea, notably the German Bight, are influenced by fluvial inputs (primarily from the rivers Rhine and Elbe) as well as Atlantic inflows (Heyen and Dippner 1998; Janssen 2002). Away from coastal waters, the influence of Atlantic inflow dominates. For the German Bight, Heyen and Dippner (1998) reported no substantial trends in sea-surface salinity (SSS) for the period 1908–1995, a result confirmed by earlier analysis of Helgoland Roads SSS for the period 1873–1993 (Becker et al. 1997) and the analyses of Janssen (2002). German Bight studies (e.g. Fig. 3.10) agree on a temporal minimum around 1982 and a maximum during the early 1990s with a difference of about 0.7 between the two. 1971–2010 ferry data (Fig. 3.8) show pentadal fluctuations with a temporal minimum and maximum also around 1982 and the early 1990s respectively.

The western English Channel (50.03°N, 4.37°W), away from the coast, is influenced by North Atlantic water, showing a similar increase in salinity in recent years (Holliday et al. 2010). Local weather effects (mixed vertically by tidal currents) add to interannual salinity variability which is much greater than in the open ocean. For example, station L4 off Plymouth experiences pulses of surface freshening after intense summer rain increases riverine input (Smyth et al. 2010). However, there is no clear trend over a century of measurements (see also E-Supplement Fig. S3.3, E-Supplement Sect. S3.2).

In the Kattegat and Skagerrak, salinities are affected by low-salinity Baltic Sea outflow. Skagerrak coastal waters in winter (January–March) were up to 0.5 more saline in the period 2000–2009 than the period 1961–1990, but further west and north around Norway their salinity decreased slightly (Albretsen et al. 2012). Shorter-term variability is larger. Salinity variability in the Kattegat and Skagerrak exceeds that in Atlantic water, owing to varying Baltic outflow (see Sect. 3.3) and net precipitation minus evaporation in catchments.

Salinity variability on all time scales to multi-decadal exceeds and obscures any potential long-term trend. For

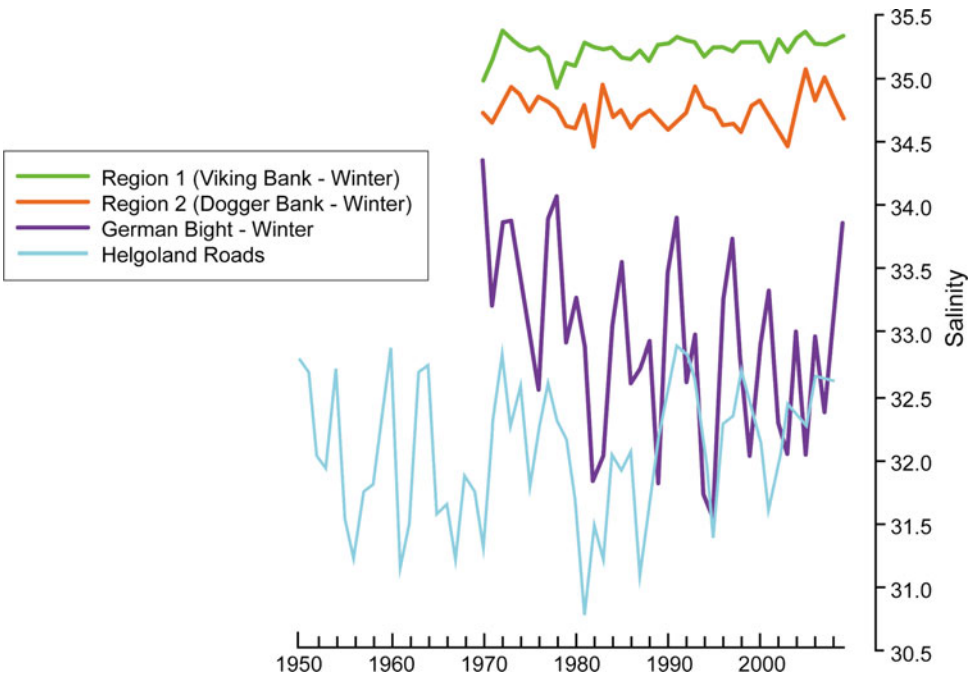

Fig. 3.10 Winter bottom salinity from the ICES International Bottom Trawl Survey (IBTS) dataset at Viking Bank, Dogger Bank and German Bight, together with annual mean salinity from Helgoland Roads (Holliday et al. 2010; see Acknowledgement)

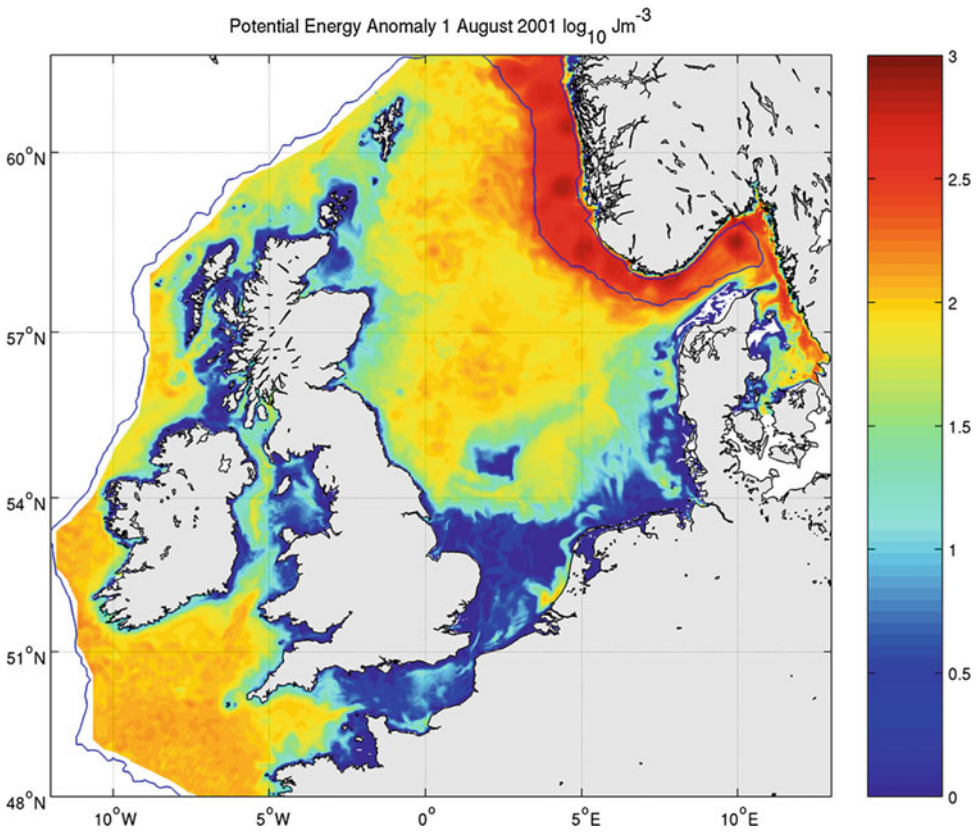

Fig. 3.11 Distribution of potential energy anomaly (energy required to completely mix the water column; log scale, 1 August 2001) (Holt and Proctor 2008)

example, in winter 2005, a series of storms drove much high-salinity Atlantic water across the north-west boundary into the North Sea as far south as Dogger Bank and bottom-water salinity exceeded 35 in 63 % of the North Sea area (Loewe 2009). Adjacent Atlantic waters in the period 2002–2010 (Hughes et al. 2011) show positive salinity anomalies of more than two (one) standard deviation in Rockall Trough (Faroe-Shetland Channel) while the North Sea has no comparably clear signal.

3.2.4 Stratification Variability and Trends

Stratification is a key control on shelf-sea marine ecosystems. Strong stratification inhibits vertical exchange of water. Spring–summer heating reduces near-surface density where tidal currents are too weak to mix through the water depth (Simpson and Hunter 1974), typically where depth is about 50 m or more. The configuration of summer-stratified regions controls much of the average flow in shelf seas (Hill et al. 2008). Mixed-layer data are available albeit only on a 2° grid.[1] The distribution of summer stratification (mainly thermal) is illustrated in Figs. 3.11 and 3.12.

Annual time series of ECOHAM4 simulated thermocline characteristics averaged over the North Sea were reported by Lorkowski et al. (2012). The maximum depth of the thermocline[2] is much more variable interannually than its mean depth. Thermocline intensity shows no trend and only moderate variability. The annual number of days with a mean thermocline greater than 0.2 °C m^{-1} ranged from 31 to 101. The warmest summer in the period simulated (2003) hardly shows in any thermocline characteristics (Lorkowski et al. 2012). In the north-western North Sea, the strength of thermal stratification varies interannually (with no clear trend but periodicity of about 7–8 years; Sharples et al. 2010). The multi-decadal hindcast by Meyer et al. (2011) for the North Sea confirmed that variability in stratification is mainly interannual. In seasonally stratified regions, Holt et al. (2012) modelling showed 1985–2004 warming trends to be greater at the surface than at depth (reflecting an increase in stratification), especially in the central North Sea, at frontal areas of Dogger Bank, in an area north-east of Scotland and in inflow to the Skagerrak. They also found this pattern in annual trends of ICES (International Council for the Exploration of the Sea) data, albeit limited by a lack of seasonal resolution.

[1] www.ifremer.fr/cerweb/deboyer/mld/home.php.

[2] Defined here as (existence of) the uppermost vertical temperature gradient $\Delta T/\Delta z \geq 0.1$; T(°C) is temperature, z (m) is depth.

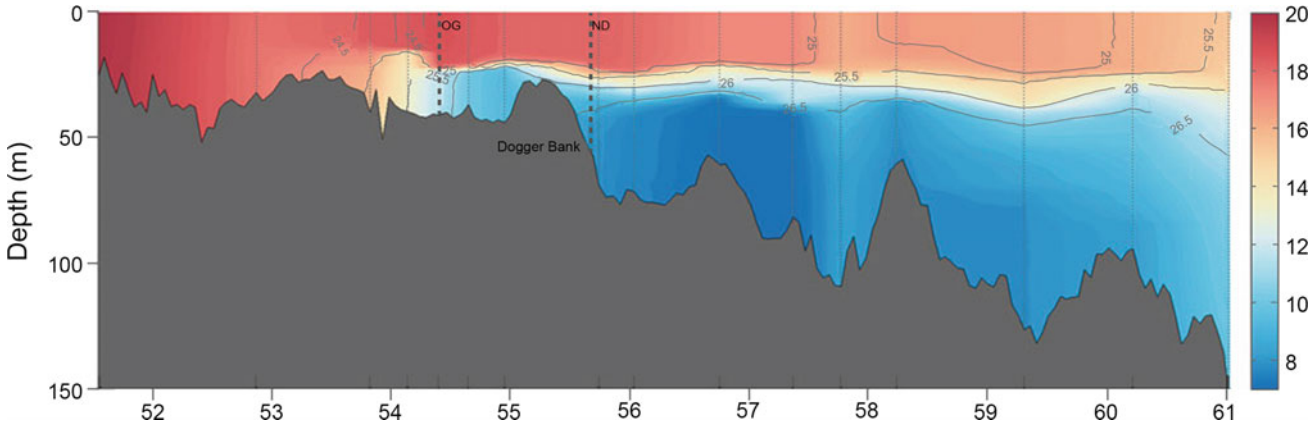

Fig. 3.12 South-north section of potential temperature (°C) near 2.5°E (but further east around Dogger Bank), August 2010 (Queste et al. 2013)

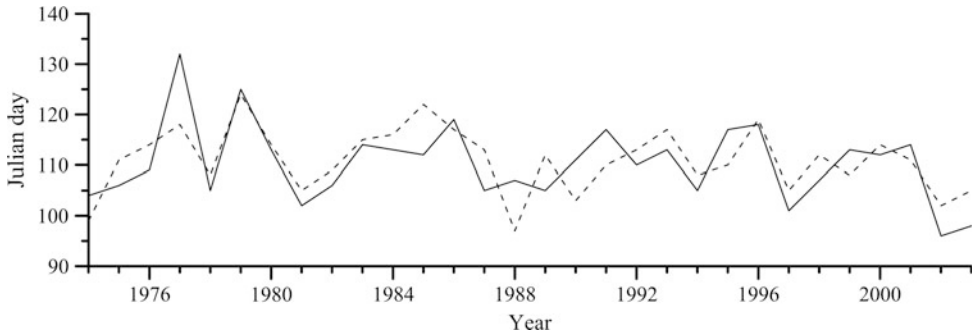

Fig. 3.13 Modelled timing (Julian day) of spring stratification (when the surface-bottom temperature difference first exceeds 0.5 °C for at least three days; *solid line*) and spring bloom (*dashed line*) between 1974 and 2003 in 60 m water depth near 1.4°W 56.2°N (reprinted from Fig. 5a of Sharples et al. 2006)

Lorkowski et al. (2012) found the time of initial thermocline development to vary between Julian days 54 and 107, with relatively large values (i.e. a late start) from 1970 to 1977. Other evidence also suggests a recent trend to earlier thermal stratification (Young and Holt 2007, albeit for the Irish Sea). The timing of spring stratification in the north-western North Sea was modelled for the period 1974–2003 and compared with observed variability by Sharples et al. (2006; Fig. 3.13). Persistent stratification typically begins (on 21 April ± three weeks range) as tidal currents decrease from springs to neaps. The main meteorological control is air temperature; since the mid-1990s its rise seems to have caused stratification to be an average of one day earlier per year with wind stress (linked to the NAO) having had some influence before the 1990s. Holt et al. (2012), modelling 1985–2004, found an extension to the stratified season in the central North Sea and north-east of Scotland.

In estuarine outflow regions, strong short-term and interannual variability in precipitation (hence fluvial inputs) and tidal mixing mask any longer-term trends in stratification (timing or strength).

3.3 Currents and Circulation

John Huthnance, John Siddorn, Ralf Weisse

3.3.1 Historical Perspective

The earliest evidence for circulation comes from hydrographic sections, for time scales longer than a day, and from drifters, observed by chance or deliberately deployed. Prior to satellite tracking (of floats or drogued buoys), typically only drifters' start and end points would be known; temporal and spatial resolution were lacking. Moored current meters record time series at one location; their use was rare until the 1960s. Within the area (5°W–13°E, 48°N–62°N) the international current meter inventory at the British Oceanographic Data Centre[3] records just 27 year-long records and 3025 month-long records to 2008; by decade from the

[3]https://www.bodc.ac.uk/data/information_and_inventories/current_meters/search.

1950s, the numbers of month-long records are 1, 32, 1306, 1201, 381, 124. Occasionally, submarine cables have monitored approximate transport across a section (notably for flow through Dover Strait; e.g. Robinson 1976; Prandle 1978a) and HF radar has given spatial coverage for surface currents within a limited range (Prandle and Player 1993).

Detail on evidence for currents, circulation and their variations is given in E-Supplement Sect. S3.3.

3.3.2 Circulation: Variability and Trends

The Atlantic Meridional Overturning Circulation (AMOC), and its warm north-eastern limb in the Subpolar Gyre, influence the flow and properties of Atlantic Water bordering and partly flowing onto the north-west European shelf and into the North Sea. The AMOC has much seasonal and some interannual variability: mean 18.5 Sv (SD ~ 3 Sv) for April 2004 to March 2009 (Sv is Sverdrup, 10^6 m^3 s^{-1}) (McCarthy et al. 2012). The AMOC probably also varies on decadal time scales (e.g. Latif et al. 2006). Longer-term trends are not yet determined (Cunningham et al. 2010) even though Smeed et al. (2014) found the mean for April 2008 to March 2012 to be significantly less than for the previous four years. The Subpolar Gyre extent correlates with the NAO (Lozier and Stewart 2008). It strengthened overall from the 1960s to the mid-1990s, then decreased (Hátún et al. 2005). While the Subpolar Gyre was relatively weak in the period 2000–2009, more warm, salty Mediterranean and Eastern North Atlantic waters flowed poleward around Britain (Lozier and Stewart 2008; Hughes et al. 2012). Negative NAO also correlates with more warm water in the Faroe-Shetland Channel (Chafik 2012). However, observations show no significant longer-term trend in Atlantic Water transport to the north-east past Scotland and Norway (Orvik and Skagseth 2005; Mork and Skagseth 2010; Berx et al. 2013).

Inflow of oceanic waters to the North Sea from the Atlantic Ocean, primarily in the north driven by prevailing south-westerly winds, has been modelled by Hjøllo et al. (2009; 1985–2007), Holt et al. (2009) and using NORWECOM/POM (3-D hydrodynamic model; Iversen et al. 2002; Leterme et al. 2008, for 1958–2003; Albretsen et al. 2012). Relative to the long-term mean, results show weaker northern inflow between 1958 and 1988; within this period, there were increases in the 1960s and early 1970s, a decrease from 1976 to 1980 and an increase in the early and mid-1980s. The northern inflow was greater than the long-term mean in 1988 to 1995 with a maximum in 1989 (McQuatters-Gollop et al. 2007) but smaller again in 1996 to 2003. This inflow is correlated positively with salinity, SST (less strongly) and the NAO (especially in winter), and negatively with discharges from the rivers Elbe and Rhine (less strongly). For the period 1985–2007, Hjøllo et al. (2009) found a weak trend of −0.005 Sv $year^{-1}$ in modelled Atlantic Water inflows (mean 1.7 Sv, SD 0.41 Sv, correlation with NAO ~0.9). Strong flows into the North Sea (and Nordic Seas) frequently correspond to high-salinity events (Sundby and Drinkwater 2007).

Dover Strait inflow, of the order 0.1 Sv (Prandle et al. 1996), was smaller than the long-term mean from 1958 to 1981 and then greater until 2003 (Leterme et al. 2008). Baltic Sea outflow variations (modelled freshwater relative to salinity 35.0) correlate with winds, resulting sea-surface elevation and NAO index; correlation coefficients with the NAO were 0.57 during the period 1962–2004 and 0.74 during 1980–2004 (Hordoir and Meier 2010; Hordoir et al. 2013). Days-to-months variability O(0.1 Sv) in North Sea—Baltic Sea exchange far exceeds the mean Baltic Sea outflow of the order 0.01 Sv or any trend therein.

North Sea outflows and inflows (plus net precipitation minus evaporation) have to balance on a time scale of just a few days. Off-shelf flow is persistent in the Norwegian Trench and in a bottom layer below the poleward along-slope flow (Holt et al. 2009; Huthnance et al. 2009). A modelled time series for 1958–1997 (Schrum and Sigismund 2001) shows an average outflow of about 2 Sv, little clear trend but consistency with the above interannual variations in inflow.

A MyOcean (project) reanalysis of the region 40°–65°N by 20°W–13°E for the period 1984–2012 was undertaken with the NEMO model version 3.4 (Madec 2008; for details on this application see MyOcean 2014). Transports normal to transects were calculated following NOOS (2010): averaging flow over 24.8 h to give a tidal mean at each model point across the transect; then area-weighting for transports, separating the mean negative and mean positive flows. For the Norway–Shetland transect, flow in the west is dominantly into the North Sea and makes a significant contribution to exchange with the wider Atlantic; circulation is partially density-driven during summer and confined to the coastal waters east of Shetland. Mean inflow is 0.56 Sv with significant seasonality and interannual variability but no obvious trend. In the east sector of the Norway–Shetland transect, flow is both into and out of the North Sea, strongly steered by the Norwegian Trench and includes the Norwegian Coastal Current, resulting in a larger outflow than inflow. Mean net flow is 1.3 Sv (SD 0.97 Sv) representing large seasonal and interannual variability, especially in the outflow.

Net circulation within the North Sea is shown schematically in Fig. 1.7. Tidal currents are important, primarily semi-diurnal with longer-period modulation (Sect. 1.4.4); locally values exceed 1.2 m s^{-1} in the Pentland Firth, off East Anglia and in Dover Strait. Other important current contributions are due to winds (Sect. 1.4.3 shows

representative flow patterns) and to differences in density (Sect. 1.4.2) including estuarine outflows (e.g. van Alphen et al. 1988), varying on time scales from hours to seasons (e.g. Turrell et al. 1992) to decades. Hence flows can be very variable in time; they also vary strongly with location.

Wind forcing is the most variable factor; water transports in one storm (typically in winter; time-scale hours to a day) can be significant relative to a year's total. 50-year return values for currents in storm surges have been estimated at 0.4–0.6 m s^{-1} in general, but exceed 1 m s^{-1} locally off Scottish promontories, in Dover Strait, west of Denmark and over Dogger Bank (Flather 1987). These extreme currents are directed anti-clockwise around the North Sea near coasts, and into the Skagerrak.

In summer-stratified areas (Sect. 3.2.4) cold bottom water is nearly static (velocity tends to zero at the sea bed due to friction). Between stratified and mixed areas, relatively strong density gradients are expected to drive near-surface flows anti-clockwise around the dense bottom water (Hill et al. 2008). These flows, of the order 0.3 m s^{-1} but sometimes >1 m s^{-1} in the Norwegian Coastal Current, are liable to baroclinic instability developing meanders, scale 5–10 km (e.g. Badin et al. 2009; their model shows eddy variability increasing in late summer with increased stratification). Such meanders are prominent north of Scotland over the continental slope and off Norway where the fresher surface layer increases stratification.

When a region of freshwater influence (ROFI) is stratified, cross-shore tidal currents may develop; for example, according to de Boer et al. (2009) surface currents rotate clockwise and bottom currents anti-clockwise in the Rhine ROFI when stratified. These authors also found cyclical upwelling there due to tidal currents going offshore at the surface and onshore below.

The winter mean circulation of the North Sea is organised in one anti-clockwise gyre with typical mean velocities of about 10 cm s^{-1} (Kauker and von Storch 2000). On shorter time scales the circulation is highly variable. Kauker and von Storch (2000) identified four regimes. Two are characterised by a basin-wide gyre with clockwise (15 % of the time) or anti-clockwise (30 % of the time) orientation. The other two regimes are characterised by the opposite regimes of a bipolar pattern with maxima in the southern and northern parts of the North Sea (45 % of the time). For 10 % of the time the circulation nearly ceased. Kauker and von Storch (2000) found that only 40 % of the one-gyre regimes persist for longer than five days while the duration of the bipolar circulation patterns rarely exceeded five days. Accordingly, short-term variability typically dominates transports; tidal flows dominate instantaneous transports (positive and negative volume fluxes across sections) and meteorological phenomena dominate residual (net) transports.

Mean residual transports are generally smaller than their variability. Many transects show strong seasonality as meteorological conditions drive surges, river runoff and ice melt. No trend in transports has been seen in these data: limited duration of available data and large variability in the transports on time scales of days, seasons and interannually makes discerning trends difficult.

In the German Bight, anti-clockwise circulation is about twice as frequent as clockwise, and prevails during south-westerly winds typical of winter storms, giving rapid transports through the German Bight (Thiel et al. 2011, on the basis of Pohlmann 2006). Loewe (2009) associated clockwise flow with high-pressure and north-westerly weather types, anti-clockwise flow with south-westerly weather types, and flow towards the north or north-west with south-easterly weather types. However, Port et al. (2011) found that the wind-current relation changes away from the coast owing to dependence on density effects, the coastline and topography.

On longer time scales the variability of the North Sea circulation and thus transports is linked to variations in the large-scale atmospheric circulation. Emeis et al. (2015) reported results of an EOF analysis (see von Storch and Zwiers 1999) of monthly mean fields of vertically integrated volume transports derived from a multi-decadal model hindcast (Fig. 3.14; see also Mathis et al. 2015). Regions of particularly high variability include the inflow areas of Atlantic waters via the northern boundary of the North Sea and the English Channel, respectively. The time coefficient associated with the dominant EOF mode overlaid with the NAO index illustrates the relation with variability of the large-scale atmospheric circulation (Fig. 3.14). Positive EOF coefficient (intensified inflow of Atlantic waters) corresponds with a positive NAO, i.e. enhanced westerly winds, which in turn result in an intensified anti-clockwise North Sea circulation (Emeis et al. 2015); opposites also hold.

In summary, multiple forcings cause currents to vary on a range of time and space scales, including short scales relative to which measurements are sparse. Hence trends are of lesser significance and hard to discern. Moreover, causes of trends in flows are difficult to diagnose; improvements are needed in observational data (quantity and quality). Reliance is placed on models, which need improvement (in formulation, forcing) for currents other than tides and storm surges.

3.4 Mean Sea Level

Thomas Wahl, Philip Woodworth, Ivan Haigh, Ralf Weisse

Changes in mean sea level (MSL) result from different aspects of climate change (e.g. the melting of land-based ice, thermal expansion of sea water) and climate variability (e.g.

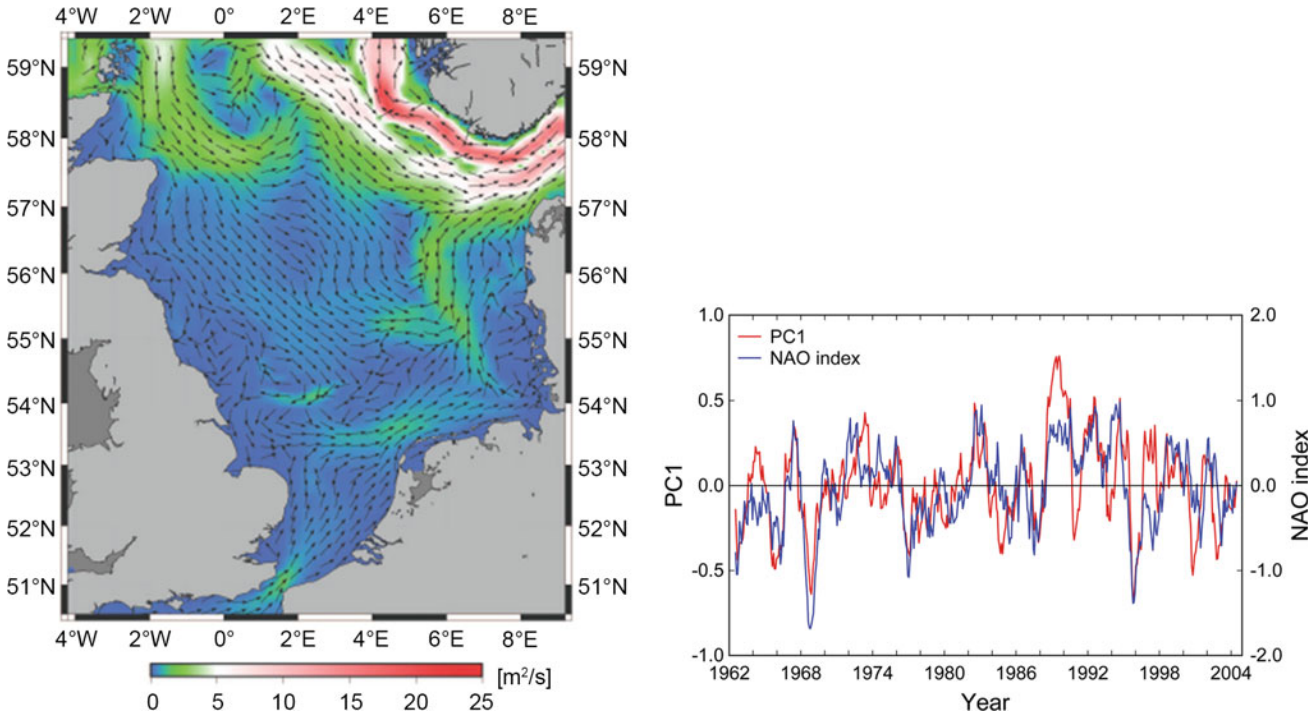

Fig. 3.14 Dominant EOF of monthly mean vertically integrated volume transports obtained from a 3D baroclinic simulation (1962–2004) explaining 75.8 % of the variability. Vectors indicate directions of transport anomalies while colours indicate magnitudes (*left* Emeis et al. 2015); Corresponding coefficient time series (*red*) and NAO index (*blue*) (*right* Hurrell et al. 2013). Shown are moving annual averages based on monthly values

changes in wind forcing related to the NAO or El Niño–Southern Oscillation) and occur over all temporal and spatial scales. MSL is sea level averaged into monthly or annual mean values, which are the parameters of most interest to climate researchers (Woodworth et al. 2011). The focus in this chapter is on the last 200 years, when direct 'modern' measurements of sea level are available from tide gauges and high precision satellite radar altimeter observations. MSL can be inferred indirectly over this period (and thousands of years earlier) using proxy records from salt-marsh sediments and the fossils within them (Gehrels and Woodworth 2013) or archaeology (e.g. fish tanks built by the Romans), and over much longer time scales (thousands to millions of years) using other paleo-data (e.g. geological records, from corals or isotopic methods).

The North Sea coastline has one of the world's most densely populated tide gauge networks, with many (>15) records spanning 100 years or longer and a few going back almost continuously to the early 19th century. The tide gauges of Brest and Amsterdam also provide some data for parts of the 18th century and are among the longest sea level records in the world. Since 1992, satellite altimetry has provided near-global coverage of MSL. The advantage of altimetry is that it records geocentric sea level (i.e. measurements relative to the centre of the Earth). By contrast, tide gauges measure the relative changes between the ocean surface and the land itself; hence, the term 'relative mean sea level' (RMSL), and it is this that is of most relevance to coastal managers, engineers and planners. Calculation from tide gauge records of changes in 'geocentric mean sea level' (sometimes referred to as 'absolute mean sea level'; AMSL) requires the removal of non-climate contributions to sea level change, which arise both from natural processes (e.g. tectonics, glacial isostatic adjustment GIA) and from anthropogenic processes (e.g. subsidence caused by ground water abstraction). Tide gauge records can be corrected using estimates of vertical land motion from (i) models which predict the main geological aspect of vertical motion, namely GIA (e.g. Peltier 2004); (ii) geological information near tide gauge sites (e.g. Shennan et al. 2012); and (iii) direct measurements made at or near tide gauge locations using continuous global positioning system (GPS) or absolute gravity (e.g. Bouin and Wöppelmann 2010). Rates of vertical land movement have also been estimated by comparing trends derived from altimetry data and tide gauge records (e.g. Nerem and Mitchum 2002; Garcia et al. 2007; Wöppelmann and Marcos 2012).

Paleo sea level data from coastal sediments, the few long (pre-1900) tide gauge records and reconstructions of MSL, made by combining tide gauge records with altimetry measurements (e.g. Church and White 2006, 2011; Jevrejeva et al. 2006, 2008; Merrifield et al. 2009), indicate that there

was an increase in the rate of global MSL rise during the late 19th and early 20th centuries (e.g. Church et al. 2010; Woodworth et al. 2011; Gehrels and Woodworth 2013). Over the last 2000 to 3000 years, global MSL has been near present-day levels with fluctuations not larger than about ±0.25 m on time scales of a few hundred years (Church et al. 2013) whereas the global average rate of rise estimated for the 20th century was 1.7 mm year^{-1} (Bindoff et al. 2007). Measurements from altimetry suggest that the rate of MSL rise has almost doubled over the last two decades; Church and White (2011) estimated a global trend of 3.2 ± 0.4 mm year^{-1} for the period 1993–2009. Milne et al. (2009) assessed the spatial variability of MSL trends derived from altimetry data and found that local trends vary by as much as −10 to +10 mm year^{-1} from the global average value for the period since 1993, due to regional effects influencing MSL changes and variability (e.g. non-uniform contributions of melting glaciers and ice sheets, density anomalies, atmospheric forcing, ocean circulation, terrestrial water storage). This highlights the importance of regional assessments. Examining whether past MSL has risen faster or slower in certain areas compared to the global average will help to provide more reliable region-specific MSL rise projections for coastal engineering, management and planning.

There have been very few region-wide studies of MSL changes in the North Sea. The first detailed study was by Shennan and Woodworth (1992), who used geological and tide gauge data from sites around the North Sea to infer secular trends in MSL in the late Holocene and 20th century (up until the late 1980s). They concluded that a systematic offset of 1.0 ± 0.15 mm year^{-1} in the tide gauge trends, compared to those derived from the geological data, could be interpreted as the regional average rate of geocentric MSL change over the 20th century; this is significantly less than global rates over this period. They also showed that part of the interannual MSL variability of the region was coherent, and they represented this as an index, created by averaging the de-trended MSL time series. Like Woodworth (1990), they found no evidence for a statistically significant acceleration in the rates of MSL rise for the 20th century.

Since then many other investigations of MSL changes have been undertaken for specific stretches of the North Sea coastline, mostly on a country-by-country basis, as for example by Araújo (2005), Araújo and Pugh (2008), Wöppelmann et al. (2006, 2008) and Haigh et al. (2009) for the English Channel; by van Cauwenberghe (1995, 1999) and Verwaest et al. (2005) for the Belgian coastline; Jensen et al. (1993) and Dillingh et al. (2010) for the Dutch coastline; Jensen et al. (1993), Albrecht et al. (2011), Albrecht and Weisse (2012) and Wahl et al. (2010, 2011) for the German coastline; Madsen (2009) for the Danish coastline; Richter et al. (2012) for the Norwegian coastline; and by Woodworth (1987) and Woodworth et al. (1999, 2009a) for the United Kingdom (UK). The most detailed analysis of 20th century geocentric MSL changes was undertaken by Woodworth et al. (2009a). They estimated that geocentric MSL around the UK rose by 1.4 ± 0.2 mm year^{-1} over the 20th century; faster (but not significantly faster at 95 % confidence) than the earlier estimate by Shennan and Woodworth (1992) for the whole North Sea and slower (but not significantly slower at 95 % confidence level) than the global 20th century rate.

A recent investigation undertaken by Wahl et al. (2013) aimed at updating the results of the Shennan and Woodworth (1992) study, using tide-gauge records that are now 20 years longer across a larger network of sites, altimetry measurements made since 1992, and more precise estimates of vertical land movement made since then with the development of advanced geodetic techniques. They analysed MSL records from 30 tide gauges covering the entire North Sea coastline (Fig. 3.15). Trends in RMSL were found to vary significantly across the North Sea region due to the influence of vertical land movement (i.e. land uplift in northern Scotland, Norway and Denmark, and land subsidence elsewhere). The accuracy of the estimated trends was also influenced by considerable interannual variability present in many of the MSL time series. The interannual variability was found to be much greater along the coastlines of the Netherlands, Germany and Denmark, compared to Norway, the UK east coast and the English Channel (Fig. 3.16).

However, using correlation analyses, Wahl et al. (2013) showed that part of the variability was coherent throughout the region, with some differences between the Inner North Sea (number 4 anti-clockwise to 26 in Fig. 3.15) and the English Channel. Following Shennan and Woodworth (1992), they represented this coherent part of the variability by means of MSL indices (Fig. 3.16). Geocentric MSL trends of 1.59 ± 0.16 and 1.18 ± 0.16 mm year^{-1} were obtained for the Inner North Sea and English Channel indices, respectively, for the period 1900–2009 (data sets were corrected for GIA to remove the influence of vertical land movement). For the North Sea region as a whole, the geocentric MSL trend was 1.53 ± 0.16 mm year^{-1}. These results are consistent with those presented by Woodworth et al. (2009a) for the UK (i.e. an AMSL trend of 1.4 ± 0.2 mm year^{-1} for the 20th century), but were significantly different from those presented by Shennan and Woodworth (1992) for the North Sea region (i.e. a geocentric MSL trend of 1.0 ± 0.15 mm year^{-1} for the period from 1901 to the late 1980s). For the 'satellite period' (i.e. 1993 to 2009) the geocentric MSL trend was estimated to be 4.00 ± 1.53 mm year^{-1} from the North Sea tide gauge records. This trend is faster but not significantly different from the global geocentric MSL trend for the same period (i.e. 3.20 ± 0.40 mm year^{-1} from satellite altimetry and

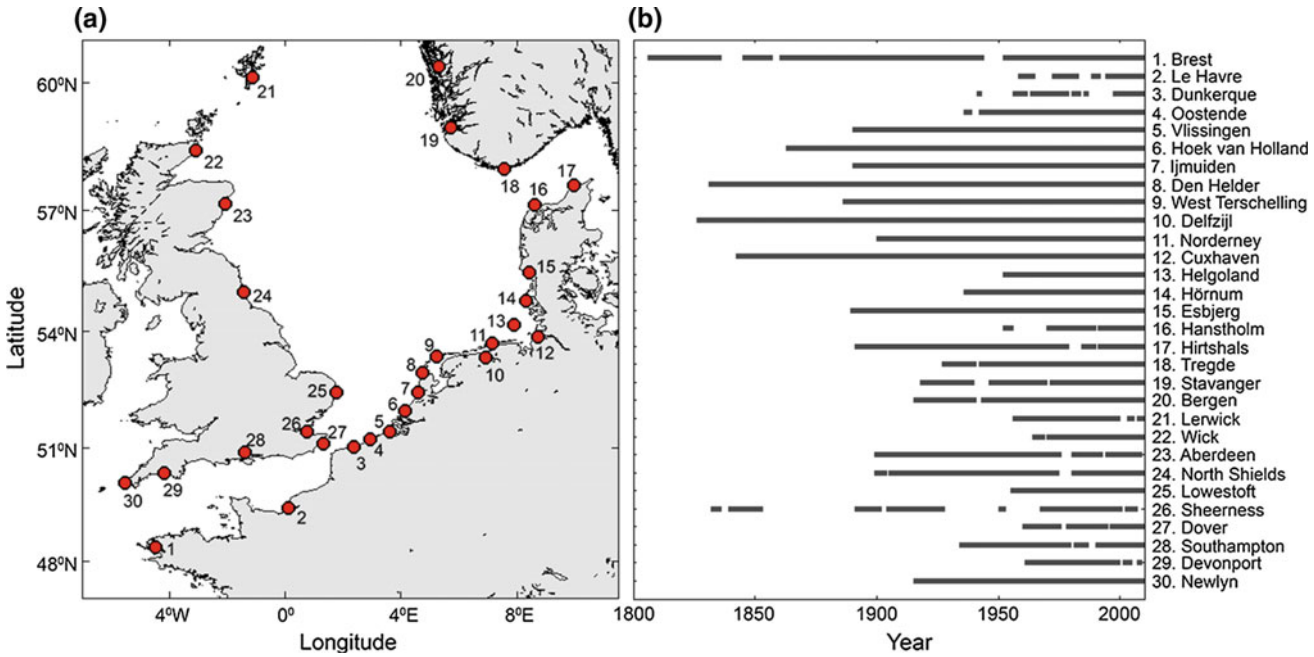

Fig. 3.15 Study area, tide gauge locations and length of individual mean sea level data sets (Wahl et al. 2013)

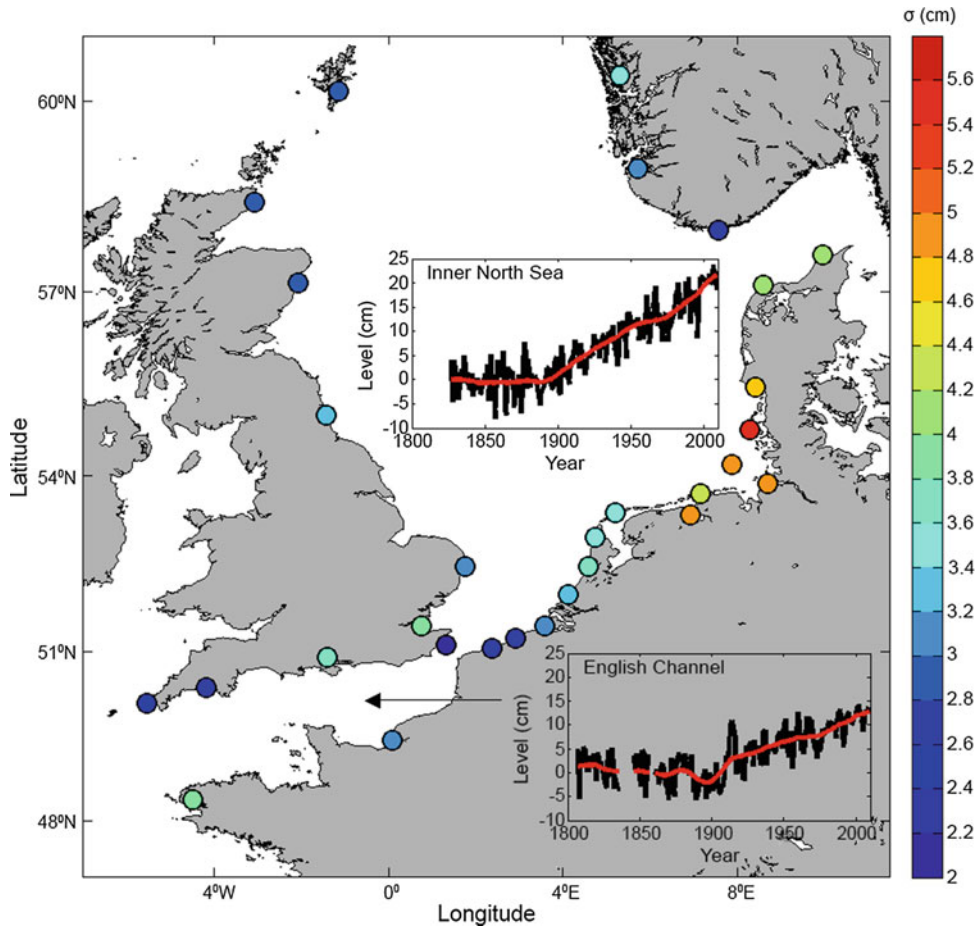

Fig. 3.16 Standard deviation from de-trended annual mean sea level (MSL) time series from 30 tide gauge sites around the North Sea; *upper inset* MSL index for the Inner North Sea (*black*) together with the non-linear sea-surface anomaly (SSA) smoothed time series (*red*); *lower inset* MSL index for the English Channel (*black*) together with the non-linear SSA smoothed time series (*red*) (after Wahl et al. 2013)

2.80 ± 0.80 mm year^{-1} from tide gauge data; Church and White 2011). In summary, the observed long-term changes in sea-level rise (SLR) in the North Sea do not differ significantly from global rates over the same period.

In recent years there has also been considerable focus on the issue of 'acceleration in rates of MSL rise'. Several methods have been applied to examine non-linear changes in long MSL time series from individual tide gauge sites and global or regional reconstructions (see Woodworth et al. 2009b, 2011 for a synthesis of these studies). Wahl et al. (2013) used singular system analysis (SSA) with an embedding dimension of 15 years for smoothing the MSL indices for the Inner North Sea and English Channel (Fig. 3.16). Periods of SLR acceleration were detected at the end of the 19th century and in the 1970s; a period of deceleration occurred in the 1950s. Several authors (e.g. Miller and Douglas 2007; Woodworth et al. 2010; Sturges and Douglas 2011; Calafat et al. 2012) suggested that these periods of acceleration/deceleration are associated with decadal MSL fluctuations arising from large-scale atmospheric changes. The recent rates of MSL rise were found to be faster than on average, with the fastest rates occurring at the end of the 20th century. These rates are, however, still comparable to those observed during the 19th and 20th centuries.

3.5 Extreme Sea Levels

Ralf Weisse, Andreas Sterl

Extreme sea levels pose significant threats (such as flooding and/or erosion) to many of the low-lying coastal areas along the North Sea coast. Two of the more recent examples are the events of 31 January/1 February 1953 and 16/17 February 1962 that caused extreme sea levels along much of the North Sea coastline and that were associated with a widespread failure of coastal protection, mostly in the UK, the Netherlands and Germany (e.g. Baxter 2005; Gerritsen 2005). Since then, coastal defences have been substantially enhanced along much of the North Sea coastline.

Extreme sea levels usually arise from a combination of factors extending over a wide range of spatial and temporal scales comprising high astronomical tides, storm surges (also referred to as meteorological residuals caused by high wind speeds and inverse barometric pressure effects) and extreme sea states (wind-generated waves at the ocean surface) (Weisse et al. 2012). On longer time scales, rising MSL may increase the risk associated with extreme sea levels as it modifies the baseline upon which extreme sea levels act; that is, it tends to shift the entire frequency distribution towards higher values.

The large-scale picture may be modified by local conditions. For example, for given wind speed and direction the magnitude of a storm surge may depend on local bathymetry or the shape of the coastline. Extreme sea states may become depth-limited in very shallow water and effects such as wave set-up (Longuet-Higgins and Stewart 1962) may further raise extreme sea levels. Moreover, there is considerable interaction among the different factors contributing to extreme sea levels, especially in shallow water. For example, for the UK coastline Horsburgh and Wilson (2007) reported a tendency for storm surge maxima to occur most frequently on the rising tide arising primarily from tide-surge interaction. Mean SLR may modify tidal patterns and several authors report changes in tidal range associated with MSL changes. For M2 tidal ranges, estimates vary from a few centimetres increase in the German Bight for a 1-m SLR (e.g. Kauker 1999) to 35 cm in the same area for a 2-m SLR (Pickering et al. 2011). So far, reasons for these differences are not elaborated on in the peer-reviewed literature.

Large sectors of the North Sea coastline are significantly affected by storm surges. A typical measure to assess the weather-related contributions relative to the overall variability is the standard deviation of the meteorological residuals (Pugh 2004). Typically, this measure varies from a few centimetres for open ocean islands hardly affected by storm surges to tens of centimetres for shallow water subject to frequent meteorological extremes (Pugh 2004). For the German Bight, values are in the order of approximately 30–40 cm indicating that storm surges provide a substantial contribution to the total sea level variability (Weisse and von Storch 2009). There is also pronounced seasonal variability with the most severe surges generally occurring within the winter season from November to February reflecting the corresponding cycle in severe weather conditions (Weisse and von Storch 2009).

Extreme sea level variability and change for Cuxhaven, Germany is illustrated in Fig. 3.17. Here a statistical approach was used to separate effects due to changes in MSL and to storm surges (von Storch and Reichardt 1997). The approach is based on the assumption that changes in MSL will be visible both in mean and in extreme sea levels as these changes tend to shift the entire frequency distribution towards higher values. Changes in the statistics of storm surges, on the other hand, will not be visible in the mean but only in the extremes. Following this idea, variations in the extremes may be analysed for example by subtracting trends in annual means from higher annual percentiles while variations and changes in the mean may be obtained by analysing the means themselves. Figure 3.17 shows the result of such an analysis for Cuxhaven, Germany. It can be inferred that the meteorological part (i.e. storm surges) shows pronounced decadal and interannual variability but no substantial long-term trend. The decadal variations are broadly consistent with observed variations in storm activity in the area (e.g. Rosenhagen and Schatzmann 2011; Weisse et al.

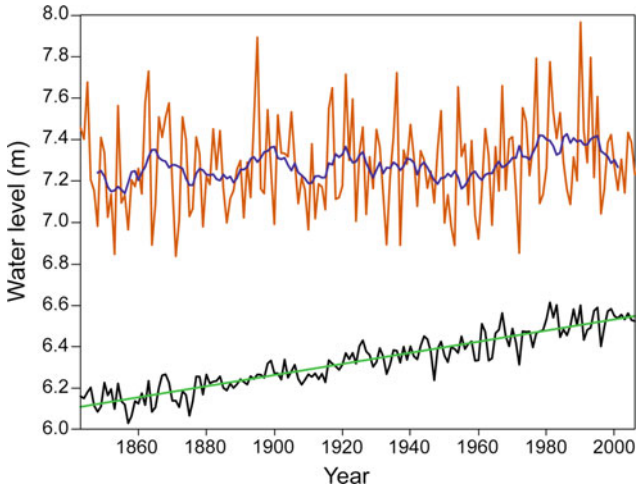

Fig. 3.17 Annual mean high water and linear trend (in m) for the period 1843–2012 at Cuxhaven, Germany (*lower*) and annual 99th percentile of the approximately twice-daily high-tide water levels at Cuxhaven after subtraction of the linear trend in the annual mean levels (*upper*); an 11-year running mean is also shown in the upper panel (redrawn and updated after von Storch and Reichardt 1997)

2012). Figure 3.17 also reveals that extreme sea levels substantially increased over the study period but that changes are primarily a consequence of corresponding changes in MSL and not of storm activity.

An alternative approach to analyse changes in extreme sea levels caused by changing meteorological conditions is by using numerical tide-surge models for hindcasting extended periods over past decades. Such hindcasts are usually set up using present-day bathymetry and are driven by observed (reanalysed) atmospheric wind and pressure fields. In such a design any observed changes in extreme sea levels result solely from meteorological changes while contributions from all other effects such as changes in MSL or local construction works are explicitly removed. Generally, and consistent with the results obtained from observations, such studies do not show any long-term trend but pronounced decadal and interannual variability consistent with observed changes in storm activity (e.g. Langenberg et al. 1999; Weisse and Pluess 2006).

In the analysis of von Storch and Reichardt (1997) annual mean high water is used as a proxy to describe changes in the mean. Climatically induced changes in annual mean high water statistics result principally from two different contributions: (i) corresponding changes in MSL and/or (ii) changes in tidal dynamics. Separating both contributions, Mudersbach et al. (2013) found for Cuxhaven from 1953 onwards that, apart from changes in MSL, extreme sea levels have also increased as a result of changing tidal dynamics. Reasons for the observed changes in tidal variation remain unclear. While increasing MSL represents a potential driver discussed by some authors (e.g. Mudersbach et al. 2013) the magnitude of the observed changes is too large compared to expectations from modelling studies (e.g. Kauker 1999; Pickering et al. 2011) and other contributions (such as those caused by local construction works) could not be ruled out (e.g. Hollebrandse 2005). Other potential reasons for changes in tidal constituents are referred to by Woodworth (2010) and Müller (2012) but have not been explored for the North Sea.

Systematic measurements of sea state parameters exist only for periods much shorter than those from tide gauges. In the late 1980s and early 1990s a series of studies analysed changes in mean and extreme wave heights in the North Atlantic and the North Sea (e.g. Neu 1984; Carter and Draper 1988; Bacon and Carter 1991; Hogben 1994). These were typically based on time series of 15 to at most 25 years and, while reporting a tendency towards more extreme sea states, all authors concluded that the time series were too short for definitive statements on longer-term changes. As for storm surges, numerical models are therefore frequently used to make inferences about past long-term changes in wave climate. Such models are either used globally (e.g. Cox and Swail 2001; Sterl and Caires 2005) or regionally for the North Sea and adjacent sea areas (e.g. WASA-Group 1998; Weisse and Günther 2007). For the North Sea, the latter found considerable interannual and decadal variability in the hindcast wave data consistent with existing knowledge on variations in storm activity.

Results from numerical studies should be complemented with those from statistical approaches. While numerical studies may represent variability and changes with fine spatial and temporal detail, the period for which such studies are possible is presently limited to a few decades. Statistical approaches may bridge the gap by providing information for longer time spans, but are usually limited in spatial and/or temporal detail. Such approaches were used by Kushnir et al. (1997), WASA-Group (1998), Woolf et al. (2002) and Vikebø et al. (2003), exploiting different statistical models between sea-state parameters and large-scale atmospheric conditions. Generally these approaches illustrate the substantial interannual and decadal variability inherent in the North Sea and North Atlantic wave climate. While longer periods are covered, the authors described periods of decreases and increases in extreme wave conditions. For example, Vikebø et al. (2003) described an increase in severe wave heights emerging around 1960 and lasting until about 1999 and concluded that this increase is not unusual when longer periods are considered. This indicates that changes extending over several decades, i.e. typical periods covered by numerical or observational based studies, should be viewed in the light of decadal variability obtained by analysing longer time series.

3.6 Carbon Dioxide, pH, and Nutrients

Helmuth Thomas, Johannes Pätsch, Ina Lorkowski, Lesley Salt, Wilfried Kühn, John Huthnance

Drivers and consequences of climate change are usually discussed from the perspective of physical processes. As such, Sects. 3.2 and 3.3 focus on aspects of physical water column properties (sea temperature, salinity and stratification) and physical interaction with adjacent water bodies (circulation and currents), and climate-change-driven alterations of these. While biogeochemical properties clearly respond to changes in physical conditions, changes can also be modulated by anthropogenic changes in the chemical conditions. These include increasing atmospheric CO_2 levels, ocean acidification as a consequence, and eutrophication/oligotrophication. Relevant time scales can co-vary with those of climate change processes, however they may also be distinctly different (e.g. Borges and Gypens 2010). Furthermore, effects of direct anthropogenic changes (such as nutrient inputs) and feedbacks between anthropogenic and climate changes (atmospheric CO_2 and warming, for example) can be synergistic (amplify each other) or antagonistic (diminish each other). Eutrophication and oligotrophication, feedbacks to changes in physical properties and their effects on productivity in the North Sea have been investigated using models (e.g. Lenhart et al. 2010; Lancelot et al. 2011). Results have been used by international bodies and regulations such as OSPAR, the European Water Framework Directive (EC 2000) and the Marine Strategy Framework Directive. A summary was recently given by Emeis et al. (2015).

The main focus of this section is on the carbonate and pH system of the North Sea and its vulnerability to climate and anthropogenic change. To address these issues, large systematic observational studies were initiated in the early 2000s by an international consortium led by the Royal Netherlands Institute of Sea Research (e.g. Thomas et al. 2005b; Bozec et al. 2006). Observational studies have been supplemented by modelling studies (e.g. Blackford and Gilbert 2007; Gypens et al. 2009; Prowe et al. 2009; Borges and Gypens 2010; Kühn et al. 2010; Liu et al. 2010; Omar et al. 2010; Artioli et al. 2012, 2014; Lorkowski et al. 2012; Wakelin et al. 2012; Daewel and Schrum 2013).

The North Sea is one of the best studied and most understood marginal seas in the world and so offers a unique opportunity to identify biogeochemical responses to climate variability and change. To better understand the sensitivity of the North Sea biogeochemistry to climate and anthropogenic change, this section first discusses some of the main responses to variability in the dominant regional climate mode—the NAO—based on observational data for 2001, 2005 and 2008. The effects of long-term perturbations on the major processes regulating biogeochemical conditions in the North Sea are then discussed based on results from multi-decadal ecosystem model runs. Observations on longer time scales exist locally off the Netherlands, Helgoland and elsewhere but are all from sites close to the coast where strong offshore gradients in nutrients and primary productivity (e.g. Baretta-Bekker et al. 2009; Artioli et al. 2014) affect CO_2.

3.6.1 Observed Responses to Variable External Forcing

In deeper areas of the North Sea, beyond the 50 m depth contour, primary production and CO_2 fixation are supported by seasonal stratification and by nutrients, which are a limiting factor and largely originate from the Atlantic Ocean (Pätsch and Kühn 2008; Loebl et al. 2009). Sinking particulate organic matter facilitates the replenishment of biologically-fixed CO_2 by atmospheric CO_2. Respiration of particulate organic matter below the surface layer releases metabolic dissolved inorganic carbon (DIC) which is either exported to the deeper Atlantic or mixed back to the surface in autumn and winter (Thomas et al. 2004, 2005b; Bozec et al. 2006; Wakelin et al. 2012). These northern areas of the North Sea act as a net annual sink for atmospheric CO_2.

By contrast, in the south (depth <50 m), the absence of stratification causes respiration and primary production to occur within the well-mixed water column. Except during the spring bloom, the effects of particulate organic carbon (POC) production and respiration cancel out and the CO_2 system is largely temperature-controlled (Thomas et al. 2005a; Schiettecatte et al. 2006, 2007; Prowe et al. 2009). Total production in this area is high in global terms; terrestrial nutrients contribute, especially in the German Bight, but in the shallow south, primary production is based largely on recycled nutrients with little net fixation of CO_2.

Beyond the biologically-mediated CO_2 controls, North Atlantic waters, flushing through the North Sea, dominate the carbonate system (Thomas et al. 2005b; Kühn et al. 2010) but may have only small net budgetary effects. The Baltic Sea outflow and river loads constitute net imports of carbon to the North Sea and modify the background conditions set by North Atlantic waters.

Basin-wide observations of DIC, pH, and surface temperature during the summers of 2001, 2005 and 2008 (Salt et al. 2013) reveal the dominant physical mechanisms regulating the North Sea pH and CO_2 system. pH and CO_2 system responses to interannual variability in climate and weather conditions (NAO, local heat budgets, wind and fluxes to or from the Atlantic, the Baltic Sea and rivers, see also Sects. 3.2 and 3.3) are also considered to be the responses that climate change will trigger. Interannual

variability appears generally more pronounced than long-term trends (e.g. Thomas et al. 2008).

The NAO index (Hurrell 1995; Hurrell et al. 2013) is commonly established for the winter months (DJF), although its impacts have been identified at various time scales. Many processes in the North Sea are reported to be correlated with the winter NAO, even if they occur in later seasons. Two aspects may explain an apparent delay between the trigger (i.e. winter NAO) and the response (the timing of the actual process): preconditioning and hysteresis (Salt et al. 2013).

An example of pre-conditioning is the water mass exchange between the North Atlantic Ocean and the North Sea. This exchange is enhanced during years of positive NAO (Winther and Johannessen 2006) and leads to an increased nutrient inventory in the North Sea and to higher annual productivity in spring and summer (Pätsch and Kühn 2008). Hysteresis can be characteristic of the North Sea's response to the NAO. Stronger westerly winds in winter, correlated with the winter NAO, push North Sea water into the Baltic Sea, a process that in turn leads to an enhanced outflow from the Baltic Sea into the North Sea in subsequent seasons (Hordoir and Meier 2010).

The bottom topographic divide of the North Sea, at about 40–50 m depth, is reflected in DIC, pH and temperature distributions (Figs. 3.18, 3.19 and 3.20) with higher DIC and temperature, and lower pH observed in the south, which is under stronger influence of terrestrial waters. In summer 2001, the year with the most negative NAO, the lowest DIC values and highest pH values were observed across the entire basin, whereas 2005 and 2008 were both characterised by higher DIC and lower pH, with some variability in these patterns across the North Sea. Summer 2005 had the coolest surface waters.

For winter NAO values, 2001 was the most negative (−1.9), 2005 was effectively neutral (0.12) and 2008 was positive (2.1). Weaker winds and circulation in the North Sea are associated with negative NAO (see Sects. 1.4.3 and 3.3.2) and reduce the upward mixing of cold winter water (Salt et al. 2013). Hence, metabolic DIC accumulated in deeper waters during the preceding autumn and winter

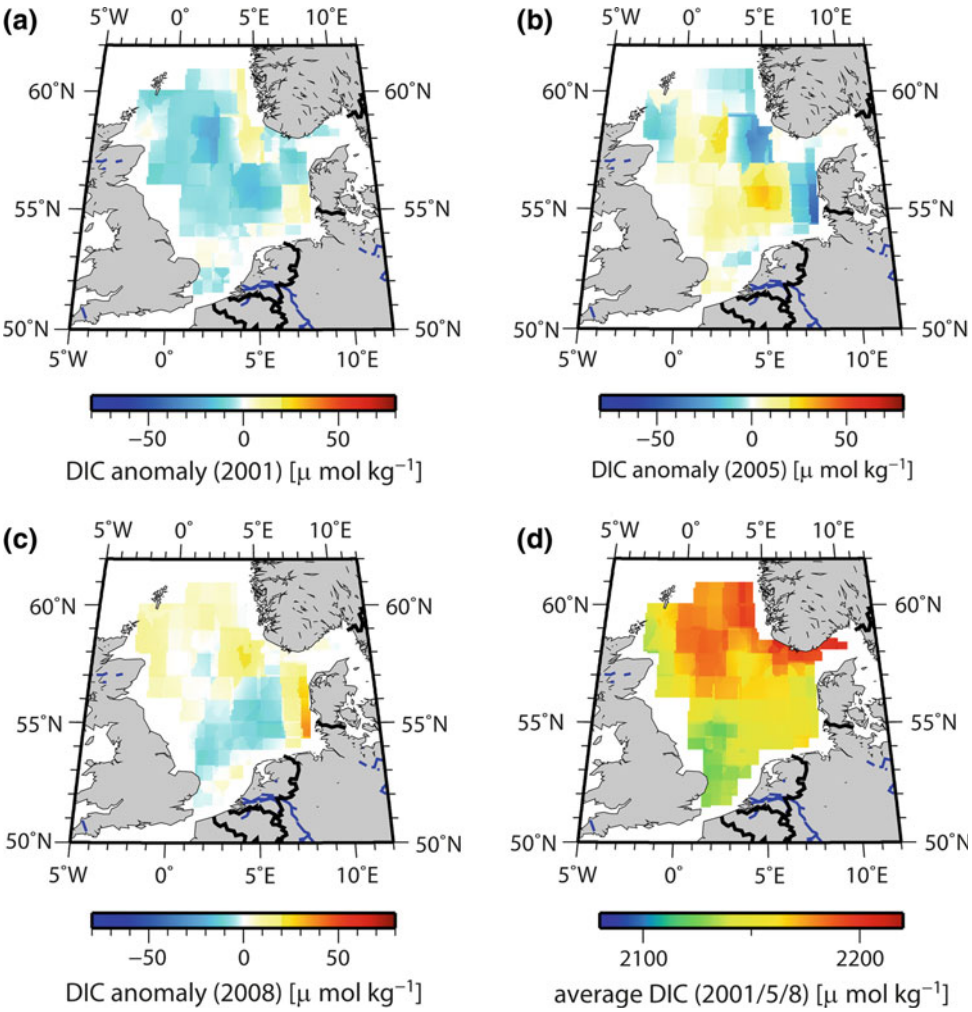

Fig. 3.18 Observed variability in surface water dissolved inorganic carbon (DIC) concentrations. All observations were made in summer (August/September) of the years 2001, 2005 and 2008 (Salt et al. 2013). Anomalies are shown relative to the average observed values for these years (also shown; figure by Helmuth Thomas, Dalhousie University, Canada)

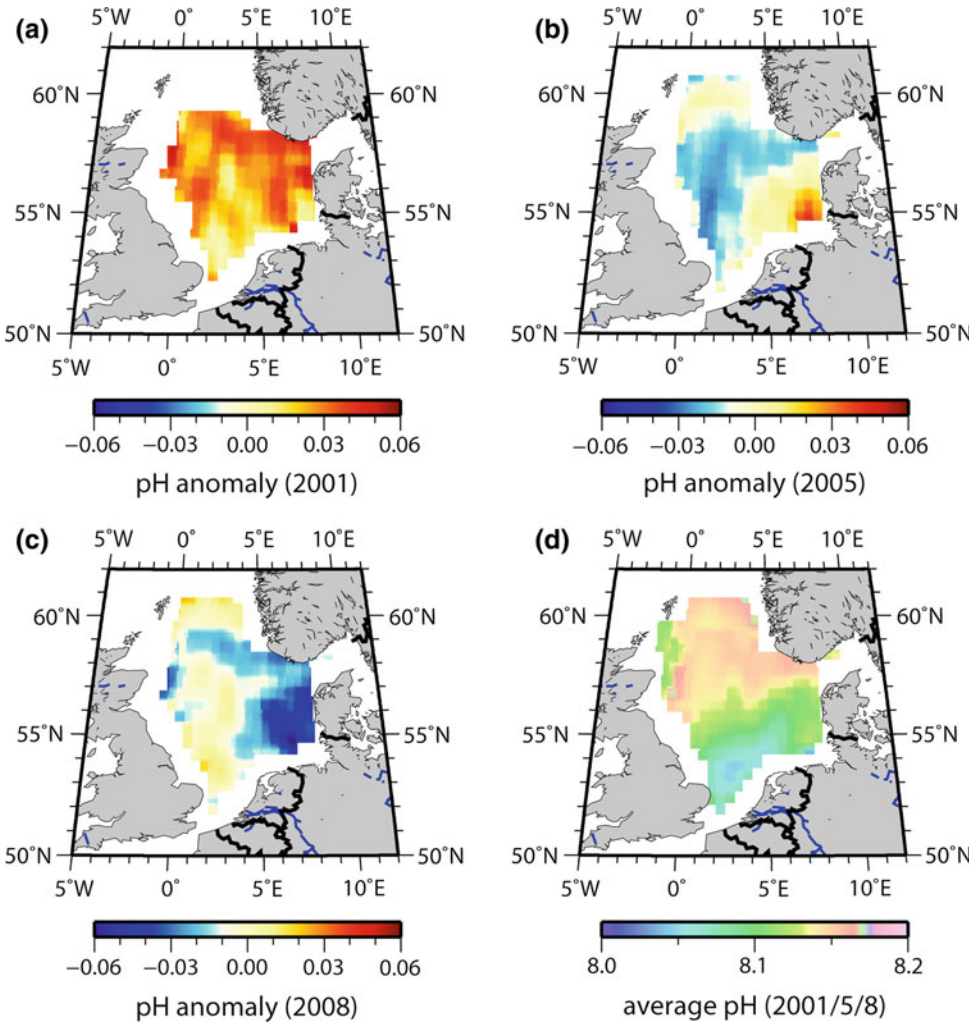

Fig. 3.19 Observed variability in surface water pH. All observations were made in summer (August/September) of the years 2001, 2005 and 2008 (Salt et al. 2013). Anomalies are shown relative to the average observed values for these years (figure by Helmuth Thomas, Dalhousie University, Canada)

(Thomas et al. 2004) was mixed into surface waters to a lesser extent in 2001 than in 2005 or 2008 when wind or circulation-driven mixing was stronger (see also Salt et al. 2013), which explained the elevated surface DIC and lower pH in 2005 and 2008 relative to 2001 (Figs. 3.18 and 3.19).

The striking difference between 2001 and 2005 in the northern North Sea (Thomas et al. 2007) was reinforced by the warmer summer with a shallower mixed layer in 2001 (Salt et al. 2013: their Fig. 5). Comparable biological activity caused the shallower mixed layer of 2001 to experience stronger biological DIC drawdown on a concentration basis, resulting in higher pH, than in 2005 (Figs. 3.18 and 3.19).

Interaction with the North Atlantic Ocean also causes variability in the CO_2 system, partly explained by NAO-dependent circulation changes (Thomas et al. 2008; Watson et al. 2009). Figure 3.21 shows the net flow of water in the first half of the three respective years. 2008 (positive NAO) has the strongest north-western inflow of DIC-enriched North Atlantic waters to the North Sea, via the Fair Isle Current and Pentland Firth, although 2001 had strong inflow from the north which recirculated out of the North Sea quickly off Norway (Lorkowski et al. 2012).

Such an influence of North Atlantic inflow is supported by strong correlations between changes in the inventories of salinity and corrected DIC (i.e. accounting for biological effects) during the periods 2001–2005 and 2005–2008 (Salt et al. 2013). Mean values of partial pressure of CO_2 (pCO_2) in the water (331.6 ppm in 2001, 352.5 ppm in 2005, 364.0 ppm in 2008) reflect the large change between 2001 and 2005 and the moderate change between 2005 and 2008. Also, strong NAO-driven anti-clockwise circulation in the North Sea in 2008 intensified the distinct characteristics of the southern and northern North Sea and sharpened the transition between them (e.g. high to low pH, see Salt et al. 2013: their Fig. 2).

Modelling results (Lorkowski et al. 2012) agree with several of these findings: a mixed layer shallower in 2001 and 2008 than in 2005, which had the coolest summer surface waters; central North Sea DIC concentrations about 10 μmol/kg less than average in 2001.

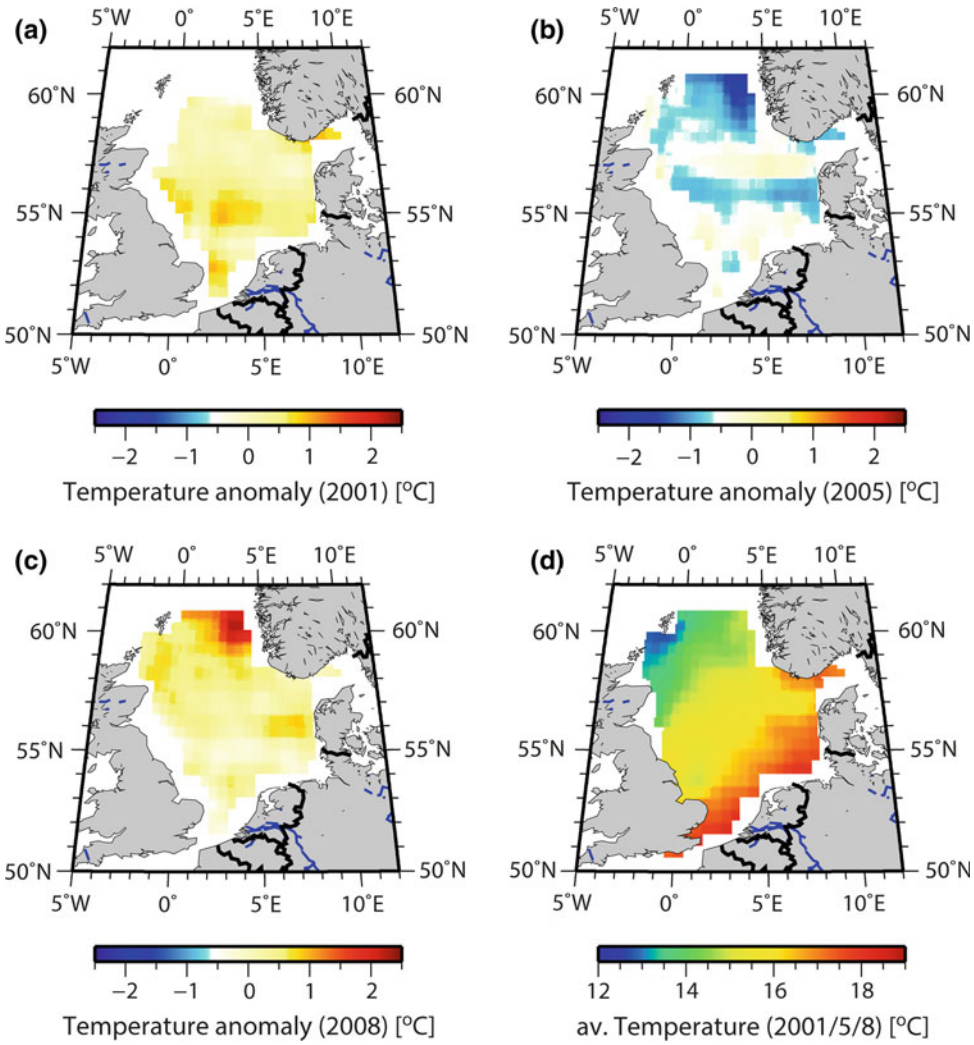

Fig. 3.20 Observed variability in sea surface temperature. All observations were made in summer (August/September) of the years 2001, 2005 and 2008 (Salt et al. 2013). Anomalies are shown relative to the average observed values for these years (figure by Helmuth Thomas, Dalhousie University, Canada)

In summary, three factors regulate the North Sea's CO_2 system and thus reveal points of vulnerability to climate change and more direct anthropogenic influences: local weather conditions (including water temperature in the shallower southern North Sea), circulation patterns, and end-member properties of relevant water masses (Atlantic Ocean, German Bight and Baltic Sea). Thus a positive NAO increases Atlantic Ocean and Baltic Sea inflow, the anti-clockwise circulation, carbon export out of the Norwegian Trench below the surface (limiting out-gassing) and hence the effectiveness of the shelf-sea CO_2 'pump' (Salt et al. 2013). If the NAO is positive together with higher SST, a shallower mixed layer favours lower surface pCO_2 and higher pH in the northern North Sea. These factors can be considered key to regulation of the North Sea's response to climate change and more direct anthropogenic influences.

3.6.2 Model-Based Interannual Variations in Nitrogen Fluxes

The North Sea is a net nitrogen sink for the Atlantic Ocean, due to efficient flushing by North Atlantic water with strong nitrogen concentrations and to large rates of benthic denitrification in the southern North Sea (Pätsch and Kühn 2008). This is the case despite large nitrogen inputs from the rivers and atmosphere. There is net production of inorganic nitrogen from organic compounds.

Pätsch and Kühn (2008) investigated nitrogen fluxes in 1995 and 1996 as the NAO shifted from very strong positive conditions in winter 1994/1995 to extreme negative conditions in winter 1995/1996. Due to enhanced ocean circulation on the Northwest European Shelf, the influx of total nitrogen from the North Atlantic was much stronger in 1995

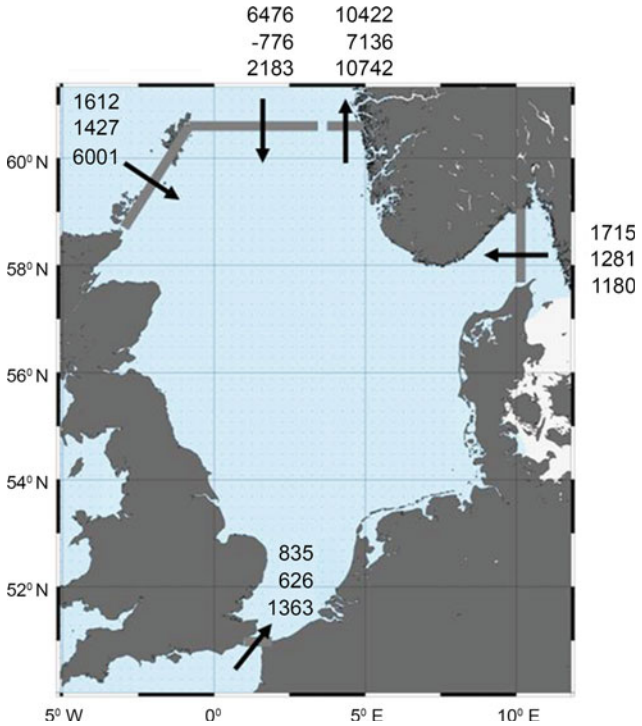

Fig. 3.21 Simulated cumulative net flux of water from 1 January to 30 June (km^3 per half year) for the years 2001 (*upper values*), 2005 (*middle values*), 2008 (*lower values*) (Lorkowski et al. 2012)

(NAO positive) than in 1996. River input of nitrogen was also larger in 1995 than 1996. While the import of organic nitrogen was similar for both years, the import of inorganic nitrogen was larger in 1995 than in 1996. The ecosystem response was stronger dominance of remineralisation over production of organic nitrogen in 1996 with negative NAO conditions.

According to this simulation, in 1996 (with extreme negative winter NAO) the net-heterotrophic state of the North Sea was stronger than in 1995. As a result, the biologically-driven air-to-sea flux of CO_2 was larger in 1995 than in 1996 (Kühn et al. 2010). In other words, in positive NAO years stronger fixation of inorganic nitrogen and inorganic carbon facilitates stronger biological CO_2 uptake. This carbon is exported into the adjacent North Atlantic in positive NAO years, as reported above. The balance between respiration and production in regulating DIC and pCO_2 conditions thus acts in synergy with the processes discussed in Sect. 3.6.1. At regional and sub-regional scales, modelling studies have investigated the concurrent impacts of eutrophication, increases in atmospheric CO_2 and climate change on the Southern Bight of the North Sea (Gypens et al. 2009; Borges and Gypens 2010; Artioli et al. 2014). The studies clearly highlight the complex effects of the individual drivers, as well as the different time scales of impact. Eutrophication, oligotrophication and temperature variability affect the CO_2 system at interannual to decadal time scales. Long-term trends of increases in atmospheric CO_2 and rising temperature have begun to cause tangible effects (e.g. Artioli et al. 2014) although, to date, these have been much less pronounced than effects at shorter time scales.

3.6.3 Ocean Acidification and Eutrophication

The interplay of the different anthropogenic and climate change processes, as well as their different, obviously overlapping time scales, can be exemplified with respect to the long-term effects of ocean acidification and the shorter-term effects of eutrophication/oligotrophication. Effects of eutrophication are closely related to the trend of ocean acidification, since both affect DIC concentrations and the DIC/A_T ratio (A_T: total alkalinity) in coastal waters, and thus CO_2 uptake capacity. Increased nutrient loads may lead to enhanced respiration of organic matter, which releases DIC and thus lowers pH. On shorter time scales, enhanced respiration overrides ocean acidification, which acts at centennial time scales (e.g. Borges and Gypens 2010; Artioli et al. 2014). (Surface-ocean pH has declined by 0.1 over the industrial era, in the North Sea as well as globally, and a hundred times faster in recent decades than during the previous 55 million years; EEA 2012).

If eutrophication-enhanced respiration of organic matter exhausts available oxygen, respiration then takes place through anaerobic pathways. Denitrification is crucial here; the biogeochemical consequences of depleted oxygen are many. Under eutrophic conditions, release of nitrate (NO_3) by enhanced respiration is controlled by the amount of available oxygen. If oxygen is depleted, NO_3 is converted to nitrogen gas (N_2). Any further input of NO_3 stimulates denitrification. The lost NO_3 is not available for biological production, thus the system is losing reactive nitrogen (Pätsch and Kühn 2008) as with eutrophication in the Baltic Sea (Vichi et al. 2004). A transition from aerobic to anaerobic processes has consequences for CO_2 uptake capacity and pH regulation: denitrification driven by allochthonous NO_3 releases alkalinity in parallel with the metabolic DIC, with a DIC/A_T ratio of 1:1.

Compared with aerobic respiration, which gives a DIC/A_T ratio of −6.6, the release of alkalinity in denitrification increases the CO_2 and pH buffer capacity of the waters, in turn buffering ocean acidification. Since denitrification is irreversible, the increased CO_2 and pH buffer capacity will persist on time scales relevant for climate change. In other words, if eutrophication yields anaerobic metabolic pathways, this constitutes a negative feedback to climate change, since more CO_2 can be absorbed from the

atmosphere, which in turn dampens the CO_2 greenhouse gas effect.

Other anaerobic pathways such as sulphate or iron reduction give even lower DIC/A_T release ratios (Chen and Wang 1999; Thomas et al. 2009); those may be reversible, however. Reduced (nitrogen-) nutrient input (i.e. oligotrophication) thus comes with a negative feedback with regard to ocean acidification: a desirable reduction in NO_3 release enhances vulnerability of the coastal ecosystem to ocean acidification, since most organic matter respiration is on or in shallow surface sediments (Thomas et al. 2009; Burt et al. 2013, 2014).

3.6.4 Variability on Longer Time Scales

Climate, CO_2 and more direct anthropogenic drivers also determine the variability of carbon fluxes in the North Sea. They can all be indicated as negative or positive feedback mechanisms for CO_2 exchange with the atmosphere and thus as feedbacks on climate change. The main direct anthropogenic impact on the carbon cycle, mostly for the southern North Sea, is the input of bio-reactive tracers, namely nutrients, via the atmosphere and rivers. Indirect anthropogenic drivers include acidification due to the ongoing increase in atmospheric pCO_2. Climate change processes (rising SST and changes in salinity distribution due to changes in circulation and winds) also induce shifts in the carbonate system and thus changes in carbon fluxes.

These anthropogenic and climate-change drivers, which act at interannual to decadal time scales, and their potential feedbacks and impacts were investigated in the model study by Lorkowski et al. (2012) for the years 1970 to 2006 (extended here to 2009). Simulation of the total system with all drivers included reproduced observations. Scenarios, mimicking anthropogenic and climate change processes, give insight into their roles and feedback mechanisms. These scenarios were generally run without biology, and with either fixed temperature or atmospheric CO_2 concentrations fixed at 1970 values. Both 'biotic' and 'abiotic' scenarios are shown here (Figs. 3.22 and 3.23, respectively), the latter to prevent biological feedbacks overshadowing the physically-driven and biogeochemically-driven responses.

The 'standard' simulation showed a decrease in CO_2 uptake from the atmosphere in the last decade (Fig. 3.22), an increase in SST by 0.027 °C year^{-1} and a decrease in winter

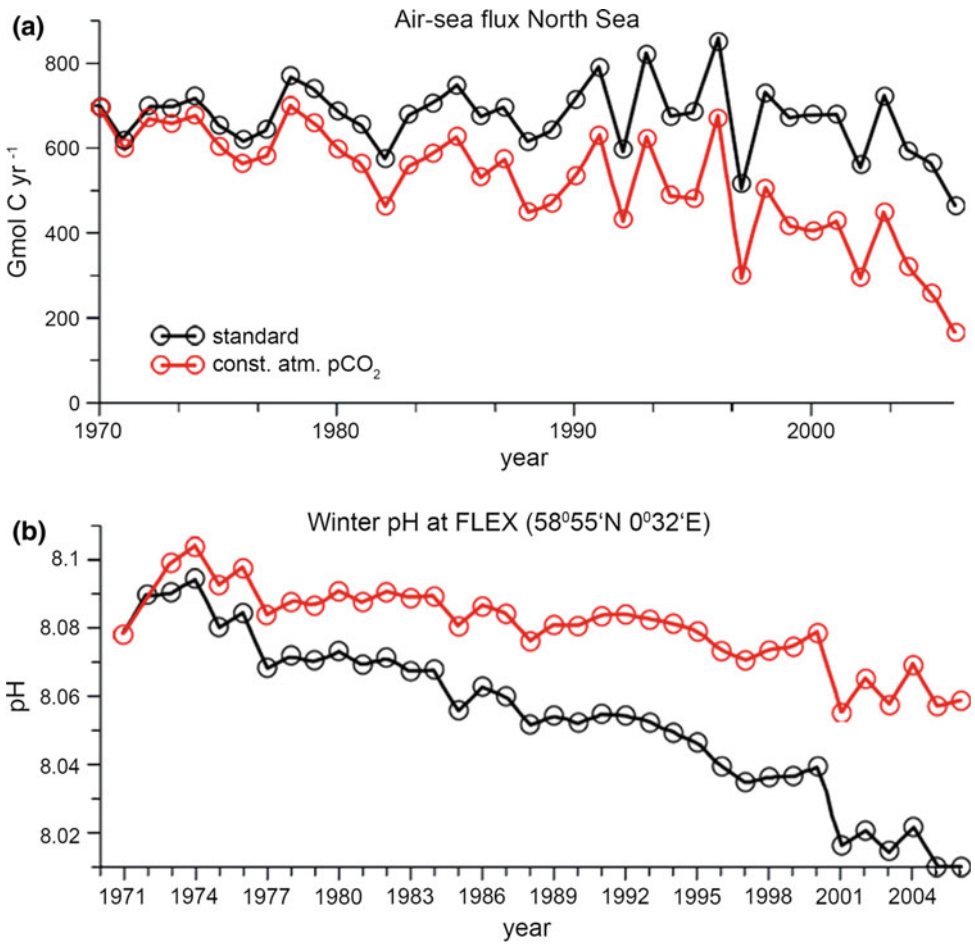

Fig. 3.22 Carbon dioxide (CO_2) air-sea fluxes for the total North Sea (*upper*, black curve reprinted from Fig. 5a in Lorkowski et al. 2012) and winter pH at one station in the northern North Sea (*lower*). Standard simulation (*black*); repeated annual cycle of atmospheric CO_2 (*red*) (figure by Helmuth Thomas, Dalhousie University, Canada)

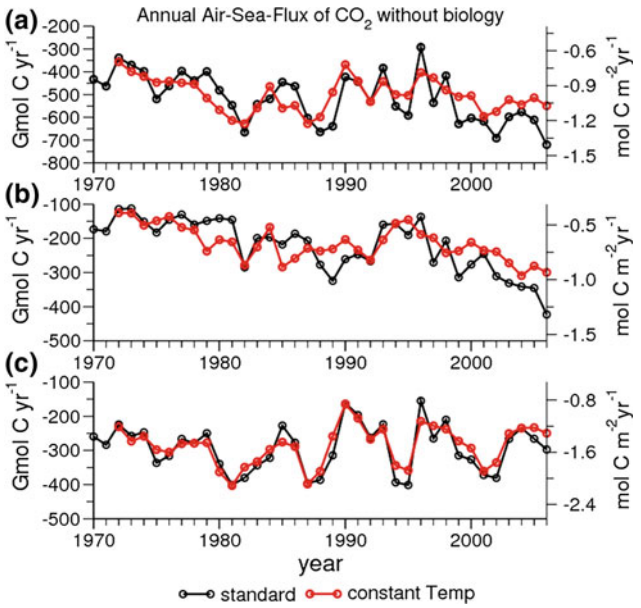

Fig. 3.23 Annual air-sea carbon dioxide (CO_2) flux for 'abiotic' simulations: total North Sea (*upper*), northern North Sea (*middle*), southern North Sea (*lower*). *Black* Results for standard conditions (Fig. 8 in Lorkowski et al. 2012); *red* results from the simulation with a repeated annual cycle of 1972 temperature. NB. Scales differ between the plots (figure by Helmuth Thomas, Dalhousie University, Canada)

pH by 0.002 year^{-1} (Lorkowski et al. 2012). Thus climate change alone (i.e. rising sea temperature) thermodynamically raises the pCO_2 and reduces CO_2 uptake in the North Sea. Furthermore, warming waters cause a lower pH, thus increased surface water acidity (Fig. 3.22).

Increasing atmospheric pCO_2 during the 'standard' simulation increases the gradient between seawater and atmospheric pCO_2 and increases the (net-) CO_2 uptake. To investigate this, the standard simulation is compared with a simulation using a repeated 1970 annual cycle of atmospheric pCO_2 (Fig. 3.22). 1970 pCO_2 (with rising temperature in common) leads to a smaller air-sea flux and less CO_2 uptake. pH decreases less than in the standard simulation (Fig. 3.22). Thus the simulations show enhanced CO_2 uptake in the North Sea as a consequence of rising atmospheric pCO_2, in turn increasing North Sea acidification as a 'local' process. This experiment also shows that for today's carbonate-system-status the increase in atmospheric CO_2 has a stronger impact on air-sea flux of CO_2 than the reduction in the buffer capacity by the ongoing acidification. This trend in acidification might be overlain on shorter time scales by advective processes (Thomas et al. 2008; Salt et al. 2013) as discussed in Sect. 3.6.1, by eutrophication (Gypens et al. 2009; Borges and Gypens 2010; Artioli et al. 2014) or by variability in biological activity.

Climate change enhances the hydrologic cycle, which means enhanced precipitation and river runoff, which drive changes in surface water salinity. Salinity decrease generally represents a dilution of DIC and A_T, with the DIC-effect dominating the A_T-effect on pCO_2 and pH (e.g. Thomas et al. 2008). Changes in salinity also alter the equilibrium conditions of the carbonate system (a minor effect): on addition of freshwater, pCO_2 decreases and pH increases. In coastal areas, precipitation-evaporation effects are confounded by changes in the mixing ratios of the dominant water masses, i.e., runoff and the oceanic end-member; higher salinity can mean a larger proportion of oceanic water relative to river runoff and vice versa. A sensitivity study, with salinity reduced by 1 (compared with the standard setup) and no biological processes, showed 10 % less outgassing, slightly counteracting the effect of rising temperature. In summary, rising temperature reduces uptake of atmospheric CO_2; increasing atmospheric pCO_2 or reduced salinity increases net uptake of atmospheric CO_2.

3.7 Oxygen

John Huthnance, Franciscus Colijn, Markus Quante

Oxygen is of concern because depletion (hypoxia) adversely affects ecosystem functioning and can lead to fish mortality. Air-sea exchange and photosynthesis tend to keep upper waters oxygenated; oxygen concentrations can be strongest in the thermocline associated with a sub-surface chlorophyll maximum (Queste et al. 2013). However, oxygen concentration near the sea bed can be reduced by organic matter respiration below stable stratification, breakdown of detrital organic matter in the sediment and lack of oxygen supply (by advection or vertical mixing). Temperature is also a factor; warmer waters can contain less oxygen but increase metabolic rates. Extra nutrients from rivers and estuaries can increase the amount of respiring organic matter. In the North Sea, most areas are well-oxygenated but some areas are prone to low oxygen concentrations near the bottom—the Oyster Grounds (central North Sea), off the Danish coast (Karlson et al. 2002) and locally near some estuaries, as in the German Bight. Climate change may influence oxygen concentrations through changes in absolute water temperature as well as through changes in temperature gradient, storm intensity and frequency, and related changes in mixing.

Data are available from the International Council for the Exploration of the Sea (ICES) for the past 100 years or so, research cruises (notably August 2010; Queste et al. 2013) and models (e.g. Meire et al. 2013; Emeis et al. 2015). The deep oxygen distribution and its relation to stratification is illustrated in Fig. 3.24.

There is strong interannual variability in the oxygen concentration of the bottom water in late summer. Published